L Viriatti

Case Inst. of Tech.

OPB

THEORY OF PULSE-DATA SYSTEMS APPLIED TO AN INPUT SELF-ADAPTIVE PULSE-DATA SYSTEM

Charles Kirkland Taft

UNIVERSITY MICROFILMS, INC.
Ann Arbor *London*

This "O-P Book" Is an Authorized Reprint of the Original Edition, Produced by Microfilm-Xerography by University Microfilms, Inc., Ann Arbor, Michigan, 1963

THEORY OF PULSE-DATA SYSTEMS APPLIED TO AN INPUT SELF-ADAPTIVE PULSE-DATA SYSTEM

A Thesis Submitted to
Case Institute of Technology
in Partial Fulfillment of the Requirements
for the Degree of
Doctor of Philosophy

by

Charles Kirkland Taft

1960

ABSTRACT

Incremental path controls employ a pulse-data system as the feedback control system. This type of system is considered in some detail. Mathematical methods of analysis are developed and described in addition to existing methods. The methods are applied to the design of a self-adaptive pulse-data system. The resulting system is a position control with superior response to ramp inputs at a wide range of desired rates. The system performance is compared experimentally with the performance of a conventional pulse-data system for a variety of inputs.

ACKNOWLEDGEMENTS

The work described herein was supported by funds from a fellowship awarded by the Charles W. Bingham Foundation and from Research Grant No. NsG 36-60 supplied by the National Aeronautics and Space Administration. Testing equipment was loaned by Minneapolis Honeywell and the Warner and Swasey Company. The author wishes to thank the many people which made this support possible.

The help extended by Professor H. W. Mergler, the author's faculty and thesis advisor, was especially helpful. The author expresses his gratitude to Professor Mergler for his assistance.

TABLE OF CONTENTS

LIST OF FIGURES

LIST OF SYMBOLS

A	Amplitude of quantizer input (quanta)
A_n	Coefficient of reference input pulses
a	Steady state velocity error (quanta)
a_n	Fourier coefficient
B	Backlash width (quanta)
B_m	Coefficient of feedback pulses
b	Distance from initial value of controlled variable to next quanta point (quanta)
b_n	Fourier coefficient
c	Location of inverse Laplace transform line integral path
$c(t)$	Quantizer output
D	Dimensionless time constant
e	Natural logarithm base 2.718
$e(t)$	Digital to analog converter output (quanta)
$\dot{e}(t)$	Derivative of $e(t)$ (quanta/sec)
$e(s)$	Laplace transform of $e(t)$ (quanta)
$e'(s)$	Laplace transform of voltage input to prime mover amplifier (volts)
$e_{average}$	Average value of $e(t)$ in steady state (quanta)
$E(t)$	Error in error criterion
$f(t)$	General function of time
$f(s)$	Laplace transform of $f(t)$
$G(s)$	Prime mover transfer function
$G'(s)$	A factor of $G(s)$

I	Smoothness factor
J	Number of quanta in a desired path
j	$\sqrt{-1}$
K	Gain
K'	Rate circuit proportionality factor (sec)
K_a	Acceleration gain constant (sec^{-2})
K_Q	Quantizer describing function
K_v	Velocity gain constant (sec^{-1})
L	Number of quanta in a desired path
$\mathcal{L}$	Laplace transformation operation
$\mathcal{L}^{-1}$	Inverse Laplace transformation
m	Integer
$N(s)$	Numerator of $G(s)$
n	Integer
Q	Quantizer transfer function
q	Exponent of s in factored form of $G(s)$
$q(t)$	Unit impulse response of $G(s)$
$q_u(t)$	Unit step response of $G(s)$
$q_{uss}(t)$	Straight line approximation to $q_u(t)$
$q_{ut}(t)$	Corrections to $q_{uss}(t)$
$r(t)$	Reference input pulses
$r'(t)$	Desired output (quanta)
$r^*(t)$	Double rate input pulses to rate sensor
s	Laplace operator (sec^{-1})
T	Prime mover time constant (sec)

T'	Time constant (sec)
T_{fm}	Time of m^{th} feedback pulse (sec)
T_L	Prime mover reactance time constant (sec)
T_m	Prime mover inertial time constant (sec)
T_r	Period of $r(t)$ when constant (sec)
T_{rn}	Time of n^{th} input pulse (sec)
t	Time (sec)
t_1	Particular value of time (sec)
$u(t)$	Unit step
X	Multiplier
x	Dummy variable
y	Dummy variable
α	Dimensionless steady state duration of $e(\tau)$
β	Dimensionless input pulse period
$\Delta\tau$	Steady state duration of $e(t)$ (sec)
$\delta(t)$	Unit impulse
ζ	Damping ratio
$\theta(t)$	Controlled variable (quanta)
$\theta'(t)$	Prime mover output in the presence of backlash (quanta)
$\dot{\theta}(t)$	Controlled variable velocity (quanta/sec)
$\theta_{ss}(t)$	Steady state controlled variable (quanta)
$\dot{\theta}_{ss}(t)$	Steady state controlled variable velocity (quanta/sec)
$\theta(s)$	Laplace transform of $\theta(t)$ (quanta)
$\dot{\theta}_{average}$	Average controlled variable velocity in the steady state (quanta/sec)

θ_1, θ_2	Limits of integration for fourier coefficient (degrees)
τ	Dimensionless time
τ_1	Dimensionless time when pass first quanta point
τ_m	Dimensionless time of maximum overtravel
φ	Phase angle (radians)
ω	Fundamental frequency of fourier series (radians/sec)

INTRODUCTION

Digital systems are being applied in a wide variety of control applications.

Modern method tools are needed to produce many parts with such complexity that a human operator is incapable of completely directing the operations. At the same time many different types of parts may be produced by the same machine. This requires setting the machine up for new parts frequently. Tolerances have also decreased in many cases. These factors have led to wide usage of digital systems for machine tools.

Chemical processes which were uncontrollable or at best only partially controllable are now being directed by digital systems. Computers have been used to provide fast and accurate computation of desired process parameter changes from measurements of process variables. Digital systems are used to translate the information of the computer to accomplish the process control.

Rockets and missiles require precise high power control. In many cases this control can best be accomplished by digital systems. This is especially true when the control is exercised from the ground. In this case the commands must travel by radio waves to the system. It has been shown that digital information is most efficiently transmitted accurately over long distances with minimum error.

A digital system receives information in a discrete digital form. This information is then manipulated by the system to accomplish some result. This result could be moving a cutter in a machine tool, changing the amount of pressure applied to a chemical process, or

firing a vernier rocket to accomplish a ' degrees correction in the course of an intercontinental ballistic m. sile.

In all of the examples above the digital system is concerned with the manipulation of a controlled variable and its time derivatives along a prescribed path. The path must be followed with extreme accuracy. A digital system is without equal in this type of application.

To exercise path control the digital system must measure the controlled variable very accurately. In the digital system the measure of a variable is indicated by the state of the transducer not a magnitude as is the case with analog transducers. This method of measurement reduces the effects of noise and permits the digital system to operate with much higher accuracies over a given range of the controlled variable. If the digital transducer is placed in a control loop this control becomes a digital system of the type described above.

There are two basic types of digital path controls with the digital transducer in the feedback loop.

(1) The absolute system shown in figure 1 measures by comparison. The control specifications of the path are translated into the desired value of the controlled variable at specified time intervals. This information is coded and fed to a comparator. The actual value of the controlled variable is encoded by a digital transducer (encoder). The difference between these two coded numbers, as obtained by the comparator, is the error. The error is converted to an

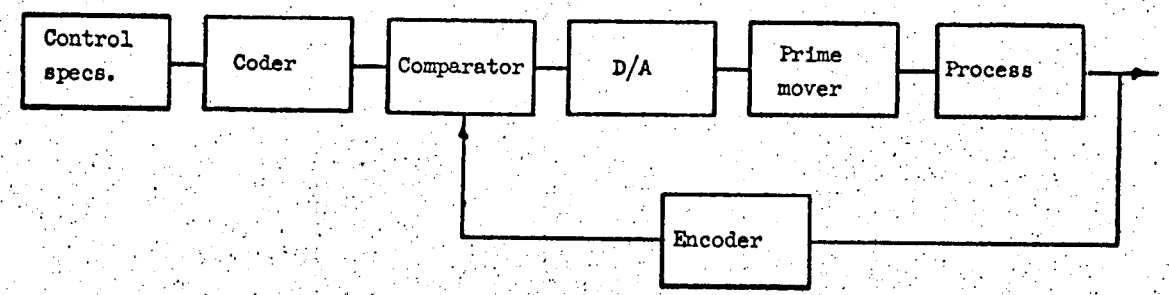

Figure 1. - Absolute system.

analog signal by the digital to analog converter (D/A). The analog error signal then directs the prime mover to manipulate the process in order to reduce the error.

(2) The incremental system shown in figure 2 measures by pulse counting. The control specifications are converted into a specific number of pulses. The number equals the desired controlled variable change in increments or "quanta". The time between pulses indicates the desired rate. These pulses are counted by a bidirectional counter (BDC) which is capable of counting up or down. The controlled variable is measured by a quantizer. This device emits a pulse whenever the controlled variable takes specified values. The pulses are counted by the bidirectional counter. The count in the counter is equal to the error. This is converted to an analog signal by the digital to analog converter (D/A). The analog error signal directs the prime mover as in the absolute system. The incremental path control is sometimes called a pulse-data system.

This thesis is concerned with the pulse-data system. This type provides high accuracy with relatively low cost. However, at low input pulse rates the controlled variable changes in a stepwise manner instead of continuously. Thus there are large errors in controlled variable rate.

The object of this thesis is twofold.

(1) Methods of analysis and synthesis of pulse-data systems are developed.

(2) A pulse data system with self-adaptive control is designed

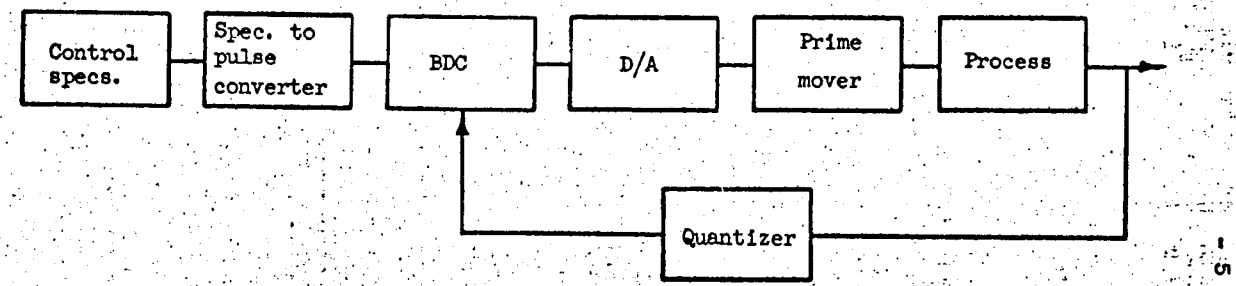

Figure 2. - Incremental system.

to manipulate the controlled variable smoothly over a wide range of input pulse rates. The methods developed in the first part are used in the design. The resulting system is then compared to the conventional pulse-data system.

CHAPTER I

PULSE-DATA SYSTEM MODEL

The object of this chapter is to describe the pulse-data system in more detail and develop a mathematical model.

Description

The basic system is shown schematically in figure 3. The waveform of the signals at various points in the circuit is also shown.

The input pulses $r(t)$ serve as the reference input. Each pulse directs the system to change the controlled variable $\theta(t)$ by one increment or "quanta". The time between pulses indicates the desired rate. These pulses are directed to either the plus or minus input of the Bidirectional Counter (BDC). If they enter the plus input the controlled variable $\theta(t)$ will increase. If the pulses are directed to the minus imput the controlled variable will decrease. The Bidirectional Counter is simply a counter which counts up when pulses are fed to its plus input and counts down when they are fed to its minus input.

The controlled variable is measured by a Quantizer. The Quantizer emits a pulse $c(t)$ whenever the controlled variable $\theta(t)$ takes on particular values equal increments apart. The points at which the Quantizer emits a pulse shall be called quanta points. The Quantizer pulses are fed to the minus input of the Bidirectional Counter if the controlled variable is increasing. If the controlled variable is decreasing they go to plus input.

In this way the state of the Bidirectional Counter is indicative of the instantaneous error when a feedback pulse is received from the Quantizer.

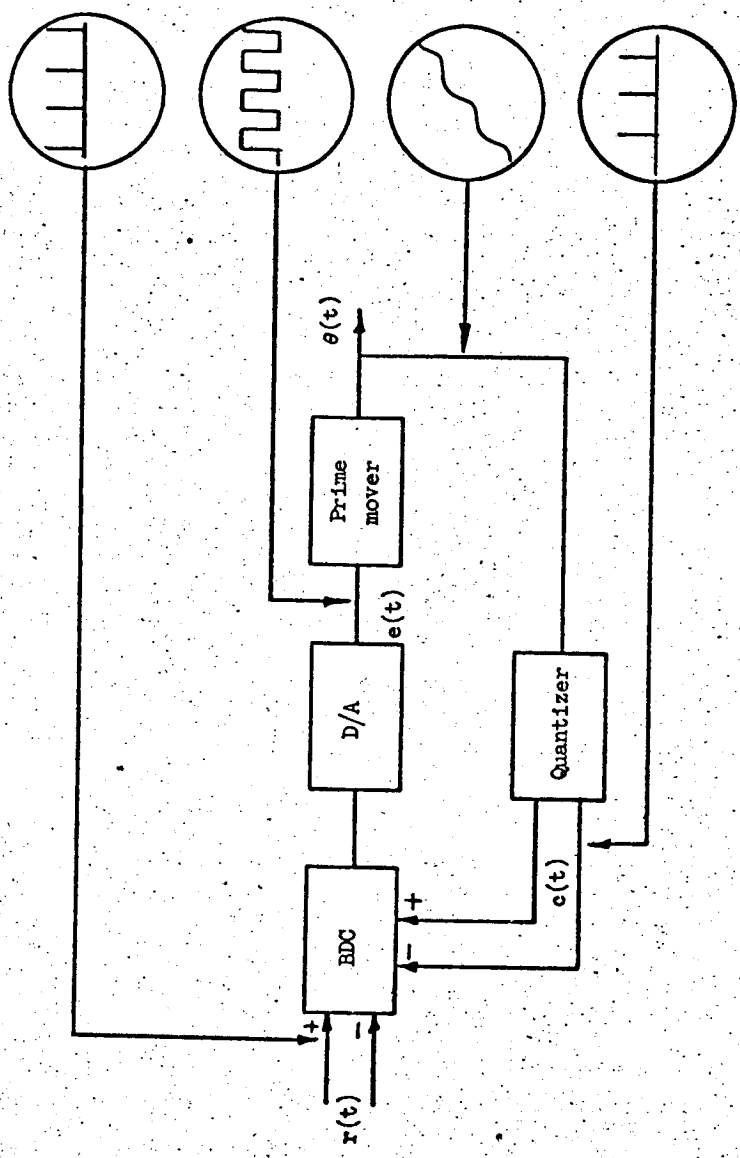

Figure 3. - Pulse-data system.

The state of the Bidirectional Counter is converted to an analog signal $e(t)$ by the Digital to Analog Converter. Thus for the input shown in figure 3 the waveform of $e(t)$ is rectangular. This signal serves to direct the Prime Mover.

The Prime Mover will be assumed to be characterized by a linear differential equation in this thesis, except where noted. The transfer function of the Prime Mover will be denoted by $G(s)$.

The integrating effect of the Prime Mover causes the output $\theta(t)$ to appear as a series of steps.

In all practical cases $G(s)$ will be of the form:

$$G(s) = \frac{KG'(s)}{s^q}$$

Where $q \geq 1$ and $G'(0) = 1$. If $q = 0$ the system would require an error $e(t)$ to hold any specific value of $\theta(t)$. Since a digital system is usually employed because of its great accuracy this would be intolerable.

Mathematical Model

The mathematical model is shown in figure 4. These mathematical representations of the variables and blocks shown in figure 3 will be developed to describe the operation of a pulsed-data system.

Reference Input $r(t)$

The reference input is a series of pulses. Because of the nature of the Bidirectional Counter model the pulses will be assumed to be unit impulses.

Thus:

$$r(t) = \sum_{n=0}^{\infty} A_n \delta(t - T_{rn})$$

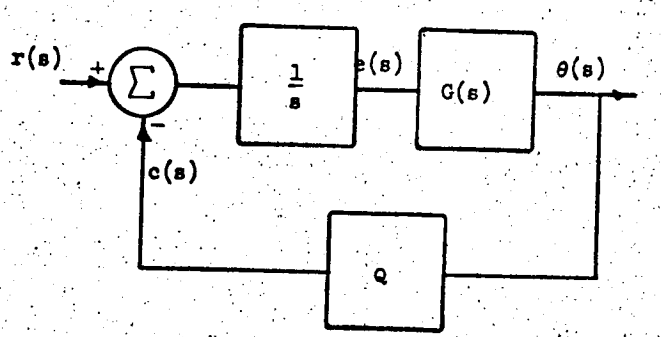

$$r(t) = \sum_{n=0}^{\infty} A_n \delta(t-T_{rn})$$

$$c(t) = \sum_{m=0}^{\infty} B_m \delta(t-T_{fm})$$

$$e(t) = \sum_{n=0}^{\infty} A_n u(t-T_{rn}) - \sum_{m=0}^{\infty} B_i u(t-T_{fm})$$

Figure 4. - Pulse-data system mathematical model.

where $\delta(t - T_{rn})$ is a pulse of unit area whose duration approaches zero which occurs at $t = T_{rn}$.

$A_n = +1$ if the n^{th} pulse is fed to the plus input of the Bi-directional Counter.

$A_n = -1$ if the n^{th} pulse is fed to the minus input of the Bi-directional Counter.

$A_n = 0$ if the pulse train stops.

Feedback Pulses $c(t)$

$c(t)$ will be represented in exactly the same way as $r(t)$.

$$c(t) = \sum_{m=0}^{\infty} B_m \delta(t - T_{fm})$$

T_{fm} = time when a quanta point is passed.

$$B_m = + \frac{\dot{\theta}(T_{fm})}{|\dot{\theta}(T_{fm})|}$$

$= 0$ when $\dot{\theta}(t) = 0$

It will be assumed that the location of the quanta points relative to $\theta(t)$ is fixed. If backlash exists in the system a new variable $\theta'(t)$ will be defined as the output of the Prime Mover. The backlash will then be assumed to exist between $\theta'(t)$ and $\theta(t)$.

Bidirectional Counter and Digital to Analog Converter

The two pulse trains enter the Bidirectional Counter where the state of the counter is equal to the algebraic sum of the A_n and B_m. This state is converted to $e(t)$ in the Digital to Analog Converter. This process can be represented by summing $c(t)$ and $r(t)$ and integrating the result. Thus:

$$e(t) = \int_0^t [r(t) - c(t)]\, dt$$

$$= \int_0^t \left[\sum_{n=0}^{\infty} A_n \delta(t - T_{rn}) - \sum_{m=0}^{\infty} B_m \delta(t - T_{fm}) \right] dt$$

A_n and B_m are constants. Since the unit step $u(t - \tau)$ is defined as:

$$u(t - \tau) = \int_0^t \delta(t - \tau)\, dt$$

An alternate representation of $e(t)$ is:

$$e(t) = \sum_{n=0}^{\infty} A_n u(t - T_{rn}) - \sum_{m=0}^{\infty} B_m u(t - T_{fm})$$

The Bidirectional Counter and Digital to Analog Converter are represented in the model by a summing point andan integrator (fig. 4).

Quantizer

The Quantizer is represented by the Q block in figure 4. This is a nonlinear element which shall be described by the relation between its input and output.

The entire range of the controlled variable $\theta(t)$ is subdivided into increments which are commensurate with the desired system accuracy. The Quantizer emits a pulse whenever the transition between one increment and another is passed. This transition point has been defined as a quanta point.

In this thesis $\theta(t)$ will be expressed in quanta thus. T_{fm} is determined by:

$$\theta(T_{fm}) = b + \sum_{m=0}^{m} B_{m-1}$$

In an incremental system no point has a special identity. Thus b locates the initial value of the controlled variable relative to the next quanta point when $t = 0$. This relationship is illustrated in figure 5.

Prime Mover

The Prime Mover includes all dynamic elements between the Digital to Analog Converter and the controlled variable. This may include process lags and actuator lags. It is assumed that these elements can be described by linear differential equations so that they are represented by a transfer function $G(s)$. If there are any lags in the Bidirectional Counter or Digital to Analog Converter they will be included in $G(s)$.

On the basis of this model several preliminary observations can be made.

(1) $e(t)$ will be a rectangular wave. In general this wave will not be periodic. If however $T_{r(n+1)} - T_{rn} = T_r$. Where T_r is fixed and the system transients have died out $e(t)$ will be periodic of period T_r. This is the case when the desired path for $\theta(t)$ is a ramp.

(2) $e(t)$ depends on $\theta(t)$ in a discontinuous manner. For this reason it is difficult to obtain $\theta(t)$ for a given $r(t)$ except by a step-by-step procedure.

(3) $\theta(t)$ can be anywhere between two quanta points with no change in system error. Thus:

$$0 < b < 1$$

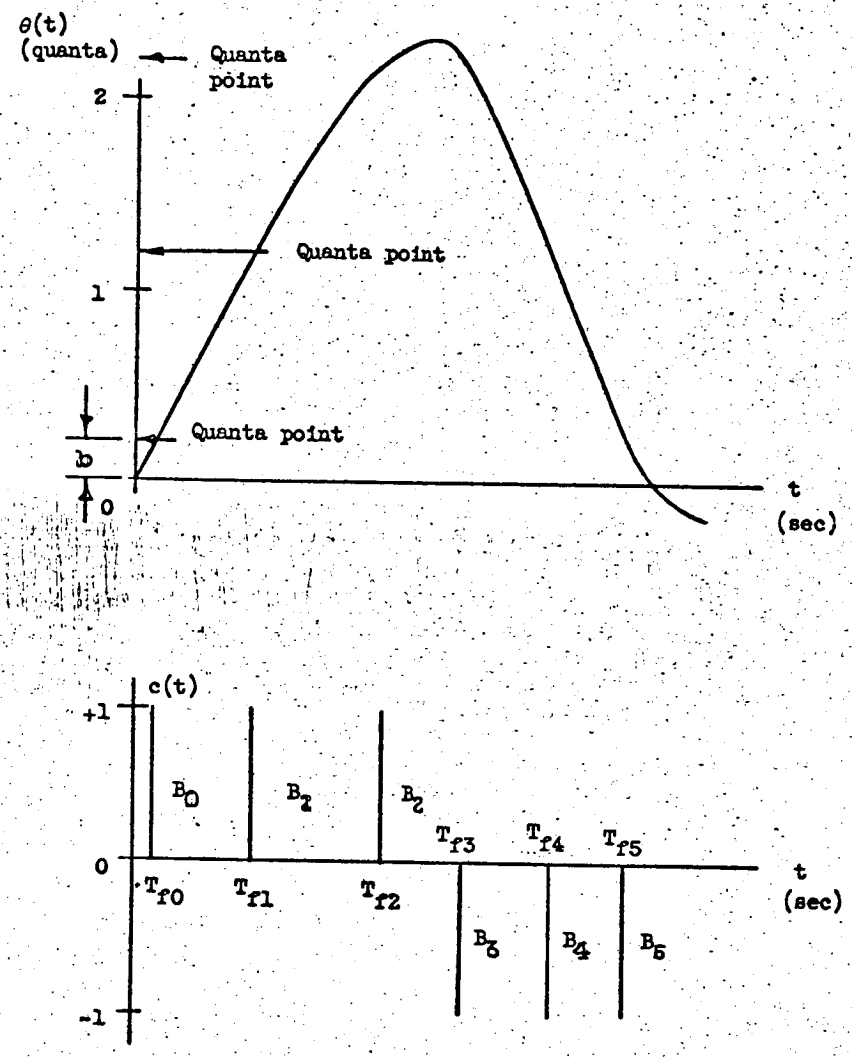

Figure 5. - Quantizer input-output relationship.

When $t = T_{r0}$, This uncertainty about location can cause $\theta(t)$ to change more or less than one quanta if a single input pulse is received. If many input pulses are received $\theta(t)$ may change more than one quanta for the first pulse. $\theta(t)$ may change less than one quanta for the second pulse etc., until equilibrium is reached. Then $\theta(t)$ changes one quanta between input pulses.

(4) As $\theta(t)$ approaches the desired position as directed by an input pulse $r(t) = \delta(t - T_{r0})$ there is no braking action as in a continuous feedback system. $e(t)$ remains fixed until a quanta point is reached. Then a feedback pulse is generated. At that time $t = T_{f0}$, $e(T_{f0}) = 0$ and the Prime Mover begins to stop. This means that there is always an overtravel beyond the quanta point. If the gain is too large $\theta(t)$ may overtravel one quanta or more causing $e(t)$ to reverse.

(5) Since there is no position feedback between quanta points the Prime Mover may drift. This is especially noticeable in systems where $q > 1$ in $G(s) = \frac{KG'(s)}{s^q}$. In an actual system drift must be kept at a minimum because it will cause the system to exhibit a limit cycle when $r(t) = 0$. $\theta(t)$ will drift to a quanta point where a feedback pulse causes $e(t)$ to reverse $\theta(t)$. $\theta(t)$ decreases until a second feedback pulse in the opposite sense makes $e(t) = 0$. $\theta(t)$ stops then starts to drift again to the quanta point where the process is repeated.

CHAPTER II

METHODS OF ANALYSIS

This chapter outlines the most useful methods which can be used in the analysis and synthesis of pulse-data systems. Wherever possible examples are chosen which illustrate the properties of pulse-data systems.

The model developed in Chapter I and shown in figure 4 will be used to represent the system.

Transient Analysis

Two methods are most useful for transient analysis. The first employs the phase plane. The method is limited to systems of low order. The second method employs the convolution integral to produce a time domain solution which is limited to Prime Movers characterized by linear differential equations of any order.

Phase Plane

This method is only useful for systems with $G(s)$ of the form:

$$G(s) = \frac{KN(s)}{s(Ts + 1)}$$

or

$$= \frac{KN(s)}{s(T^2s^2 + 2\zeta Ts + 1)}$$

or

$$= \frac{KN(s)}{s^2(Ts + 2\zeta Ts + 1)}$$

If the system $G(s)$ has more than two nonzero poles the phase space must be used which greatly complicates the analysis.

The method consists of defining a new variable equal to the time derivative $\dot{\theta}(t)$ of the controlled variable $\theta(t)$. The order of the differential equation may then be reduced by one. The resulting

equation may be used to trace the system trajectory in a $\dot{\theta}(t)$, $\theta(t)$ plane with increasing time given the initial conditions.

In general the phase plane method is much more laborious to apply than the time domain methods. However, if the Prime Mover exhibits significant nonlinearities the phase plane method will yield useful results while the time domain methods are not applicable. This thesis will be concerned with systems where the Prime Mover can be characterized by a linear differential equation. Thus this method is described only briefly. A more detailed explanation of the phase plane can be obtained from Cunningham[1], Truxal[2], or Savant[3]. The main usefulness of this method lies in the fact that one of the coordinates of the plane is $\theta(t)$. This defines the point where $e(t)$ changes and hence regions of constant $e(t)$ can be specified.

Time Domain Solution

When the Prime Mover can be characterized by a linear differential equation the principle of superposition can be applied to obtain a solution.

C. Lepage suggests a method which is described by J. C. Gille[4] who employs it in the analysis of relay servomechanisms. The output of the relay is decomposed into a series of unit steps. The overall system response is then a summation of a series of unit step responses.

This is applied to a pulse-data system as follows.

---

[1]The superscript numerals refer to the Bibliography.

Referring to the model shown in figure 4 the Laplace transform of $\theta(t)$ can be written.

$$\mathcal{L}[\theta(t)] = \theta(s) = e(s)\, G(s)$$

But:

$$e(t) = \sum_{n=0}^{\infty} A_n u(t - T_{rn}) - \sum_{m=0}^{\infty} B_m u(t - T_{fm})$$

Obviously this is a series of unit steps. A_n and T_{rn} are specified but B_m and T_{fm} are determined by $\theta(t)$. Thus the solution must be carried out in a step by step manner.

$$e(s) = \sum_{n=0}^{\infty} \frac{A_n e^{-T_{rn}s}}{s} - \sum_{m=0}^{\infty} \frac{B_m e^{-T_{fm}s}}{s}$$

Thus:

$$\theta(s) = \sum_{n=0}^{\infty} \frac{A_n G(s) e^{-T_{rn}s}}{s} - \sum_{m=0}^{\infty} \frac{B_m G(s) e^{-T_{fm}s}}{s}$$

Define $q_u(t) = \mathcal{L}^{-1}[G(s)/s)] \equiv$ the Prime Mover response to a unit step with zero initial conditions. Then:

$$\theta(t) = \sum_{n=0}^{\infty} A_n q_u(t - T_{rn})\, u(t - T_{rn})$$

$$- \sum_{m=0}^{\infty} B_m q_u(t - T_{fm})\, u(t - T_{fm})$$

Where $q_u(t - T_{rn})\, u(t - T_{rn})$ is the unit step response delayed by $t = T_{rn}$. The transient response can be determined by a step-by-step graphical procedure.

(1) The unit step response $A_0 q_u(t)$ of the Prime Mover is plotted. The response $\theta(t)$ starts at $t = T_{r0}$ and is positive if $A_0 = +1$

and negative if $A_0 = -1$. It is usually more convenient to measure time from $t = T_{r0}$ but not necessary.

(2) When the controlled variable $\theta(t)$ reaches a quanta point a feedback pulse occurs. This specifies B_0 and T_{f0}. A unit step response $-B_0 q_u(t - T_{f0})$ is started from this time. It is positive if $-B_0$ is positive and negative if $-B_0$ is negative.

(3) The value of $\theta(t)$ is then the algebraic sum of the ordinates of $A_0 q_u(t)$ and $-B_0 q_u(t - T_{f0})$ at time t. This is continued and is correct until another quanta point is reached or another reference pulse is received.

(4) Whenever a reference pulse $r(t) = A_n \delta(t - T_{rn})$ or a feedback pulse $c(t) = B_m \delta(t - T_{fm})$ is received another unit step response is started.

Once the values for B_m and T_{fm} are determined by the above method the response of the pulsed data system may be expressed analytically.

This method is illustrated by the following example:

$$G(s) = \frac{K_v}{s(Ts + 1)}$$

Let:

$$\sqrt{\frac{T}{K_v}}\,\tau = t$$

Then:

$$G(s) = \frac{1}{s\left(s + \frac{1}{\sqrt{TK_v}}\right)}$$

Let $D \equiv \sqrt{TK_v} = 1.1$. The inverse Laplace transform is:

$$q_u(\tau) = \sum_{\text{Poles of } G(s)} \text{residues} \left[\frac{e^{s\tau}}{s^2\left(s + \frac{1}{D}\right)}\right]$$

$$= D^2 e^{-\frac{\tau}{D}} + \frac{d}{ds}\left[\frac{e^{s\tau}}{s + \frac{1}{D}}\right]_{s=0}$$

$$= D^2 e^{-\frac{\tau}{D}} + \tau D - D^2$$

$$= 1.1\tau + 1.21\left(e^{-\frac{\tau}{1.1}} - 1\right)$$

It will also be assumed that there is backlash between the Prime Mover output and the controlled variable. Define:

$\theta'(\tau) \equiv$ the Prime Mover output (quanta)

$B \equiv$ backlash (quanta)

The backlash will be of the form shown in figure 6. The nature of the backlash is such that $\theta'(\tau)$ may be as far as $B + 1$ quanta from its value when a quanta point is passed.

In this example let $B = 0.8$ quanta and $\theta'(0) = 1.8$ quanta from the next quanta point.

The graphical procedure is shown in figure 7. $\theta'(\tau)$ is plotted vs τ.

At $\tau = 0$ a reference pulse $r(t) = \delta(\tau)$ is received. This initiates a unit step response at $\tau = 0$. The initial position is $\theta'(0) = 0$. Thus when $\theta'(\tau) = 1.8$ the first feedback pulse $c(t) = -\delta(\tau - 2.7)$ occurs. At this point a second unit step response $-u(\tau - 2.7)\ q_u(\tau - 2.7)$ starts. When $\tau = 4.75$ the system passes another quanta point at $\theta'(\tau) = 2.8$. This initiates another unit step response $-u(\tau - 4.75)\ q_u(\tau - 4.75)$ due to another feedback pulse $c(t) = +\delta(t - 4.75)$. The algebraic sum of these three responses

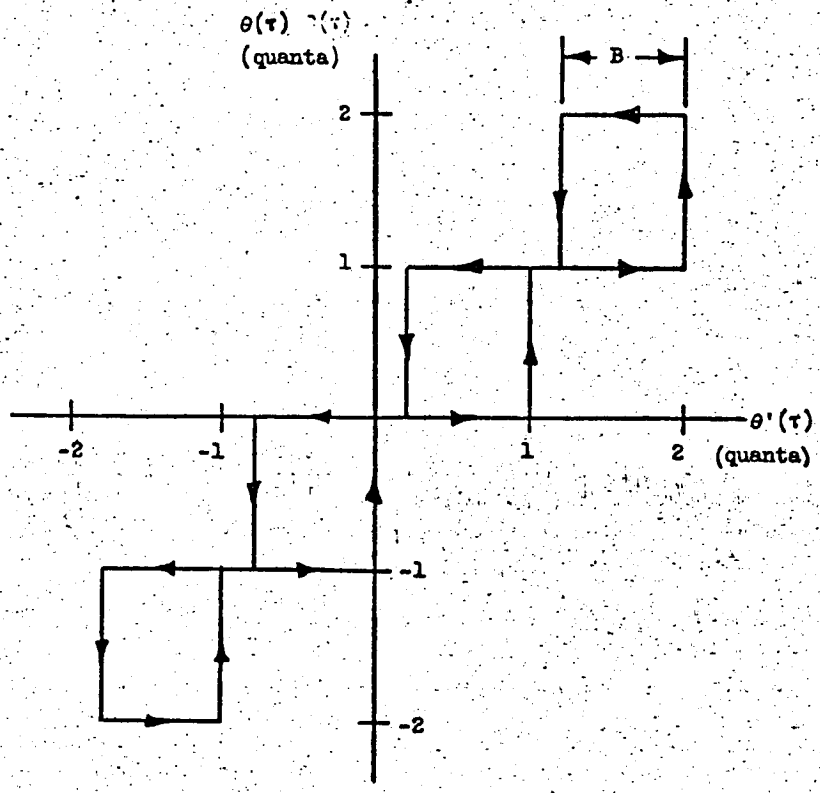

Figure 6. - Backlash description.

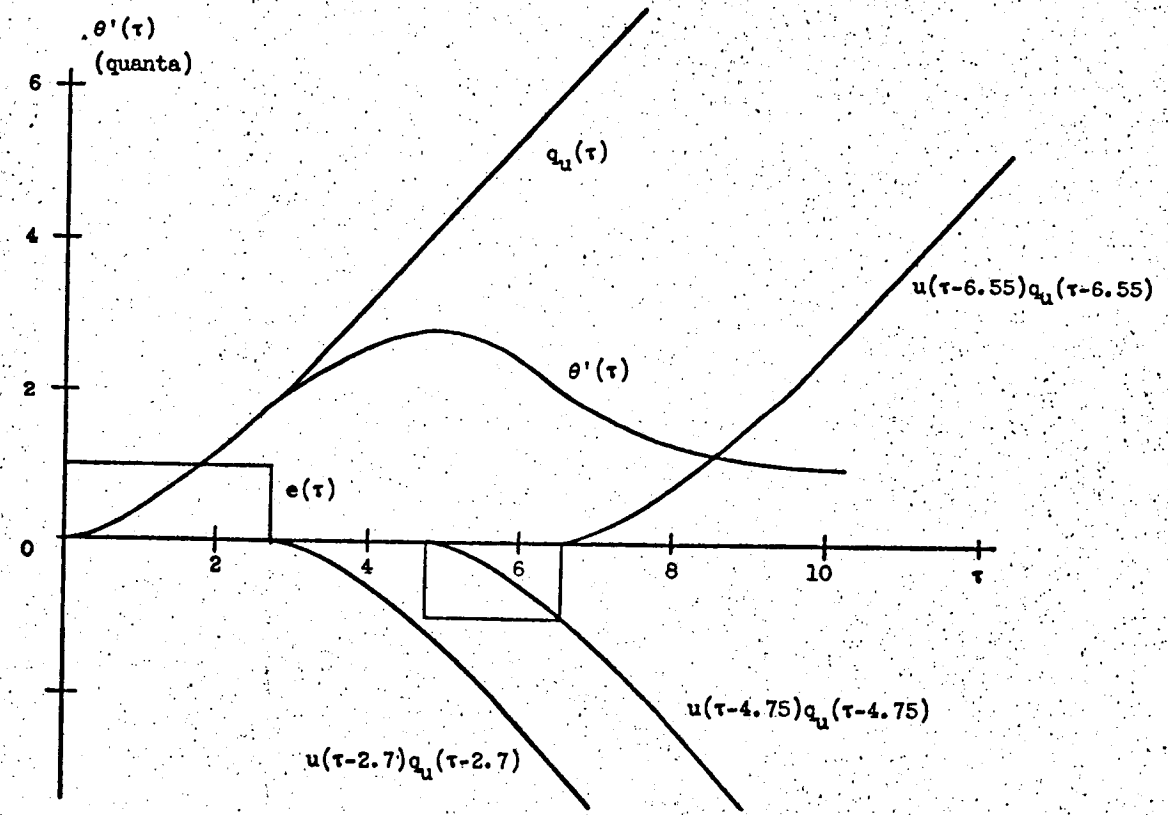

Figure 7. - Graphical construction of pulse-data system prime mover output.

determines $\theta'(\tau)$ which reverses at $\tau = 5$. Because of the backlash $\theta(\tau)$ does not reverse until $\theta'(\tau) = 2.05$. At $\theta'(\tau) = 2$ a feedback pulse $c(t) = \delta(t - 6.55)$ is produced by the quantizer which causes another unit step response $u(\tau - 6.55)q_u(\tau - 6.55)$. This process can be continued until the system comes to rest at $\tau = 10$. If another reference pulse occurred at any time the unit step response at that time could be plotted in the same way. $e(\tau)$ can be plotted as shown.

This example illustrated how the response of a pulse-data system with backlash can be analyzed. It also points out the fact that if the analysis is to extend over a very long time τ errors can develop. For example at $\tau = 8$ four ordinates are added algebraically to produce $\theta'(8)$. Three of these are greater than the value of $\theta'(8)$. This situation can lead to errors.

In all practical cases $q_u(\tau)$ will be a ramp function as discussed in chapter I. Thus an improvement in the method can be achieved.

It is more practical to decompose $q_u(\tau)$ into a delayed ramp and a transient correction. The ramps can then be combined to yield a straight line approximation to the response. The ordinates of the transient corrections are then added algebraically to obtain corrections to the approximate response. The exact response is obtained with much better accuracy by this method.

This modification is illustrated in figure 8. The example is the same as the one shown in figure 7, however the straight line approximation with corrections is used. The unit step response $q_u(t)$ is represented by a ramp $u(\tau - 1.1)1.1(\tau - 1.1)$ and a transient correction. When $\tau = 2.7$ the quanta point is passed. A transient correction is plotted starting at this time. At $\tau = 2.7 + 1.1$ the slope of the

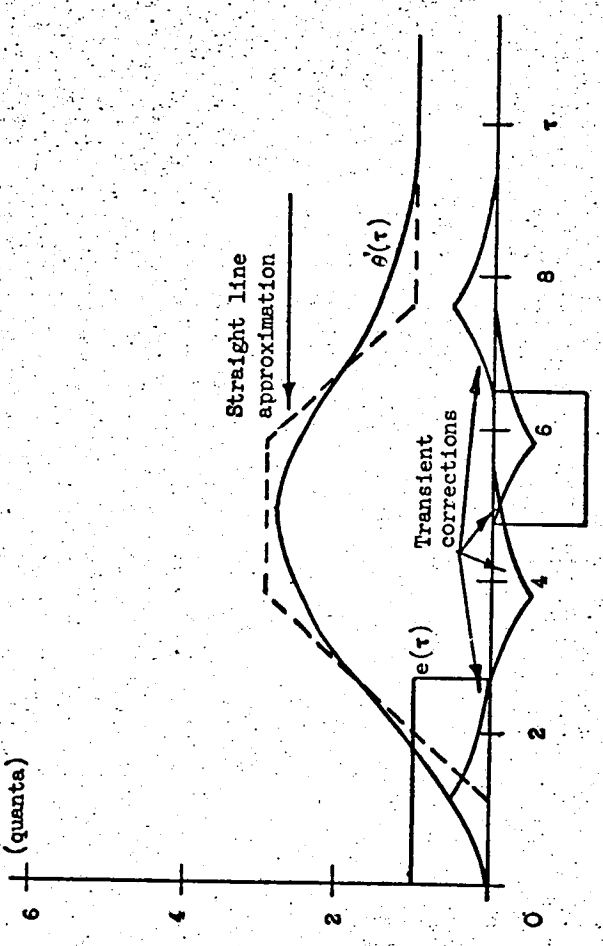

Figure 8. - Graphical construction using straight line approximation.

straight line approximation must be zero since the two ramp functions cancel. When $\tau = 4.75$ another feedback pulse occurs. A transient correction is started at this time. At $\tau = 4.75 + 1.1$ the straight line approximation slope becomes -1.1. Thus the slope of the straight line approximation is determined by the ramp function. The transient corrections determine the exact curve. This greatly reduces the magnitude of ordinates to be compared. In this way it improves the accuracy.

These methods lead to a method of much greater utility. The final method is based on the convolution integral.

The Laplace transform of a function $f(t)$ is:

$$f(s) = \int_0^\infty f(t)\, e^{-st}\, dt = \mathcal{L}[f(t)]$$

The transform of the controlled variable is:

$$\theta(s) = G(s)\, e(s)$$

Which multiplying and dividing by s yields:

$$\theta(s) = \left[\frac{G(s)}{s}\right] [s\, e(s)]$$

However:

$$\frac{G(s)}{s} = \mathcal{L}[q_u(t)] = \int_0^\infty q_u(x)\, e^{-sx}\, dx$$

Here x is a dummy variable.

Also:

$$s\, e(s) = \mathcal{L}[\dot{e}(t)] = \int_0^\infty \dot{e}(y)\, e^{-sy}\, dy$$

Where y is a dummy variable.

Then:

$$\theta(s) = \left[\frac{G(s)}{s}\right][s\, e(s)]$$

$$= \left[\int_0^\infty q_u(x)\, e^{-sx}\, dx\right]\left[\int_0^\infty \dot{e}(y)\, e^{-sy}\, dy\right]$$

$$= \int_0^\infty \int_0^\infty q_u(x)\, \dot{e}(y)\, e^{-s(x+y)}\, dx\, dy$$

Since each variable is a constant with respect to the other variable of integration the double integral and the integral product is the same.

Define new variables.

$$t = x + y$$

$$\tau = x$$

The element of area $dx\, dy$ can be related to $d\tau\, dt$ by the Jacobian.

$$dxdy = \left|\begin{vmatrix} \frac{\partial x}{\partial t} & \frac{\partial x}{\partial \tau} \\ \frac{\partial y}{\partial t} & \frac{\partial y}{\partial \tau} \end{vmatrix}\right| d\tau\, dt$$

$$x = \tau$$

$$y = t - \tau$$

Thus:

$$dxdy = |0 \cdot -1 - 1 \cdot 1|\, d\tau dt$$

$$= d\tau dt$$

The limits of integration also change. The definition for the Laplace transform only holds for $y \geq 0$, $x \geq 0$. Since $t = \tau + y$, τ cannot be greater than t. Thus:

$$\theta(s) = \int_0^\infty \left[\int_0^t q_u(\tau)\, \dot{e}(t - \tau)\, d\tau\right] e^{-st}\, dt$$

According to the definition of the Laplace transform:

$$\theta(t) = \int_0^t q_u(\tau)\, \dot{e}(t - \tau)\, d\tau$$

This relation is one form of the convolution integral.

In the case of a pulse-data system represented by the model in figure 4 $\dot{e}(t - \tau)$ has a very useful form.

$$\dot{e}(t) = \sum_{n=0}^{\infty} A_n \delta(t - T_{rn}) - \sum_{m=0}^{\infty} B_m \delta(t - T_{fm})$$

$$\dot{e}(t - \tau) = \sum_{n=0}^{\infty} A_n \delta(t - T_{rn} - \tau) - \sum_{m=0}^{\infty} B_m \delta(t - T_{fm} - \tau)$$

If τ is the independent variable this is a train of positive and negative unit impulses plotted with τ increasing negatively. The train is advanced in τ by an amount $t = \tau$.

The definition of a unit impulse is:

$$\int_0^t \delta(t - \tau_1)\, f(\tau)\, d\tau = f(\tau_1)$$

Thus:

$$\int_0^t q_u(\tau)\, A_n \delta(t - T_{rn} - \tau)\, d\tau$$

$$= A_n q_u(t - T_{rn})$$

To obtain $\theta(t)$ at $\tau = t$ the unit step response $q_u(\tau)$ is convolved with a train of positive and negative unit impulses. The train is reversed in time and shifted forward by $\tau = t$. $\theta(t)$ then becomes an algebraic sum:

$$\theta(t_1) = \int_0^{t_1} \dot{e}(t_1 - \tau)\, q_u(\tau)\, d\tau$$

$$= \int_0^{t_1} \left[\sum_{n=0}^{\infty} A_n \delta(t_1 - T_{rn} - \tau) - \sum_{m=0}^{\infty} B_m \delta(t_1 - T_{fm} - \tau) \right] q_u(\tau)\, d\tau$$

To obtain better accuracy $q_u(\tau)$ may be decomposed into a transient $q_{ut}(\tau)$ and a straight line portion $q_{uss}(\tau)$.

$$q_u(\tau) = q_{uss}(\tau) + q_{ut}(\tau)$$

The graphical solution is carried out as follows:

(1) $q_{uss}(\tau)$ and $q_{ut}(\tau)$ are plotted.

(2) A strip of paper is located parallel to the τ axis. $\tau = 0$ is marked. At $\tau = T_{r0}$ the $\tau = 0$ mark is lined up with $\tau = T_{r0}$ and a second mark is made on the strip opposite the $\tau = 0$ point on the τ axis. The mark is noted as + or - depending on whether A_0 is plus or minus. The input pulse at $\tau = T_{r0}$ initiates a ramp $u(t - T_{r0})q_{uss}(t - T_{r0})$. This is the straight-line approximation. Throughout this analysis this straight-line approximation is used just as was done in the example shown in figure 8.

(3) The value of $\theta(t_1)$ is determined by moving the strip to $\tau = t_1$. The ordinate of $q_{ut}(\tau)$ above the mark located on the strip opposite $\tau = t_1 - T_{r0}$ is the correction term applied to the straight line approximation. The sign adjacent to the mark on the strip determines whether the correction is positive or negative.

(4) When $\theta(t)$ equals the value at a quanta point $t = T_{f0}$ a mark is made on the strip opposite $\tau = 0$. The sign is determined by B_m where:

$$B_m = + \frac{\dot{\theta}(T_{f0})}{|\theta(T_{f0})|}$$

The straight-line approximation slope is changed to account for the $u(t - T_{f0})\, q_{uss}(t - T_{f0})$ ramp.

(5) The process is continued. The strip has a series of marks with

+ or - adjacent to each. At any $t = t_i$ the $\tau = 0$ mark on the strip is lined up with the $\tau = t_i$ abscissa on the $\theta(\tau)$ and $q_u(\tau)$ vs τ plot. The ordinates $q_{ut}(\tau)$ above each mark are added algebraically to obtain the corrections to the straight line approximation.

Thus the straight line approximation is obtained in a step-by-step manner with the convolution integral method supplying the corrections to form the exact solution. If desired, only the values of $\theta(\tau)$ near quanta points need to be determined. The values for B_m and T_{fm} may be determined quickly by this method. $q_{uss}(\tau)$ and $q_{ut}(\tau)$ are plotted only once reducing the labor considerably.

The following example illustrates the method:

$$G(s) = \frac{K_v T}{s(s^2 + 2\zeta s + 1)}$$

Note: Any $G(s) = \frac{K_v}{s(T^2 s^2 + 2\zeta T s + 1)}$ can be reduced to this form by letting $T\tau = t$. Let $K_v T = 0.5$. $\zeta = 0.3$.

$$q_u(\tau) = K_v T \left[\tau - 2\zeta + \frac{e^{-\zeta\tau}}{\sqrt{1 - \zeta^2}} \sin\left(\sqrt{1 - \zeta^2}\tau + \varphi\right) \right]$$

Where:

$$\varphi = \tan^{-1} \frac{2\zeta\sqrt{1 - \zeta^2}}{2\zeta^2 - 1}$$

or

$$q_u(\tau) = 0.5[\tau - 0.6 + 1.05e^{-0.3\tau} \sin(0.955\,\tau + 2.529)]$$

This is plotted in figure 9. Also $q_{uss}(\tau)$ and $q_{ut}(\tau)$ are plotted.

The controlled variable $\theta(t)$ is measured from the initial position. The initial position is assumed to be one quanta away from the next quanta point, $b = 1$. At $t = 0$ a reference pulse is received with

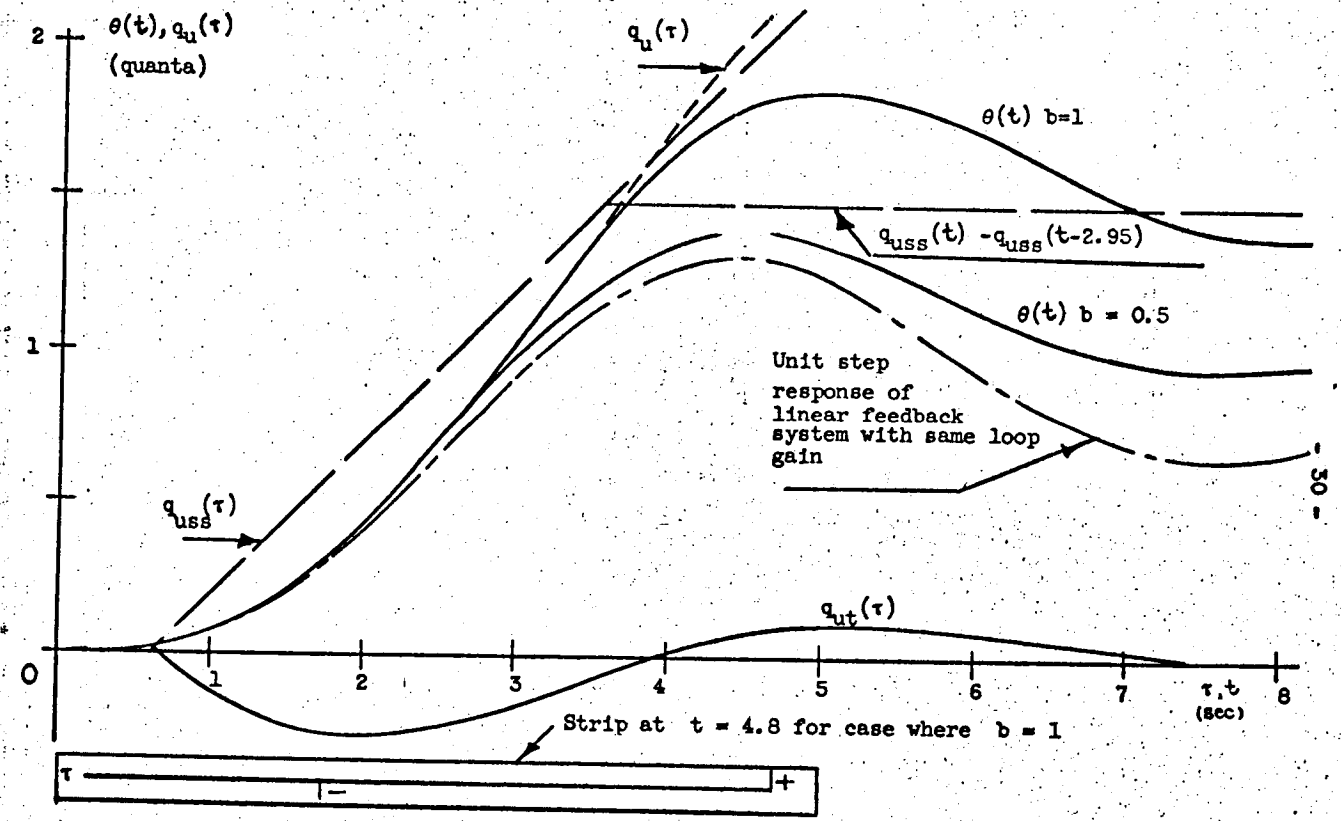

Figure 9. - Graphical method using convolution integral $K_v T = 0.5$.

$A_0 = +1$. A mark is made on the paper strip with a plus sign adjacent to it. At $t = 0.6$, $q_{uss}(\tau)$ starts. The corrections to this path are determined by adding $q_{ut}(t_i)$ to $q_{uss}(t_i)$ when the mark on the strip is opposite $\tau = t_i$ on the abscissa of the plot. When $t = 2.95$ a quanta point is passed. The straight line approximation is now $q_{uss}(t) - q_{uss}(t - 2.95)$. A mark is made on the strip opposite $\tau = 0$ when the original mark is opposite $\tau = 2.95$. A minus sign is placed adjacent to the mark since

$$-B_m = -\frac{\dot{\theta}(2.95)}{|\dot{\theta}(2.95)|} = -1$$

The process is continued. The method of determining $\theta(t)$ is shown for a typical point at $t = 4.8$. The strip is aligned so that the first mark representing the input pulse is opposite $\tau = 4.8$. The straight-line approximation to $\theta(4.8)$ is 1.48. The correction due to $q_{ut}(4.8)$ is +0.09. The correction due to the feedback pulse is $q_{ut}(1.75)$ whose value is $(-1)(-0.26) = +0.26$. Thus $\theta(4.8) = 1.48 + 0.09 + 0.26 = 1.83$.

The resulting response shows the overtravel characteristic of a pulse-data system. The final position is 1.45 quanta from the initial position. The response is also shown for an initial starting position of $b = 0.5$ quanta from a quanta point. The final position for this starting point is 1.06 quanta from the starting point. It is of interest to note that the maximum overtravel of $\theta(t)$ is greater when $b = 0.5$ than it is when $b = 1$. This will be explored later. The response of a linear system with the same $G(s)$ and unity feedback is also shown for an input step of one quanta. The overshoot is similar but the settling time is longer.

This method of obtaining the response $\theta(t)$ to an input $r(t)$ is quite useful in analyzing the response of a pulse-data system. It will be used throughout this thesis in the analysis. It is not confined to second order systems. It can also be used to determine response in the presence of backlash as was illustrated in figure 7.

The method could also probably be programed on a digital computer to yield results with less computational effort on the part of the investigator.

Steady State Analysis

When a pulse-data system is used to direct the controlled variable over a desired path the path is often described by straight line segments. The desired path is then transcribed into a reference input $r(t)$ of the form:

$$r(t) = \sum_{n=0}^{J} A_0\delta(t - nT_{r0}) + \sum_{n=K+1}^{L} A_1\delta(t - nT_{r1}) + \cdots$$

A_0, A_1, . . . determine the desired direction of $\theta(t)$. J, L, . . . determine the length of the straight line segments. T_{r0}, T_{r1}, . . . specify the desired rate of $\theta(t)$. Each of these series of pulses is equivalent to a ramp input to a continuous control. Since this type of input is often applied to a pulse data system it is of interest to examine the system response to this type of input.

The transfer function of the prime mover is assumed to be of the form:

$$G(s) = \frac{K_v G'(s)}{s} \quad \text{where} \quad G'(0) = 1$$

The pulse-data system is incapable of maintaining $\dot{\theta}(t) = 1/T_r$ except under certain circumstances. When $r(t) = \sum_{n=0}^{K} A\,\delta(t - nT_r)$

and the system is in the steady state $e(t)$ has the form shown in figure 10. Under these conditions $e(t)$ is periodic with period T_r. It has the magnitude of $a + 1$ quanta for $\Delta\tau$ of every period and equals a quanta the remainder of the period. a is the minimum number of quanta velocity error in the steady state. Unless $\Delta\tau$ is zero $\dot{\theta}(t) \neq 1/T_r$.

In the steady state $\theta(t)$ must change by one quanta during the time between reference pulses. If it does not then a correction will take place until it does. Thus:

$$\int_0^{T_r} \dot{\theta}_{ss}(t)\, dt = 1$$

Where $\dot{\theta}_{ss}(t)$ is the velocity of the controlled variable during one period of $e(t)$ in the steady state. This relation will be used to determine $\Delta\tau$ in a rigorous manner. For the present a much less rigorous approach will be used to illustrate important aspects of the steady state response.

In the steady state:

$$\dot{\theta}_{\text{average over one period}} = 1/T_r$$

$$= K_v e_{\text{average}}$$

$$e_{\text{average}} = a + \frac{\Delta\tau}{T_r}$$

Thus:

$$\frac{1}{T_r} = K_v \left[a + \frac{\Delta\tau}{T_r} \right]$$

or

$$\Delta\tau = \frac{1}{K_v} - aT_r$$

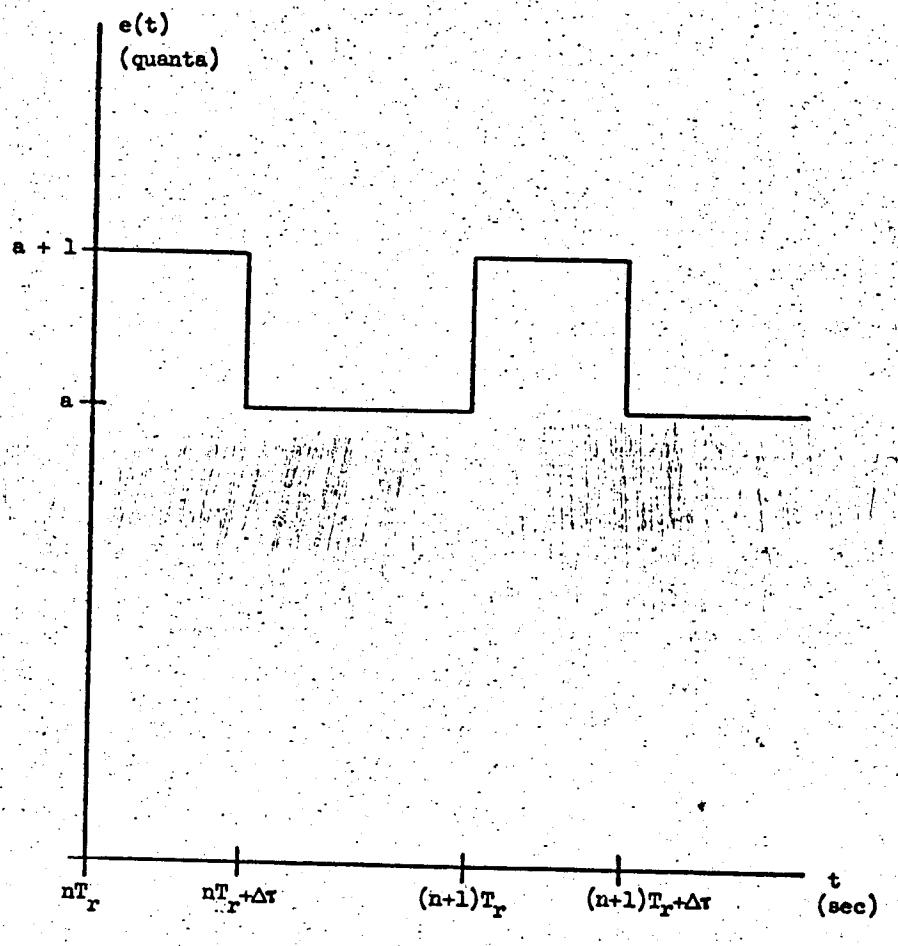

Figure 10. - Steady state output of digital to analog converter.

Note that for $a = 0$, $\Delta\tau$ is independent of T_r. This is illustrated in figure 11 for $G(s) = 1/s(s+.9)$ at three input rates. The system starts at rest when $r(t)$ is applied.

$$r(t) = \sum_{n=0}^{\infty} \delta(t - nT_r)$$

In all cases $\Delta\tau$ approaches 0.9 in the steady state. At the lower rates it takes longer to reach the steady state.

The steady state response $\theta(t)$ can be evaluated by determining the response of the prime mover to an input $e(t)$ of the form shown in figure 10. This is simply the response of $G(s)$ to a periodic input plus a fixed input. This can be accomplished in many ways:

(1) The Fourier series representation of $e(t)$ can be evaluated. $\theta(t)$ can then be specified as a Fourier series.

(2) Steady state operational calculus can be applied to obtain the steady state solution for $\theta(t)$ over one period.

(3) The pulse-data system can be represented by an open loop sampled-data model. Then $e(t)$ would be represented by a constant plus the output of a sampler and zero order hold circuit. The hold time would be $\Delta\tau$. The input to the sampler would be unity. Advanced z transforms could then be used to evaluate $\theta(t)$. z transform sampled data system analysis is described by Ragazzini[5].

(4) The sampled-data model described in (3) could be considered an open loop sampled-data system with finite pulse width $\Delta\tau$. Farmanfarma[6] presents a group of transforms which can be used to evaluate $\theta(t)$.

The most useful of these four methods is the second one. This will be the method used in this thesis to describe the steady state behavior of a pulse-data system.

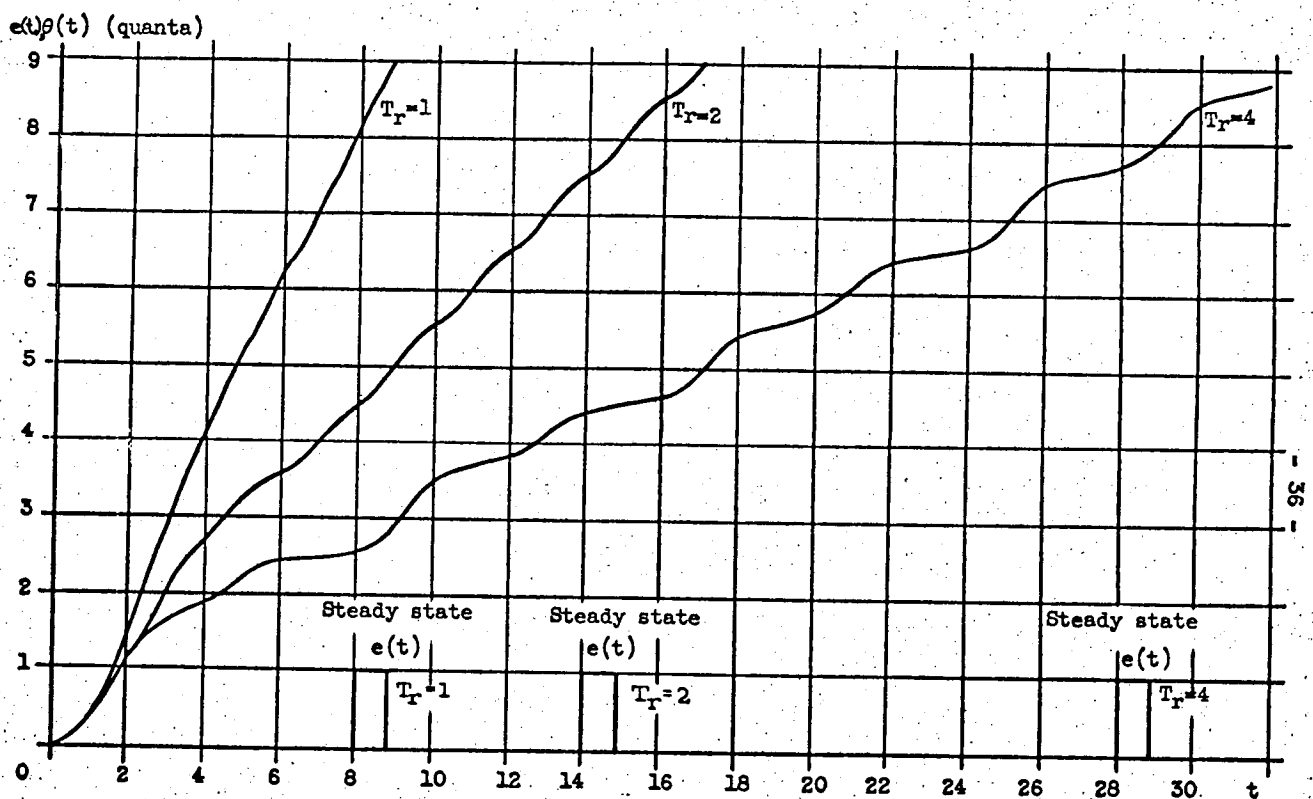

Figure 11. - Pulse-data system ramp response $G(s) = \frac{1}{s(s+0.9)}$.

Steady State Operational Calculus

Waidelich[7] developed a method of determining the steady state response of a linear system to a periodic input. This method was applied by Hinde[8] to a pulse data system with:

$$G(s) = \frac{K_v}{s(Ts + 1)}$$

The method is also described by Truxal[2] and Seshu[9]. A rigorous proof is developed in Seshu.

The method is performed as follows:

(1) The transient response of the system to a periodic input is determined.

(2) The total response during the first period of a periodic input is determined.

(3) The total response for the first period minus the transient response is the steady state response over any period.

This is applied to a pulse-data system in the following way:

$$e(t) = a + \sum_{n=0}^{\infty} [u(t - nT_r) - u(t - nT_r - \Delta\tau)]$$

Describes $e(t)$ in the steady state as shown in figure 10. It is useful to normalize the time variable by letting:

$$T\tau = t$$

Where T is the major time constant of $G(s)$.

$$e(\tau) = a + \sum_{n=0}^{\infty} \left[u\left(\tau - \frac{nT_r}{T}\right) - u\left(\tau - \frac{nT_r}{T} - \frac{\Delta\tau}{T}\right)\right]$$

Let:

$$\frac{T_r}{T} = \beta \quad \text{and} \quad \frac{\Delta\tau}{T} = \alpha$$

Then take the Laplace transform of $e(\tau)$.

$$e(s) = \frac{a}{s} + \sum_{n=0}^{\infty} \frac{e^{-n\beta s}(1 - e^{-\alpha s})}{s}$$

$$\sum_{n=0}^{\infty} e^{-n\beta s} = \frac{1}{1 - e^{-\beta s}}$$

since,

$$(1 - x)^{-1} = 1 + x + x^2 + x^3 + \cdots$$

Thus:

$$e(s) = \frac{a}{s} + \frac{(1 - e^{-\alpha s})}{s(1 - e^{-\beta s})}$$

As an example let:

$$G(s) = \frac{K_v T}{s(s + 1)}$$

Then:

$$\theta(s) = \frac{K_v T\, e(s)}{s(s + 1)}$$

The transient response $\theta_t(\tau)$ can be determined by evaluating the inverse Laplace transform.

$$\theta(t) = \frac{1}{2\pi j} \int_{c-j\infty}^{c+j\infty} \theta(s)\, e^{st}\, ds$$

This can be evaluated as a contour integral in the complex plane.

$$\theta(t) = \sum \begin{matrix}\text{residues of } \theta(s)\, e^{st} \\ \text{at poles of } \theta(s)\end{matrix}$$

$$= \sum \begin{matrix}\text{residues of } \theta(s)\, e^{st} \\ \text{at poles of } G(s)\end{matrix} + \sum \begin{matrix}\text{residues of } \theta(s)\, e^{st} \\ \text{at poles of } e(s)\end{matrix}$$

The residues of $\theta(s)\, e^{st}$ at poles of $G(s)$ yield the transient part $\theta_t(t)$. The second term will yield a Fourier series of the steady state part $\theta_{ss}(t)$. However $e(s)$ and $G(s)$ cannot have any poles in common or the method does not work.

In all of the examples considered here $G(s) = K_v G'(s)/s$ where $G'(0) = 1$. This always has a pole in common with $e(s)$. This pole at $s = 0$ can be eliminated by examining $\dot{\theta}(\tau)$. In the present example the Laplace transform of $\dot{\theta}(t)$ can be formed.

$$\int_0^\infty \dot{\theta}(\tau)\, e^{-s\tau}\, d\tau = \frac{K_v T e(s)}{s+1} + \frac{\dot{\theta}(0^+)}{s+1}$$

$$= \frac{K_v T}{s+1}\left[\frac{a}{s} + \frac{(1 - e^{-\alpha s})}{s(1 - e^{-\beta s})}\right] + \frac{\dot{\theta}(0^+)}{s+1}$$

$$\dot{\theta}_t(\tau) = \sum_{\substack{\text{residues} \\ \text{pole: at} \\ s = -1}} \mathcal{L}[\dot{\theta}(\tau)]\, e^{s\tau}$$

$$= -K_v T\left[a e^{-\tau} + \frac{(1 - e^{\alpha})}{(1 - e^{\beta})} e^{-\tau}\right] + \dot{\theta}(0^+) e^{-\tau}$$

The total response over the first period is now determined.

$$e(s) = \frac{a + 1 - e^{-\alpha s}}{s} \quad \text{for} \quad 0 < \tau < \beta$$

Thus:

$$\mathcal{L}[\dot{\theta}(\tau)] = \frac{K_v T}{s+1}\left[\frac{a + 1 - e^{-\alpha s}}{s}\right] + \frac{\dot{\theta}(0^+)}{s+1}$$

$$\dot{\theta}(\tau) = \sum_{\substack{\text{residues} \\ \text{poles of} \\ e(s)G(s)}} \mathcal{L}[\dot{\theta}(\tau)]\, e^{st}$$

$$= K_v T\,[(a + 1)(1 - e^{-\tau}) + u(\tau - \alpha)(e^{-(\tau-\alpha)} - 1)] + \dot{\theta}(0^+)\, e^{-\tau}$$

$$\text{for} \quad 0 < \tau < \beta$$

The steady state response over one period is then the difference.

$$\dot{\theta}_{ss}(\tau) = K_v T\,[(a + 1)(1 - e^{-\tau}) + u(\tau - \alpha)(e^{-(\tau-\alpha)} - 1)] + \dot{\theta}(0^+)\, e^{-\tau}$$

$$- \left\{-K_v T\left[a e^{-\tau} + \frac{(1 - e^{\alpha})}{(1 - e^{\beta})} e^{-\tau}\right] + \dot{\theta}(0^+)\, e^{-\tau}\right\}$$

$$= K_v T\left[a + 1 - e^{-\tau} + \left(\frac{1 - e^{\alpha}}{1 - e^{\beta}}\right) e^{-\tau} + u(\tau - \alpha)(e^{-(\tau-\alpha)} - 1)\right]$$

Where $\tau = 0$ at the time when a reference pulse $\delta(t - nT_r)$ occurs. Then this solution is valid for $0 < \tau < \beta$.

$\Delta\tau$ may be evaluated by making use of the fact that the controlled variables changes by one quanta between reference pulses. Thus:

$$\int_0^\beta \dot{\theta}_{ss}(\tau)\, d\tau = K_v T \int_0^\beta \left[a + 1 - e^{-\tau} + \left(\frac{1 - e^{\alpha}}{1 - e^{\beta}} \right) e^{-\tau} \right] d\tau$$

$$+ K_v T \int_\alpha^\beta \left(e^{-(\tau - \alpha)} - 1 \right) d\tau$$

$$= K_v T \left[(a + 1)\,\beta + e^{-\beta} - 1 - \left(\frac{1 - e^{\alpha}}{1 - e^{\beta}} \right)(e^{-\beta} - 1) \right.$$

$$\left. - e^{\alpha - \beta} + 1 - \beta + \alpha \right]$$

$$= K_v T \left[a\beta + \alpha \right]$$

but,

$$\int_0^\beta \dot{\theta}_{ss}(\tau)\, d\tau = 1$$

Thus:

$$\alpha = \frac{1}{K_v T} - a\beta$$

or,

$$\Delta\tau = \frac{1}{K_v} - aT_r$$

As was shown before.

Graphical Steady State Analysis

The time domain solution which employs the convolution integral can also be applied to obtain information about the steady state response. Once T_r and $G(s)$ are determined $\Delta\tau$ may be determined by the methods of steady state operational calculus or by the graphical time domain solution. The form of $e(t)$ is then specified. $\dot{\theta}_{ss}(t)$ can then be determined by the following procedure:

1. Plot $q(t)$, the impulse response of $G(s)$. This is the velocity response to a step input.

2. The convolution integral then can be used to determine $\dot{\theta}(t)$.

$$\dot{\theta}(t_i) = \int_0^{t_i} \dot{e}(t_i - \tau)\, q(\tau)\, d\tau$$

3. The form of $\dot{e}(t_i - \tau)$ in the steady state is a periodic series of unit impulses. This series of impulses is marked on a strip of paper with τ as the dependent variable.

4. The strip is moved along the t axis of the $q(t)$ plot until the ordinate of $q(t)$ opposite the $\tau = 0$ point on the strip is in the steady state.

5. The method then proceeds just as in the case of the time domain transient solution. Except the strip now has the marks already on it. The value of $\dot{\theta}_{ss}(t)$ at any time is the algebraic sum of the ordinates of $q(t)$ above the marks on the strip.

The values of $\dot{\theta}_{ss}(t)$ over one period of T_r may be determined very quickly by this method. The method is applied to determine theoretical values for I in appendix I. Thus $\dot{\theta}_{ss}(t)$ can be used to determine the steady state ripple for a given value of K_vT and T_r.

Synthesis Methods

It is desirable to have some criterion by which the system gain or some other system parameter can be specified.

In a linear system the Root Locus, the Nyquist or the Bode methods can be employed. In general the specification of stability criterion for a nonlinear system are not nearly as easy to systematize.

For inputs which cause the pulse-data system errors to be large the quantized and discontinous nature of $e(t)$ would appear to be less important. Thus it might be reasonable to replace the system model with one which had the same transfer function with unity feedback for large errors. One way to determine if this is possible is to apply the describing function method.

Describing Function

A new model of the system is developed in figure 12 from the model shown in figure 4. A new input $r'(t)$ is defined as the desired output. This is quantized to produce $r(t)$. The integration block may then be moved beyond the summing point. This is done by replacing it with two integrating blocks. One on each of the inputs to the summing point (fig. 12(a)). A describing function will be developed for the Quantizer and integrator combined. This will yield an equivalent gain K_Q which is dependent on the amplitude of the input to the Quantizer. This is shown in figure 12(b). This model could then be used for stability investigations using the describing function. A further refinement is shown in figure 12(c) where the K_Q block is moved back through the summing point. In this model the gain K_Q can be related to the error.

The gain K_Q is determined by applying a sine wave to the Quantizer input. The output of the Quantizer is integrated. The first harmonic of the integrator output is compared with the Quantizer input. The ratio of the output amplitude to the input amplitude is K_Q.

The Quantizer and integrator input-output relation is shown in figure 13. For a sine wave input to the Quantizer the output may be

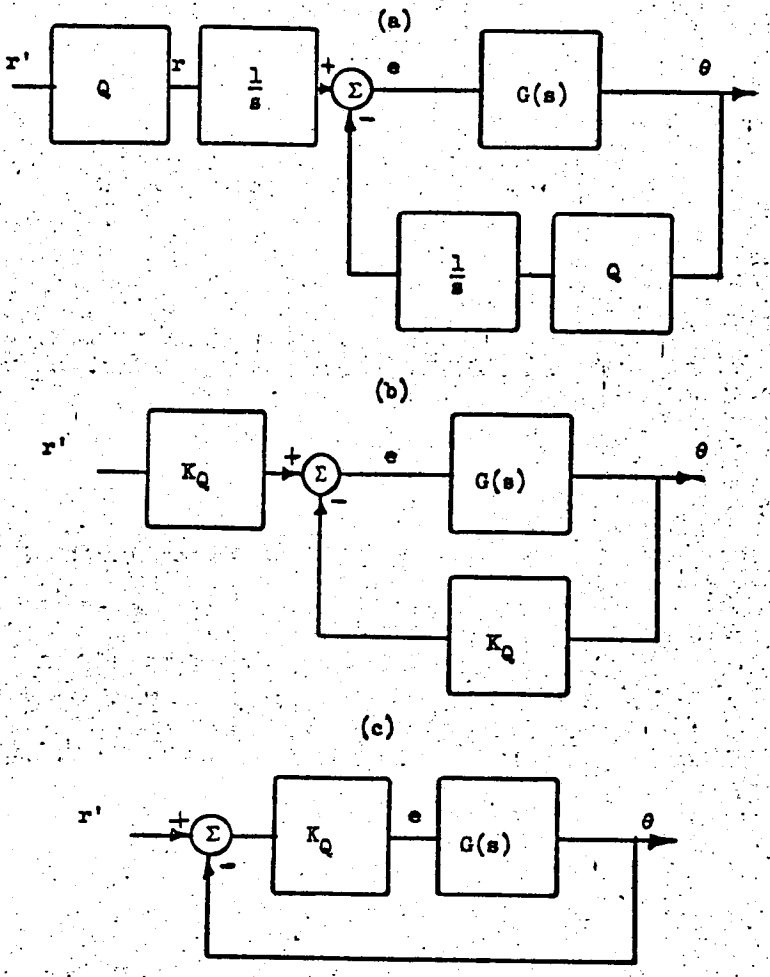

Figure 12. - Describing function model.

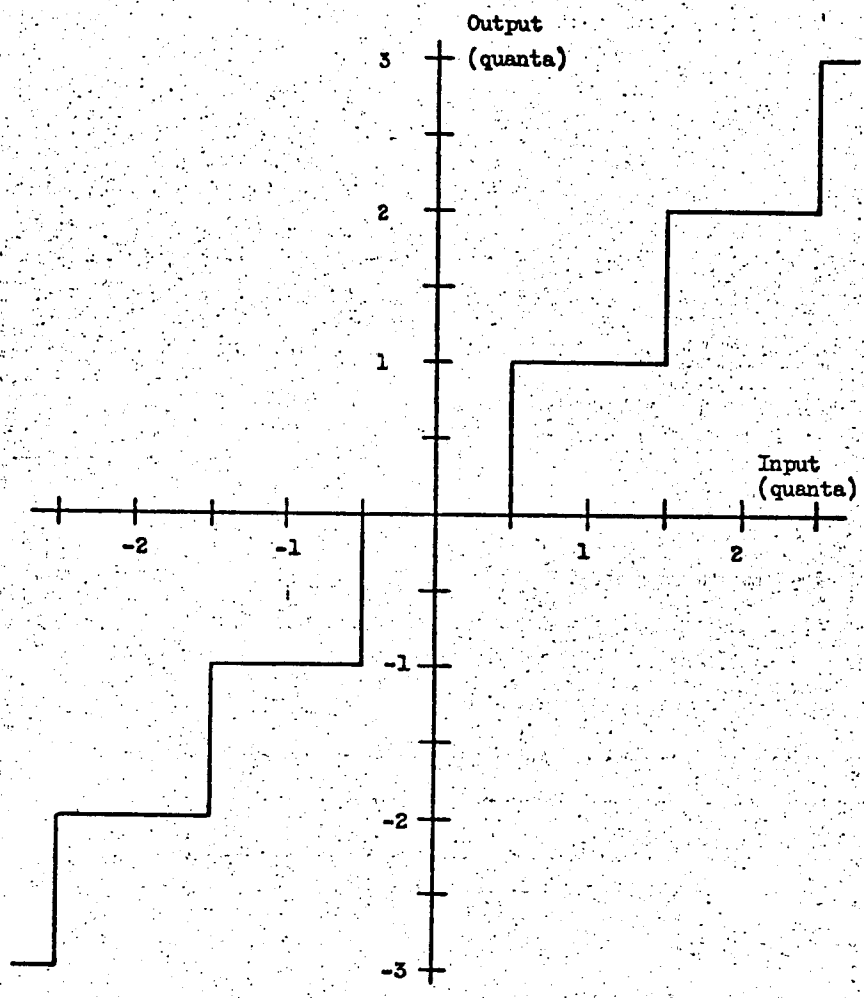

Figure 13. - Quantizer input-output relation.

expressed as a Fourier series.

$$f(t) = \sum_{n=1}^{\infty} a_n \cos n\,\omega t + b_n \sin n\,\omega t + \frac{a_0}{2}$$

Where:

$$\frac{a_0}{2} = \frac{1}{2\pi}\int_{-\pi}^{\pi} f(\omega t)\, d\omega t$$

$$a_n = \frac{1}{\pi}\int_{-\pi}^{\pi} f(\omega t) \cos n\,\omega t\, d\omega t$$

$$b_n = \frac{1}{\pi}\int_{-\pi}^{\pi} f(\omega t) \sin n\,\omega t\, d\omega t$$

The output of the integrator for a Quantizer sine wave input of two quanta amplitude is shown in figure 14.

$$a_n = 0 = a_0$$

Since the integrator output is an odd function this integral will vanish.

$$b_n = \frac{1}{\pi}\left\{-\int_{-\pi+\theta_1}^{-\pi+\theta_2} \sin n\,\omega t\, d\omega t - \int_{-\pi+\theta_2}^{-\theta_2} 2\sin n\,\omega t\, d\omega t - \int_{-\theta_2}^{-\theta_1} \sin n\,\omega t\, d\omega t \right.$$
$$\left. + \int_{\theta_1}^{\theta_2} \sin n\,\omega t\, d\omega t + \int_{\theta_2}^{\pi-\theta_2} 2\sin n\,\omega t\, d\omega t + \int_{\pi-\theta_2}^{\pi-\theta_1} \sin n\,\omega t\, d\omega t \right.$$

$n = 1$ for the first harmonic thus:

$$b_1(2) = \frac{4}{\pi}\left[\cos\theta_1 + \cos\theta_2\right]$$

Where:

$$A \sin\theta_1 = 0.5 \qquad A = 2$$

Thus:

$$\theta_1 = 14.5^\circ$$

$$A \sin\theta_2 = 1.5$$

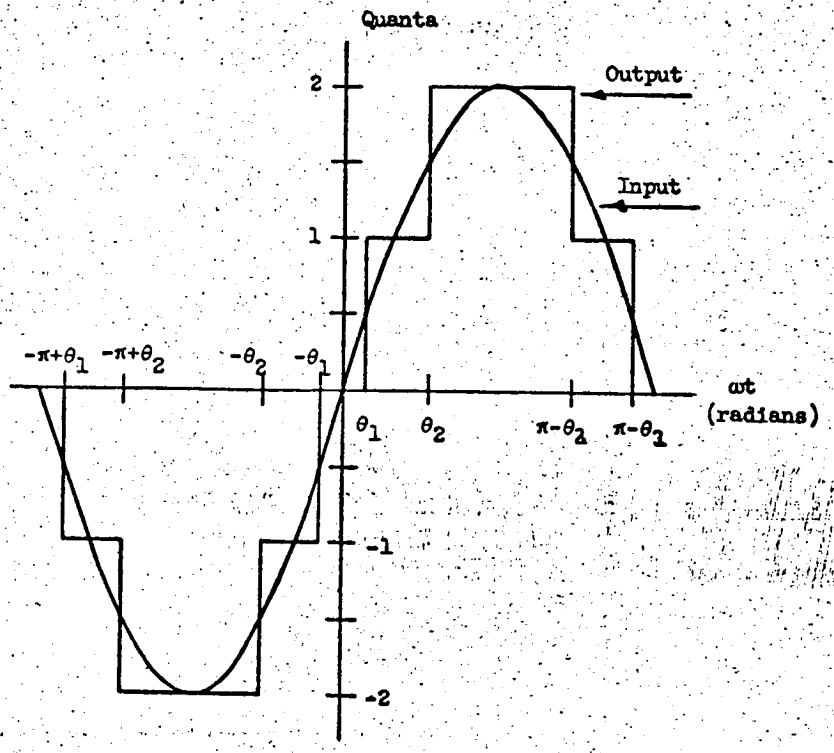

Figure 14. - Quantizer output for an input of 2 sin ωt.

$$\theta_2 = 48.5^\circ$$

$$b_1(2) = 2.08$$

In this way b_1 can be determined for several input amplitudes A. The value of K_Q is then determined by the relation:

$$K_Q = \frac{b_1(A)}{A}$$

The resulting relation between K_Q and A is shown in figure 15. K_Q varies from 0 to 1.275. The highest gain occurs for a sine wave input of amplitude 0.7 quanta. As the input amplitude increases the effective gain K_Q oscillates about the value one with decreasing amplitude. For inputs of amplitude less than 0.5 quanta the gain is zero. In this region it behaves as an open loop system.

This result seems to substantiate the claim that the pulse-data system approaches a continuous system when its error is large. In figure 12(c) the loop transfer function approaches G(s) for large errors.

The describing function could now be used to approximate the system gain for stable operation at all input amplitudes. If G(s) is the open loop transfer function and $K_Q(e)$ is the describing function (there is no phase change with amplitude) then the closed loop transfer function is:

$$\frac{G(s)}{\frac{1}{K_Q(e)} + G(s)}$$

This is stable if the denominator has no zeros with positive real parts. The Nyquist diagram serves to investigate this by plotting the locus of the $G(j\omega)$ vector in the complex plane as $-\infty < \omega < \infty$. As

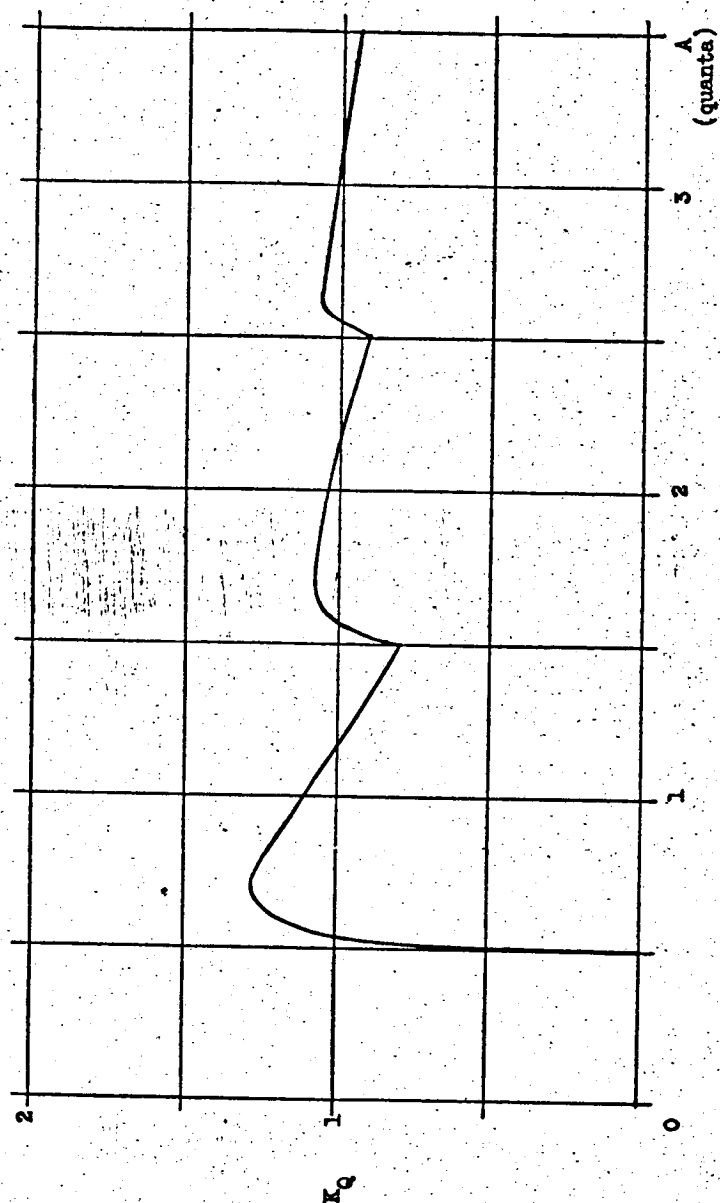

Figure 15. - Describing function for quantizer.

this locus is traveled when ω goes from $-\infty$ to $+\infty$ the $-\frac{1}{K_Q(e)}$ point must always lie on the left. In this case the critical point would be $1/1.275 = 0.784$ instead of 1.

The describing function, however, appears to be quite conservative. In figure 9 the response of a pulse-data system is shown. Where

$$G(s) = \frac{K_v T}{s(s^2 + 0.6s + 1)}$$

with continuous feedback this system would be unstable if $K_v T = 0.6$. Since Routh's criterion shows:

$$1 + G(s) = K_v T + s + 0.6s^2 + s^3$$

The Routh table is:

$$\begin{array}{cc} 1 & 1 \\ 0.6 & K_v T \\ 0.6 - K_v T & \end{array}$$

If $K_v T > 0.6$ the continuous system is unstable. Using the describing function the pulse-data system should be unstable for $K_v T > 0.47$. The response shown in figure 9 has $K_v T = 0.5$ and the error is certainly greater than 0.7 quanta. Thus it appears desirable to have a more accurate stability criterion.

Stability Criterion

The describing function indicates that stability of a pulse-data system is the most critical at small errors. The describing function is approximate, however. Its accuracy depends on how well the output of the quantizer and integrator can be represented by a sine wave. Also the bandwidth characteristics of $G(s)$ are important.

In order to develop a more accurate method of specifying a parameter of a pulse-data system the response to a single input pulse will be examined.

Figure 16 shows the two basic types of response to a single pulse. The initial value of the controlled variable is $b-1$ quanta from the next quanta point. An input pulse $r(\tau) = \delta(\tau)$ is received at $\tau = 0$. The controlled variable $\theta(\tau)$ will increase with time until the system passes a quanta point at $\theta(\tau) = 1$. This time is designated τ_1. At this time the value of $e(\tau)$ goes to zero. The controlled variable continues to increase but the velocity decreases. In one case the controlled variable overtravels less than one quanta beyond the quanta point. The response for an underdamped system in this case will reach a maximum value $\theta(\tau_m)$ at $\tau = \tau_m$. In the other case if $\theta(\tau_m) > 1 + b$ the system has overtraveled more than one quanta. $e(\tau)$ will become negative causing the system to take longer to settle down. In general b and $G(s)$ will determine if the system will overtravel by more than one quanta. A procedure for determining if a given pulse-data system will overtravel more than one quanta will now be developed. This will provide a way of specifying system response in the region where the pulse-data system is most nonlinear.

The prime mover block and its typical input and output during the response of a pulse-data system to a single input pulse is shown in figure 17. An input pulse is received at $\tau = 0$. This causes $e(\tau)$ to become one. At $\tau = \tau_1$ a quanta point is passed causing $e(\tau)$ to become zero. At τ_m the value of $\theta(\tau)$ is a maximum. Thus:

$$\theta(\tau) = q_u(\tau) - u(\tau - \tau_1)\, q_u(\tau - \tau_1)$$

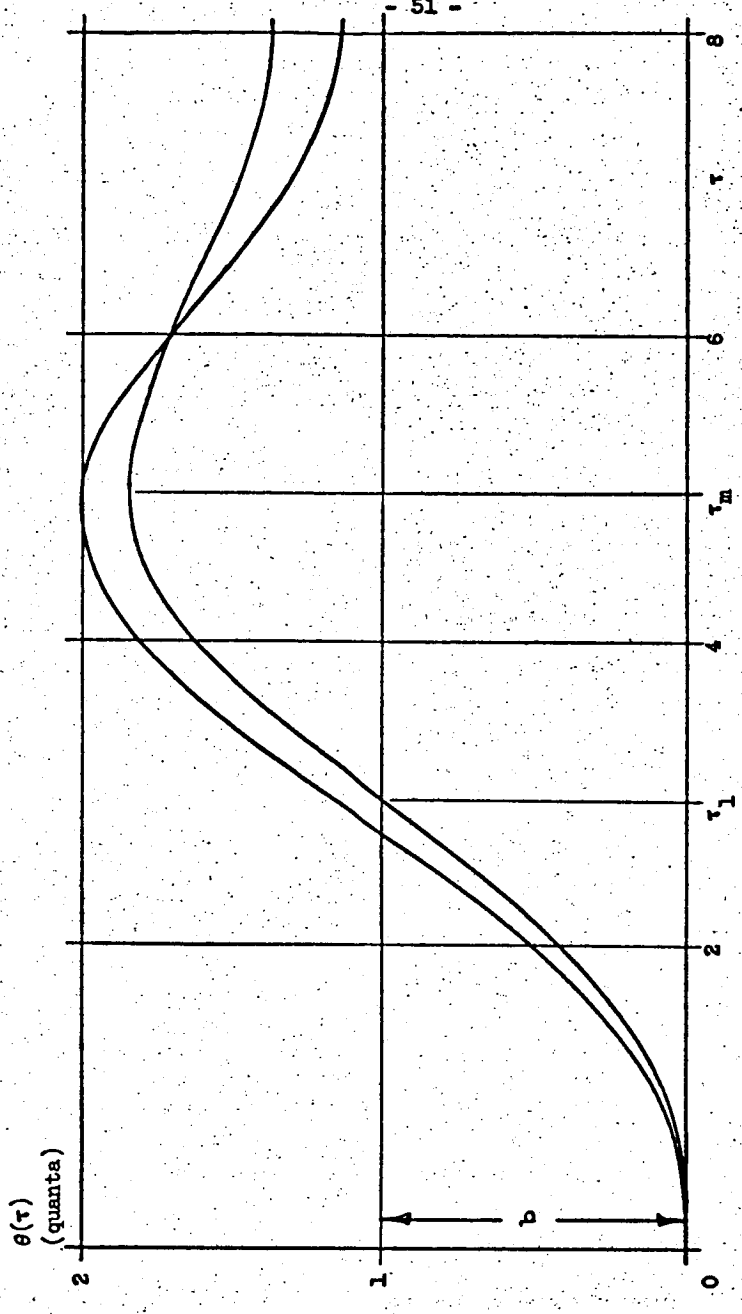

Figure 16. - Pulse-data system response.

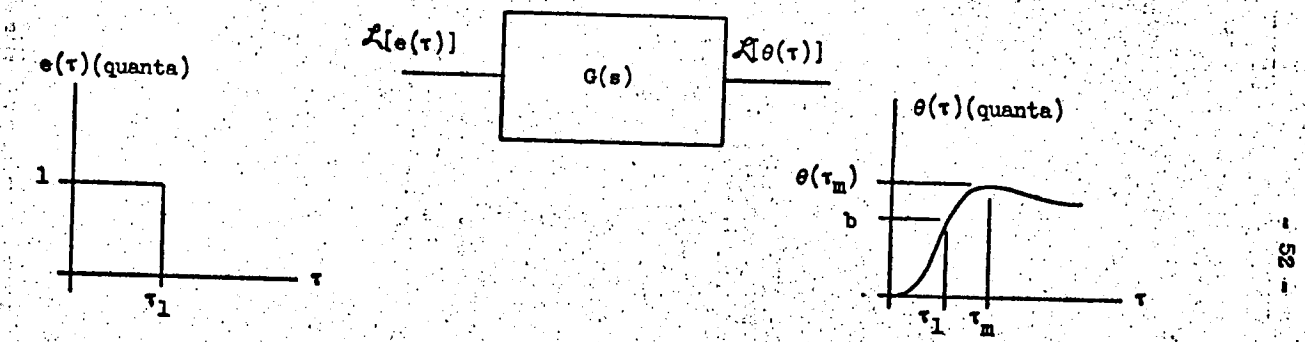

Figure 17. - Prime mover input and output for single pulse input.

The requirement for no overtravel is:

$$\theta(\tau)_{maximum} < b + 1$$

There are two cases which must now be considered.

Case I $\theta(\tau)$ exhibits no overshoot.

Case II $\theta(\tau)$ does overshoot.

Case I

In this case $G(s)$ has no complex poles. The final value of $\theta(\tau)$ is the maximum value.

$$\theta(\tau)_{maximum} = \lim_{\tau \to \infty} \theta(\tau)$$

The final value theorem of Laplace transform theory states:

$$\lim_{s \to 0} sF(s) = \lim_{\tau \to \infty} f(\tau)$$

In this case the Laplace transform of $\theta(\tau)$ is:

$$\theta(s) = \frac{G(s)(1 - e^{-\tau_1 s})}{s}$$

Thus:

$$\theta(\tau)_{max} = \lim_{s \to 0} \left[\frac{sG(s)(1 - e^{-\tau_1 s})}{s} \right]$$

For example if:

$$G(s) = \frac{K_v T}{s(s + 1)(T's + 1)}$$

where $K_v T$ is to be specified.

$$\theta(\tau)_{max} = \lim_{s \to 0} \left[\frac{K_v T(1 - e^{-\tau_1 s})}{s(s + 1)(T's + 1)} \right]$$

The numerator and denominator approach zero so that this is indeterminate. However, L' Hospital's rule can be applied.

$$\theta(\tau)_{max} = \lim_{s \to 0} \left[\frac{K_v T \frac{d}{ds} (1 - e^{-\tau_1 s})}{\frac{d}{ds} (T's^3 + (1 + T')s^2 + s)} \right]$$

$$= \lim_{s \to 0} \left[\frac{K_v T \tau_1 e^{-\tau_1 s}}{3T's^2 + 2(1 + T')s + 1} \right]$$

$$= K_v T \tau_1$$

In this case the overtravel criterion is:

$$K_v T \tau_1 \leq b + 1$$

Thus the method for overdamped systems is:

(1) Plot $q_u(\tau)$ for various values of the parameter which is to be specified.

(2) From this plot determine τ_1 with respect to b for the parameter values.

(3) Plot $\theta(\tau)$ maximum with respect to b for the parameter values. The limiting parameter value is that for which the $\theta(\tau)_{maximum}$ curve falls below the $b+1$ line at all points except one.

Case II

In this case the final value of $\theta(\tau)$ is not the maximum value. Let τ_m be the time at which $\theta(\tau)$ is a maximum. The maximum value occurs where the slope of $\theta(\tau)$ is zero. That is:

$$\frac{d}{dt} \theta(\tau) = 0 = \frac{d}{dt} [q_u(\tau) - u(\tau - \tau_1) q_u(\tau - \tau_1)]$$

or,

$$\frac{d}{dt} [q_u(\tau_m)] = \frac{d}{dt} [u(\tau_m - \tau_1) q_u(\tau_m - \tau_1)]$$

Let $q(\tau)$ be the impulse response of $G(s)$, then $\frac{d}{dt} [q_u(\tau)] = q(\tau)$.

Thus:

$$q(\tau_m) = u(\tau_m - \tau_1)\, q(\tau_m - \tau_1)$$

The value of τ_m may be obtained by plotting the impulse response $q(\tau)$. A second plot of $q(\tau)$ is delayed in time by τ_1. Then the time τ at which these two curves cross is τ_m. If there are several τ_{mi} where the two curves cross all of the values are noted. The desired τ_m is the one which causes $\theta(\tau_{mi})$ to be the largest. Once τ_m is found $\theta(\tau)$ maximum is determined. If $b + 1 > \theta(\tau_m)$ the pulse-data system will overtravel less than one quanta.

The method for underdamped systems is:

(1) Plot $q_u(\tau)$ for various values of the parameter which is to be specified.

(2) From this plot determine τ_1 with respect to b for the parameter values.

(3) Plot $q(\tau)$ twice. Delay one plot by τ_1 to determine τ_m the time at which the curves cross. Determine τ_m as a function of τ_1.

(4) Using $\theta(\tau)_{max} = q_u(\tau_m) - u(\tau_m - \tau_1)\, q_u(\tau_m - \tau_1)$ and the plots developed in (1), (2), and (3) plot $\theta(\tau_m)$ as a function of b.

(5) The curve of $\theta(\tau_m)$ less than the $b + 1$ line at all points except one determines the critical parameter value.

Note: If it is desired to vary the open loop gain K_vT alone an alternate step (4) is suggested. (4) (alternate) Plot $\theta(\tau_m)/K_vT$ as a function of τ_1. Then for various values of K_vT plot $\theta(\tau_m)$ as a function of b.

The method for underdamped systems is illustrated by the following example:

Let

$$G(s) = \frac{K_v T}{s(s^2 + 0.6s + 1)}$$

The critical value of $K_v T$ will be selected.

(1) Figure 18 shows $q_u(\tau)/K_v T$ as a function of τ.

(2) τ_1 as a function of b for various values of $K_v T$ is shown in figure 19. These are obtained by choosing a value of $K_v T$. This value specifies the ordinates in figure 18. Then the value of τ for which $q_u(\tau) = b$ is τ_1. For example if $K_v T = 0.5$ for $b = 0.8 = q_u(\tau)$, $\tau = 2.56$. In this way figure 19 is developed.

(3) Figure 20 shows $q(\tau)/K_v T$ and $q(\tau - \tau_1)/K_v T$ for $\tau_1 = 1$. The curves cross twice at $\tau_m = 3.8$ and 7.1 sec. $\theta(\tau)/K_v T$ is largest for $\tau_m = 3.8$ sec. This comparison of $q(\tau)$ and $q(\tau - \tau_1)u(\tau - \tau_1)$ is carried out for enough values of τ_1 to plot the τ_m versus τ_1 relation. The resulting τ_m versus τ_1 plot is shown in figure 21.

(4) Then given τ_1, τ_m is determined from figure 21. These two values may then be used in the relation:

$$\theta(\tau_m) = q_u(\tau_m) - u(\tau_m - \tau_1)\, q_u(\tau_m - \tau_1)$$

The values of $q_u(\tau_m)$ and $q_u(\tau_m - \tau_1)$ are determined from figure 18. For $\tau_1 = 1$ sec figure 21 yields $\tau_m = 3.8$ sec. Then figure 18 shows $\frac{q_u(3.8)}{K_v T} = 3.28$ quanta and $\frac{q_u(2.8)}{K_v T} = 1.93$ quanta. Thus:

$$\frac{\theta(3.28)}{K_v T} = 1.35 \text{ quanta for } \tau_1 = 1$$

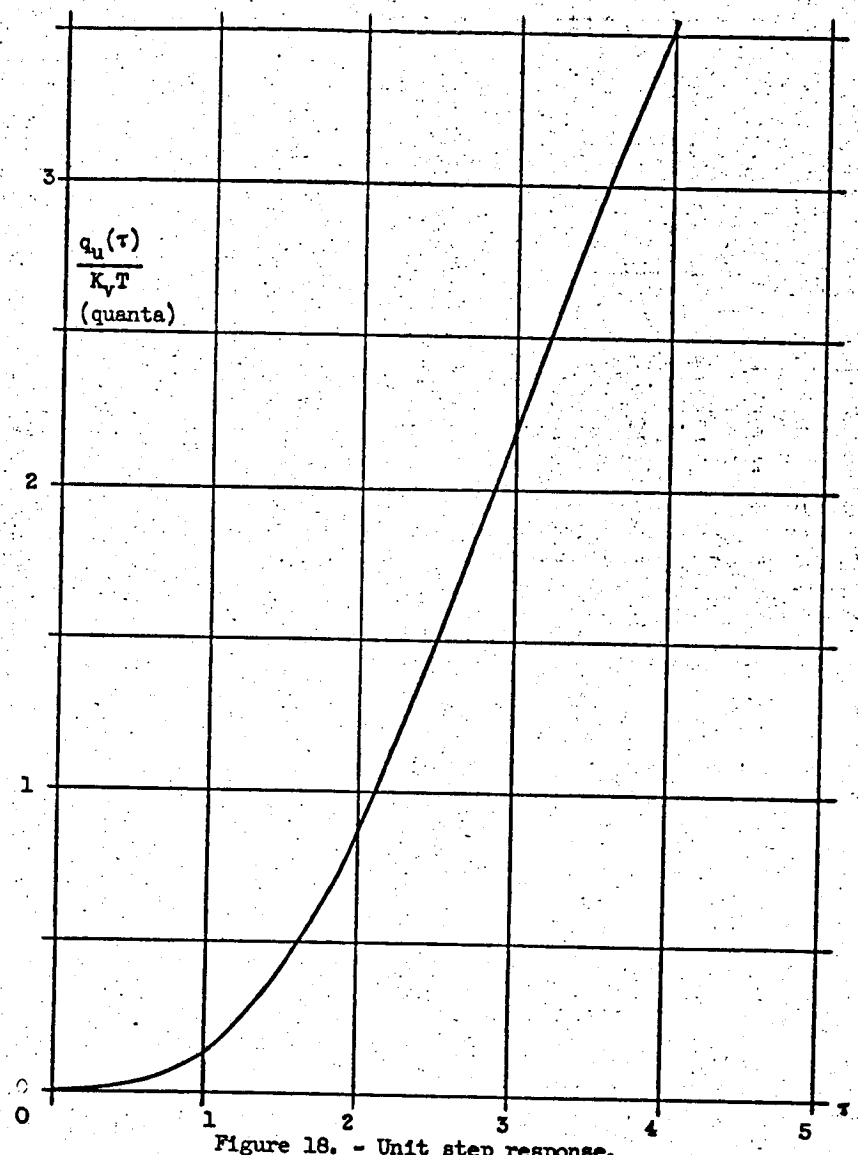

Figure 18. - Unit step response.

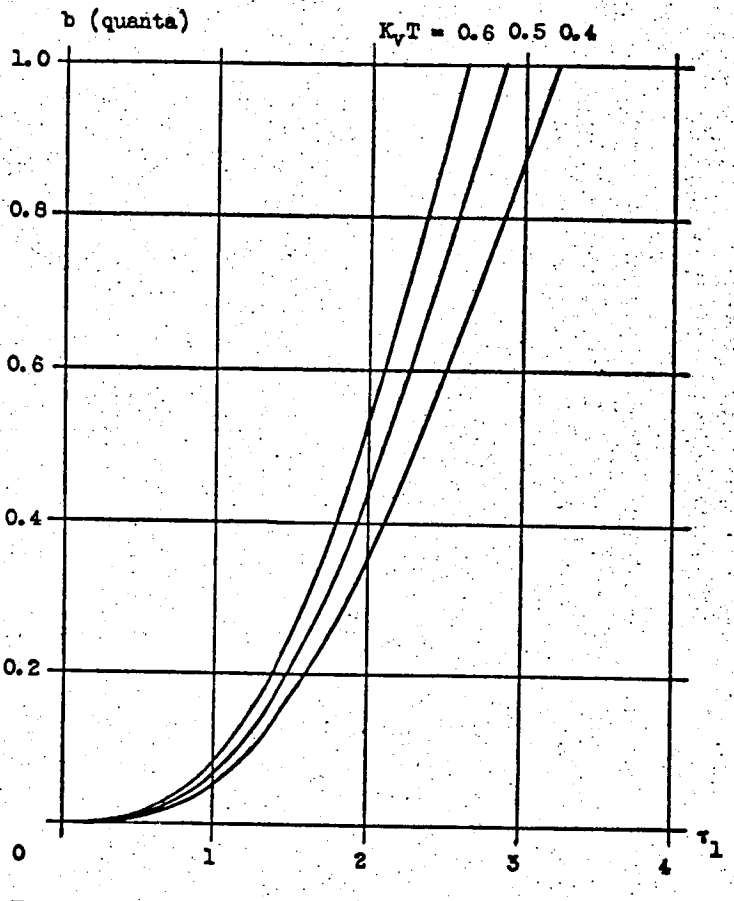

Figure 19. - Distance to first quanta point versus time to first quanta point.

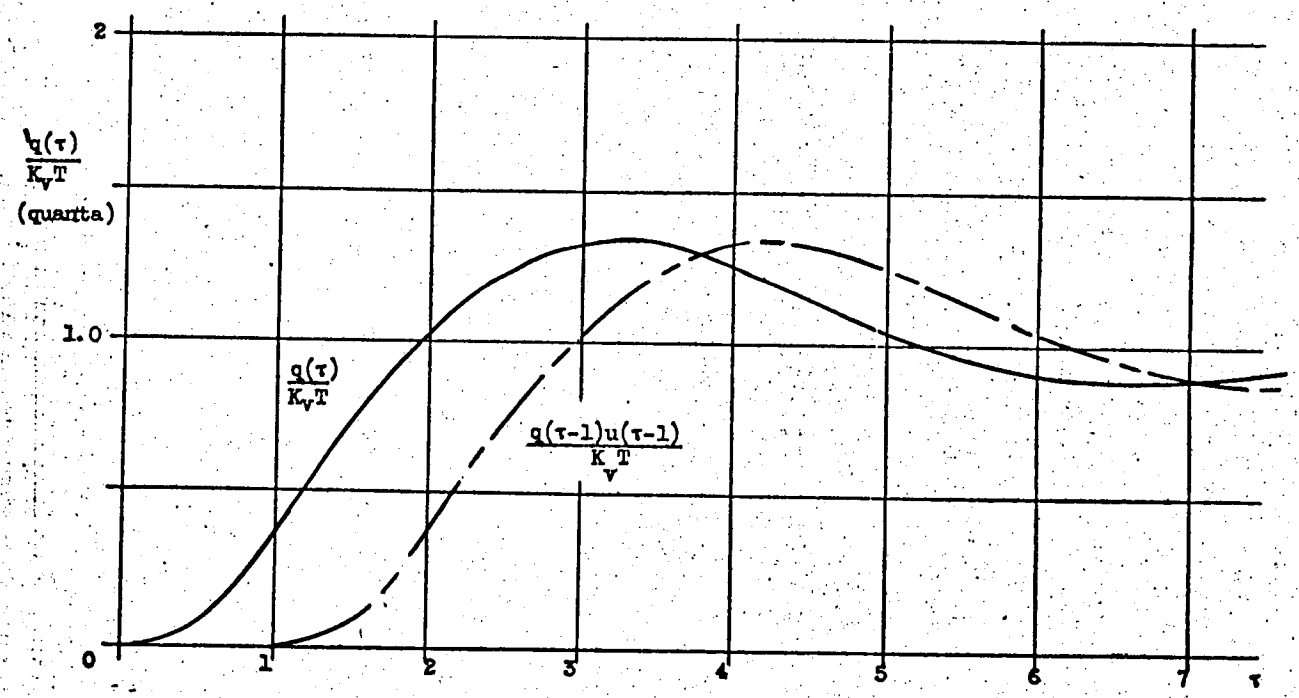

Figure 20. - Determination of time of maximum overtravel τ_m.

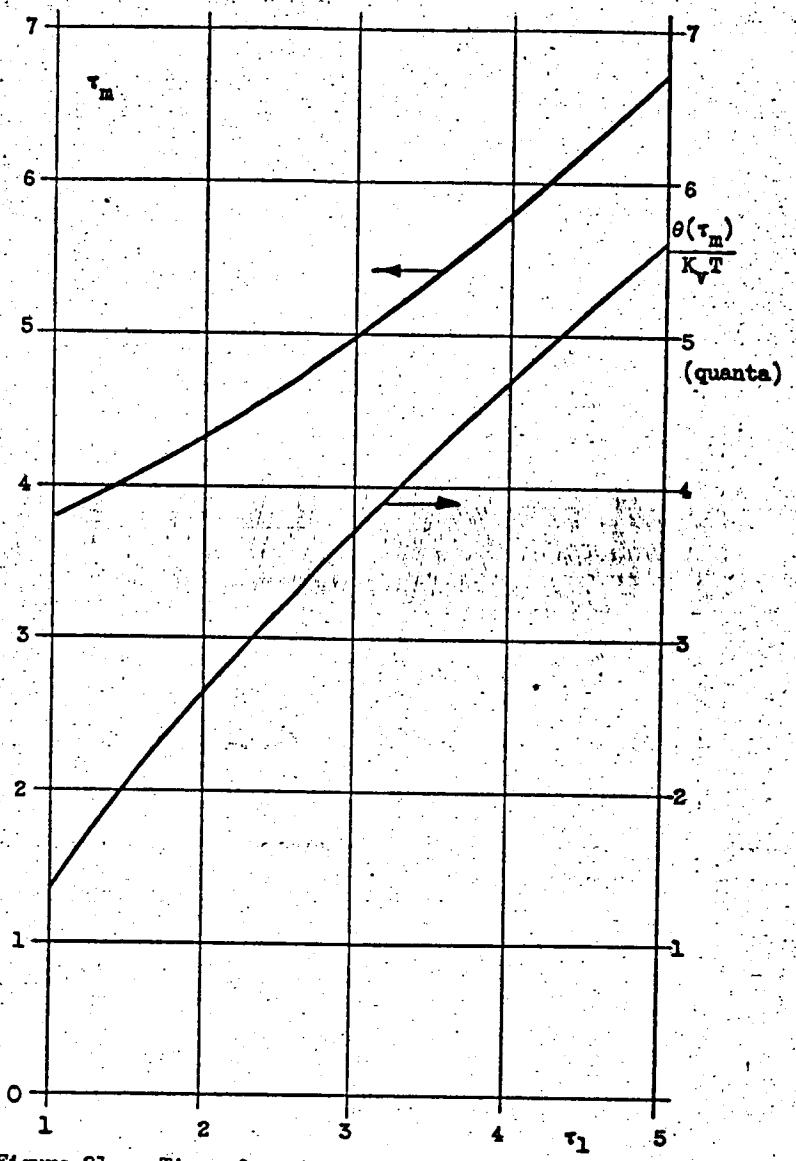

Figure 21. - Time of maximum overtravel and maximum travel versus time of first quanta point.

This development is used to obtain $\theta(\tau_m)/K_vT$ as a function of τ_1 as shown in figure 21.

(5) Now the curves of $\theta(\tau_m)$ as a function of b for various values of K_vT are plotted in figure 22. This is done by selecting a value of K_vT. Then for every b there is a τ_1 from figure 19. The value of τ_1 specifies $\theta(\tau_m)/K_vT$ in figure 21. This value is multiplied by K_vT to obtain a value of $\theta(\tau_m)$ for b at the specified K_vT. Thus for $K_vT = 0.5$ and $b = 0.6$ quanta, $\tau_1 = 2.26$ sec from figure 19. At $\tau_1 = 2.26$ sec, $\theta(\tau_m)/K_vT = 2.95$ quanta. Thus $\theta(\tau_m) = 2.95 \times 0.5 = 1.475$ quanta. The curves shown in figure 22 are developed in this way. The critical value of K_vT is:

$$0.5 < K_vT < 0.6$$

This is shown by the fact that the $\theta(\tau_m)$ curve for $K_vT = 0.5$ lies entirely below the $1 + b$ line. $\theta(\tau_m)$ for $K_vT = 0.6$ has portions above the $1 + b$ line.

The analysis shown yields much more information in addition to the maximum value of a system parameter for a specified overtravel. The following information is also available:

(1) The time of the first feedback pulse τ_1 as a function of starting position and a system parameter.

(2) The time at which $\theta(\tau)$ is a maximum τ_m as a function of the same parameter.

(3) The distance between $1 + b$ and $\theta(\tau_m)$ indicates the amount by which the system fails to overtravel one quanta.

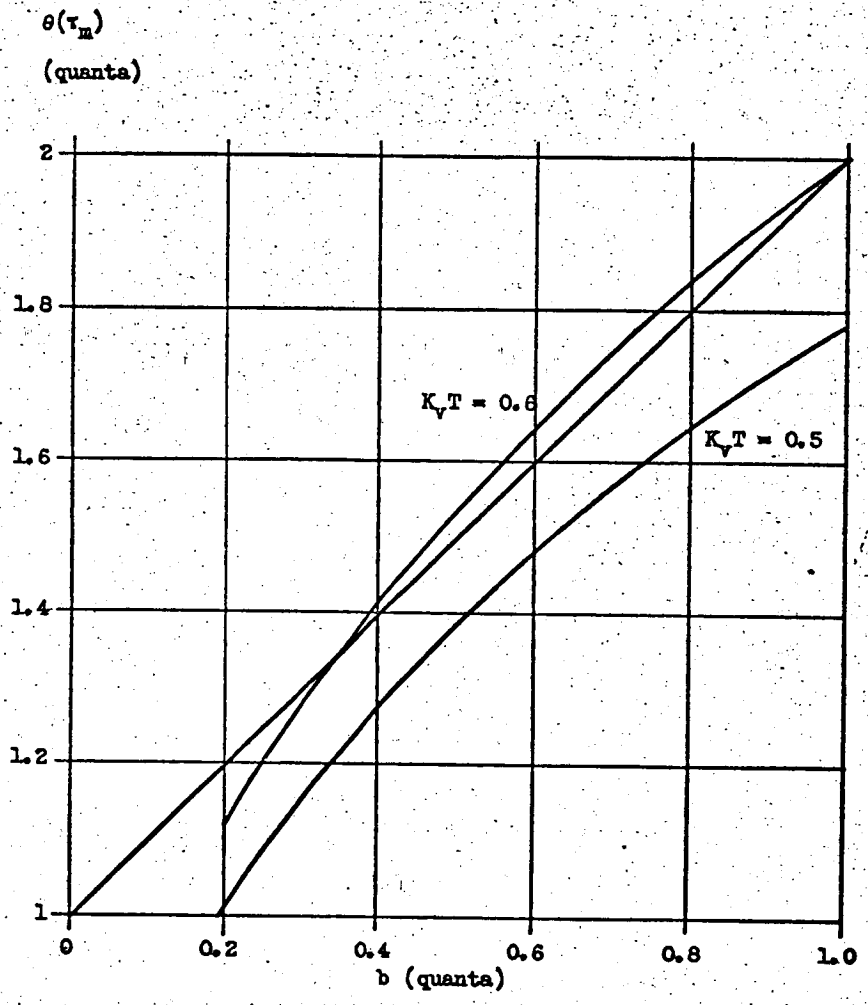

Figure 22. - Determination of critical value of gain K_vT.

Thus many of the essential characteristics of the system response to a single input pulse are obtained. The method appears to be more exact than the describing function since it specifies the response of the system shown in figure 9.

The three methods outlined in detail in this chapter can be used to design a pulse-data system to meet specific requirements. This will be illustrated in the appendix for a specific system.

CHAPTER III

ACCURACY AND SMOOTHNESS

This chapter will be concerned with the definition of accuracy and smoothness of the controlled variable in a pulse-data system. The system considered has a prime mover characterized by:

$$G(s) = \frac{K_V G'(s)}{s}$$

where $\lim_{s \to 0}$ of $G'(s) = 1$. A smoothness criterion will be developed to evaluate the smoothness of the controlled variable $\theta(t)$. The method of translating a desired path into an input $r(t)$ will be defined.

The pulse-data system is capable of extremely high accuracy. However, its resolution is limited by the quanta size. The original specifications that describe the desired path that the controlled variable should follow must be transcribed into pulse-data. The path is expressed as a series of one quanta steps. The resulting information is in the form of a pulse train $r(t)$, see figure 4. Each pulse directs the system to move one quanta. The time between pulses determines the desired instantaneous rate. It will be assumed that the desired path is made up of a series of straight lines or ramps. The actual pulse-data system will not follow the ramp paths exactly because of overtravel and the lack of resolution between quanta points. However the errors can be reduced if the translation is carried out in a specific way.

It is desired to have the controlled variable describe in a ramp at a rate of $1/T_r$ quanta per second. This information can be transcribed in one of two ways:

Method I

The input pulses $r(t)$ start as soon as the desired ramp is to start. Figure 23(a) shows the steady state response for several values of gain K_v with this method.

Method II

The input pulses $r(t)$ start when the desired ramp has reached a height of one quanta (fig. 23(b)).

If method I is used the controlled variable starts to change at the instant that the desired ramp starts (fig. 23(a)). With gain $K_v = 1/T_r$ the controlled variable will follow the desired path quite closely. For gain $K_v > 1/T_r$ the controlled variable will lead the desired path by one quanta or more. If gain $K_v < 1/T_r$ it will lag the desired path.

If method II is used the controlled variable starts T_r seconds late. If gain, $K_v > 1/T_r$ the path of the controlled variable oscillates about the desired path (fig. 23(b)). For gain $K_v \leq 1/T_r$ the controlled variable lags behind the desired path.

Method II penalizes the pulse-data system except when $K_v > 1/T_r$. However, it corresponds to the continuous feedback system where the controlled variable lags the desired path by an amount determined by K_v and the rate.

Since the translator can choose either method it will be assumed that both methods are applied as follows:

(1) When $K_v > 1/T_r$ method II is used to transcribe the desired path into pulse-data.

(2) When $K_v \leq 1/T_r$ method I is used.

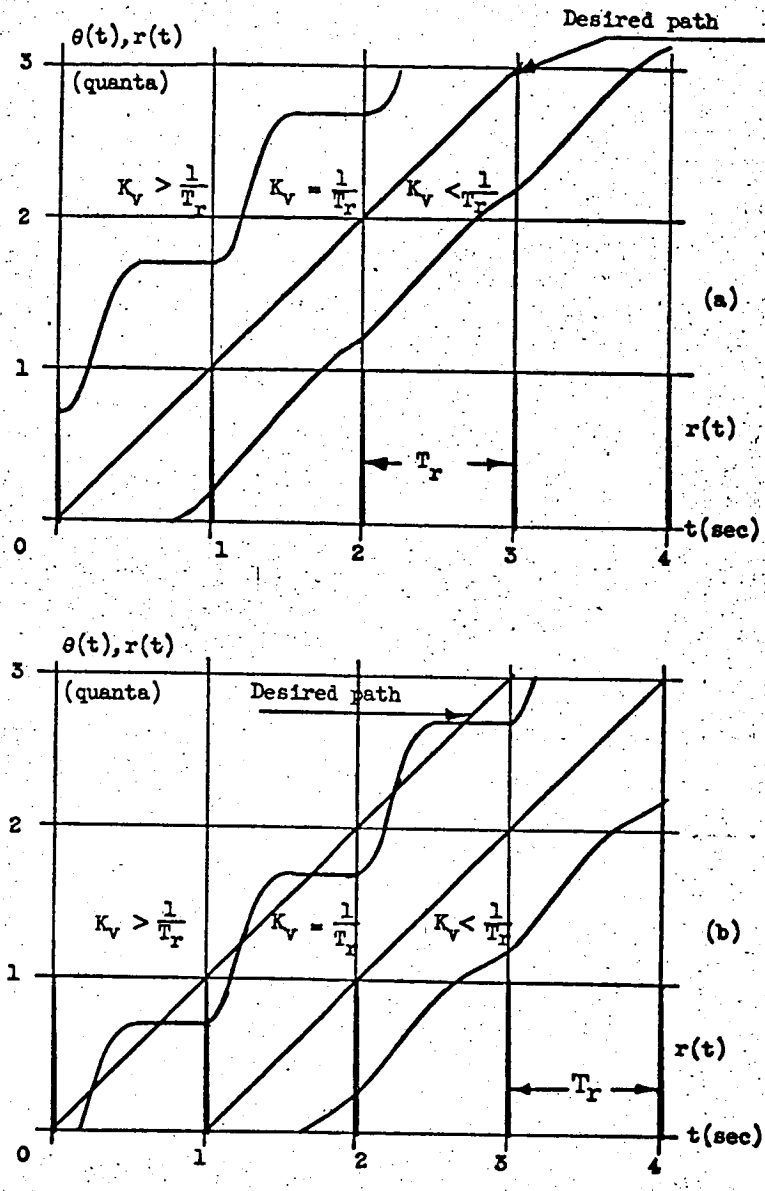

Figure 23. - Ramp input response.

In this way the accuracy of the pulse-data system for ramp inputs of various rates can be improved. This will be used to compare the response of the adaptive and nonadaptive pulse-data systems.

Figure 23 also illustrates one of the disadvantages of the pulse-data system. At low input pulse rates it tends to follow a "staircase" path. The rate of the controlled variable is not continuously equal to the desired rate. The amount of this deviation will be indicated by a smoothness criterion.

The most common types of error criteria involve the integration of error or powers of the error. This tends to smooth or average the error.

The problem involved with the integral criterion is illustrated for the mean-square error criterion where

$$I = \frac{1}{T}\int_0^T [E(t)]^2 \, dt$$

Figure 24 shows the velocity of a pulse-data position system with $G(s) = K_v/s$ at a fixed input pulse period T_r.

$$I = \frac{1}{T_r}\left[\left(K_v - \frac{1}{T_r}\right)^2 \Delta\tau + \left(\frac{1}{T_r}\right)^2 (T_r - \Delta\tau)\right]$$

But $\Delta\tau = 1/K_v$ when $1/K_v < T_r$ as was shown in chapter II.

$$I = \frac{1}{T_r}\left[K_v - \frac{2}{T_r} + \frac{1}{T_r^2 K_v} + \frac{1}{T_r} - \frac{1}{T_r^2 K_v}\right]$$

$$= \frac{K_v T_r - 1}{T_r^2}$$

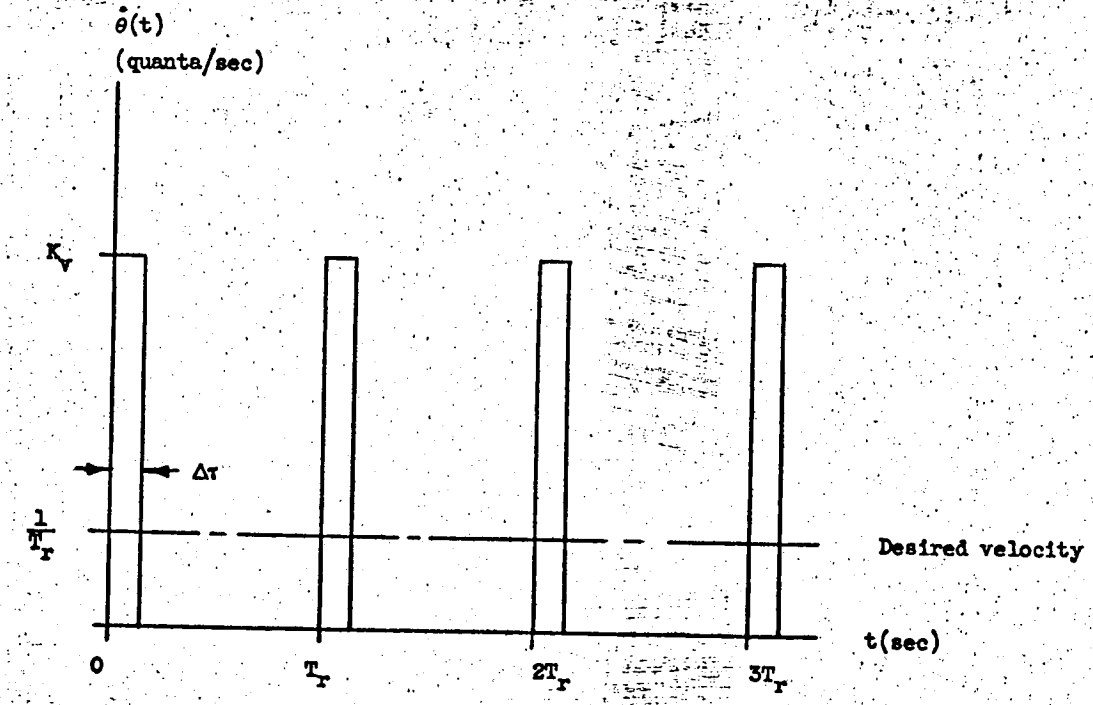

Figure 24. - Typical pulse-data ramp response.

Thus I varies with T_r for a fixed K_v. I has a maximum value for:

$$T_r = \frac{2}{K_v}$$

When T_r becomes large I becomes small due to the averaging effect. In a machine tool, for example, a response of the type shown in figure 24 would be just as serious if T_r was large as it would be for T_r small.

The integral error criteria are useful in systems with random or nonperiodic inputs. In the present case a criterion is needed to evaluate the smoothness of the steady state response of a pulse-data system. This response is periodic. Thus an error criterion which does not have the "averaging" feature is useful.

One possible error or smoothness criterion is the maximum error between the controlled variable velocity and the desired velocity.

$$I = | 1 - \dot{\theta}_c(t)\ T_r |_{max}$$

This criterion will be used to evaluate the smoothness of the adaptive and nonadaptive system responses.

CHAPTER IV

PATH CONTROL SYSTEMS WITH SMOOTHER RESPONSE

One of the reasons that a pulse-data system is used is that it possesses high accuracy. Thus at high input pulse rates it is desirable to have the position loop gain as high as possible to minimize the error. At low rates the gain should be small so that the controlled variable will follow the desired path at the desired velocity. The two requirements cannot be met by the pulse-data system with fixed position loop gain.

There are several solutions that were investigated.

(1) The loop gain could be made adaptive with the input rate. For example if $G(s) = K_v/s$ the controlled variable will follow the desired path if $K_v = 1/T_r$. Thus K_v could be controlled by $1/T_r$.

(2) Integral plus proportional control could be used. Then $G(s)$ would have the form:

$$G(s) = \frac{K_a(Ts + 1)}{s^2 D(s)}$$

This system has small steady state errors and is capable of following low input pulse rates. However the transient errors are quite large. The system would be quite difficult to stabilize in the presence of even small amounts of backlash. Drift problems are accentuated in a system of this type which increases the possibility of a limit cycle of small amplitude.

(3) Feed-forward techniques could be used. An analog signal proportional to the desired rate could be added to the digital to

analog converter output $e(t)$. This type of system has large transient errors. Also slight changes in the analog rate signal or the controlled variable rate would lead periodic pulses in the output speed. These pulses would be due to the correction of accumulated position errors.

(4) A sampled-data control could be used with the position feedback supplied by an encoder. This is an absolute path control. This system would be considerably more expensive than the pulse-data system. The quanta size would have to be made much smaller than the size used in the pulse-data system to obtain much improvement.

(5) The quanta size of the pulse-data system could be reduced. This would have the effect of reducing T_r for a given desired input rate. At the same controlled variable rate $\dot{\theta}(t)$ the "d-c level" a of $r(t)$ would increase providing smoother operation. Thus the system would operate with the same absolute error and the same gain K_vT but the number of quanta error would increase. As was illustrated by the describing function in chapter II the pulse-data system approaches a linear system as the error, in quanta increases. This system has the disadvantage that the capacity of the bidirectional counter and digital to analog converter must be increased. The "fineness" of the quantizer must be increased. Backlash between the quantizer and the actuator will now increase in importance. As the amount of the backlash approaches one quanta in magnitude stability problems can develop. The work involved in transforming the desired path into a pulse train $r(t)$ increases as many more input pulses are required to move the same distance.

The best overall system appears to be the first one. This system has the lowest transient error. It will operate reliably in the presence of large system parameter variations. It is no more succeptable to drift problems than the basic pulse-data system. The range of smooth operating speed can be larger than any of the other methods with the possible exception of the integral control. The cost of the adaptive control is less than that of any of the other methods. The adaptive system was selected on the basis of these advantages. This method was implemented by a system which is described in the next chapter.

CHAPTER V

SELF-ADAPTIVE PULSE-DATA SYSTEM

As was discussed in chapter IV the self-adaptive pulse-data system appears to be the best overall solution to the problem of low speed smoothness and high speed accuracy. The system is shown in block diagram form in figure 25. This system was constructed and tested to show the improvements in smoothness. The circuit consists of a pulse-data system as described in chapter I and shown in figure 3. In addition there is a self-adaptive section (inside the dotted area) which makes the position loop gain proportional to input pulse rate. The purpose of this chapter is to describe the self-adaptive system. Special attention will be directed to those parts not described in chapter I. A detailed description of the system is contained in appendix II.

Basic Pulse-Data Section

The section of the self-adaptive pulse-data system outside the dotted lines in figure 25 consists of seven physical subsections whose operation will be described briefly.

Synchronizer

The input pulses r(t) enter a Synchronizer (sync. in fig. 25) along with the feedback pulses c(t). This circuit, developed by D. R. McRitchie[10], prevents the Bidirectional Counter (BDC in fig. 25) from receiving more than one pulse at a time. It is possible that an input pulse and a feedback pulse could occur at the same time. If the Bidirectional Counter received these two pulses in a time interval which was too short it would malfunction. The Synchronizer consists of four

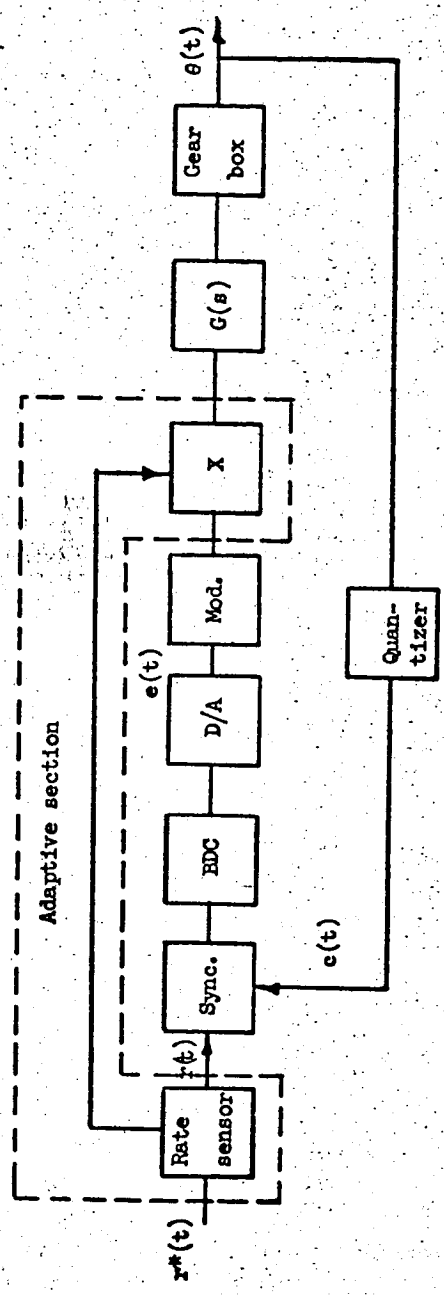

Figure 25. - Self-adaptive pulse-data system.

sections. One section for each of the plus and minus input lines and one for each of the plus and minus feedback lines. Whenever a pulse is received by the Synchronizer in one of these lines it is stored. A clock operating at a high rate opens each of the four sections in succession allowing the stored pulses to enter the Bidirectional Counter at specified times. In this way no two pulses can enter the Bidirectional Counter simultaneously. The unit does, however, introduce a delay due to the pulse storage time. In the system constructed this delay is 0.005 sec.

Bidirectional Counter

The Synchronizer output is in one of two lines at any given time. A pulse in one of the lines directs the Bidirectional Counter to count one bit up, in the other line it directs it to count down. The interconnections between stages of the Bidirectional Counter determine whether it counts up or down.

In each stage these interconnections are controlled by two gates. The gates which operate as electronic switches are controlled by whether the pulse enters in the "up" or the "down" input line. When a pulse enters, the appropriate gates are activated for a time which is long enough to allow the counter to change state one bit.

At the null position the counter is set half full. In this way it can count up or down by the same amount before it overflows. The counter capacity is ±63 counts. This is considerably in excess of the maximum system error.

Digital to Analog Converter

The state of the Bidirectional Counter is converted to a d-c voltage by the Digital to Analog converter (D/A in fig. 25). The circuit used is described by Susskind[11]. It consists of a ladder network with equal current sources each activated by a stage of the counter. The resulting output voltage varies from +190 volts to +166 volts with +178 volts output when the counter is at null. The voltage deviation from +178 volts is proportional to the count in the counter.

Modulator

The d-c voltage produced by the Digital to Analog converter is modulated on a 60 cycle per second carrier. The signals in the actuator driving section are all 60 cycle per second a-c voltages. The Modulator (mod. in fig. 25) accomplishes this with an electromechanical chopper. The amplitude of the 60 cycle per second a-c voltage is proportional to the number of quanta error in the pulse-data system. This is e(t) in the system shown in figure 3. This voltage controls the actuator in a normal pulse-data system. In the adaptive system the magnitude of this voltage for a given error is proportional to the input pulse rate. This is accomplished by multiplying e(t) by a signal proportional to input pulse rate in the Multiplier (X in fig. 25).

Prime Mover

The signal e(t) or $K'e(t)/T_r$ in the adaptive system directs the Prime Mover (G(s) in fig. 25). A two phase a-c 15 watt servomotor driven by a push-pull power amplifier is used as the Prime Mover. The motor speed is measured by a tachometer to provide velocity feedback.

This feedback is used to reduce the time constant between input signal and motor speed. The motor is capable of speeds of up to 3550 rpm at no load.

Gear Box

The output speed of the motor is geared down to the Quantizer. The Gear Box is breadboarded on an aluminum plate by means of hangers clamped to the plate to support the gear shafts. The motor turns at 17.5 times the speed of the Quantizer.

Quantizer

The controlled variable $\theta(t)$ is measured by the Quantizer (fig. 25). This is an electromagnetic device which produces two outputs. The outputs are modulated on a 45 kilocycle carrier. These two outputs are shown in figure 26(a) for a constant Quantizer speed in the plus direction. Notice that they are 90^{o} out of phase. These signals are demodmulated and amplified to produce two square waves A and B (fig. 26(b)). Wave B is also inverted to produce -B (fig. 26(b)). Both of the B waves are differentiated to produce the waveforms in figure 26(c). dB/dt and -dB/dt are each fed to a gate which is open to positive pulses when signal A is positive. Thus since the positive -dB/dt pulses occur when A is not positive the output of that gate which we call the minus gate is zero. The dB/dt positive pulses occur when A is positive. Thus the output of that gate which we call the plus gate is shown in figure 26(d). When the Quantizer is rotating in the minus direction the waveforms are as shown in figure 27. The positive -dB/dt pulses occur when A is positive. Thus the output

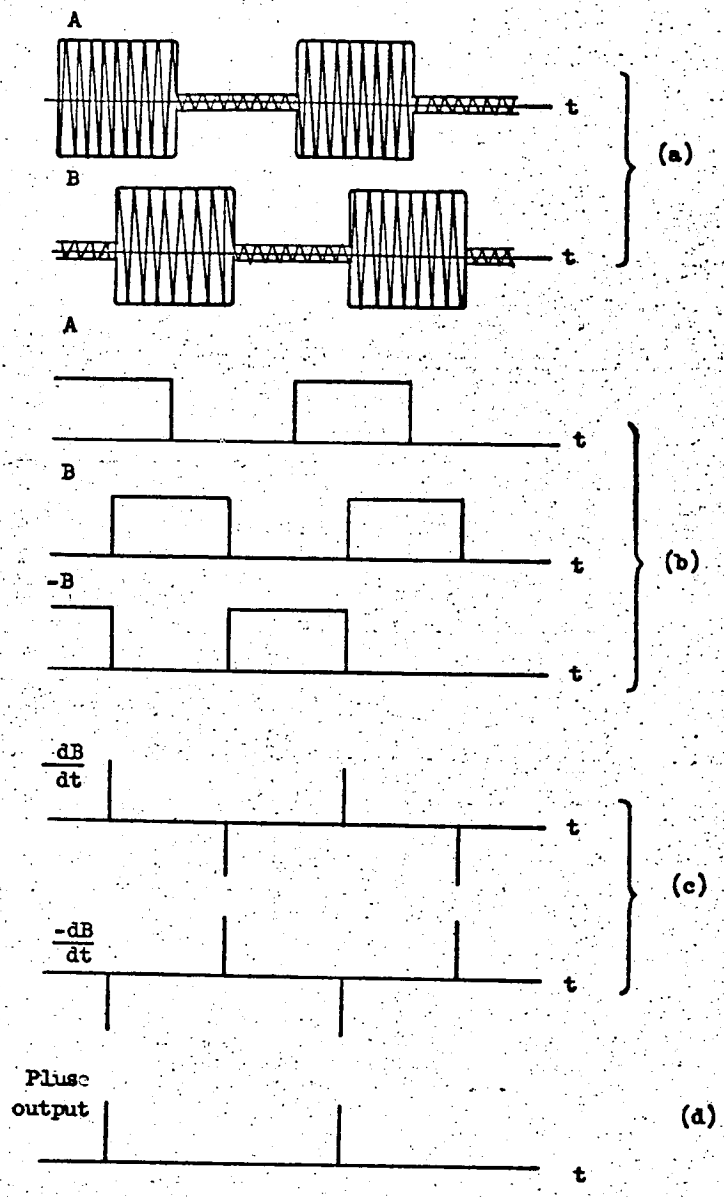

Figure 26. - Quantizer waveforms in plus direction.

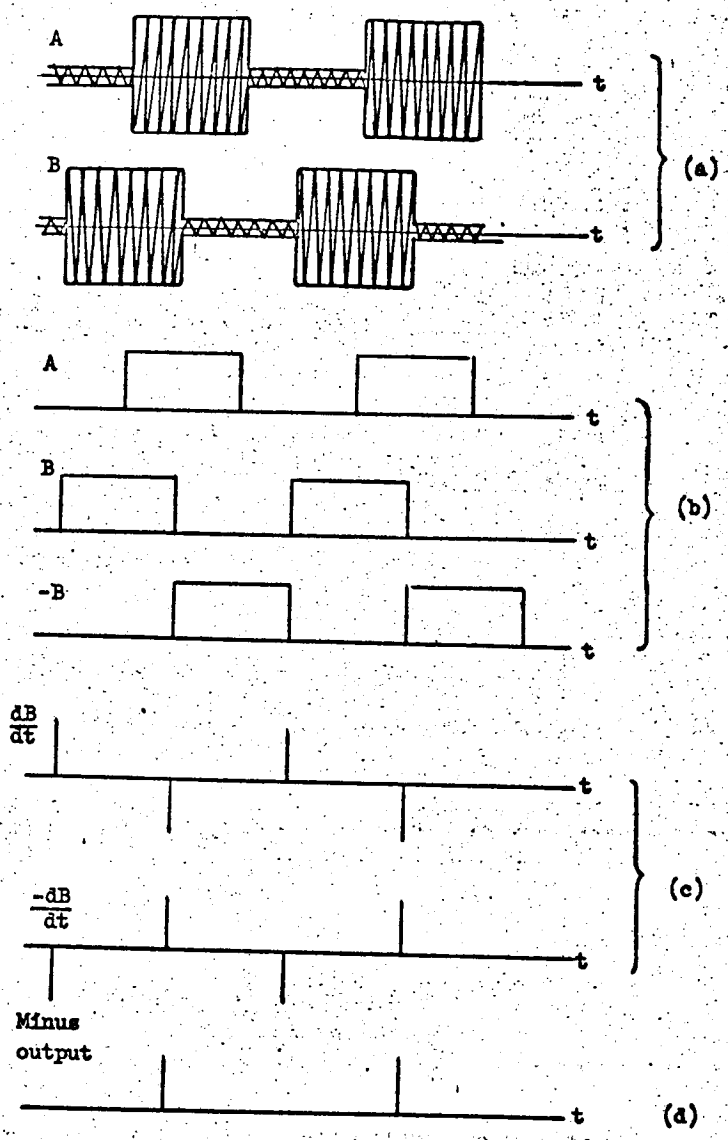

Figure 27. - Quantizer waveforms in minus direction.

of the minus gate is shown in figure 27(d). The positive dB/dt pulses occur when A is not positive thus the output of the plus gate is zero. The values of $\theta(t)$ where the B output goes from 0 to plus when the Quantizer is rotating in the plus direction are the quanta points. The Quantizer used produced 100 pulses per revolution of the electromagnetic unit.

This completes the description of the basic pulse-data system.

Self Adaptive Section

The position loop gain of the basic pulse-data system is controlled by the Self-Adaptive Section. This is accomplished by a Multiplier as briefly described in the Modulator description above. The signal which controls the Multiplier is developed by the Input Rate Sensor (fig. 25).

Input Rate Sensor

The Rate Sensor measures the input pulse rate. It accomplishes this purpose by measuring one half the input pulse period.

The circuit requires that twice as many input pulses at one half the period of $r(t)$ are fed to it. This is shown in figure 28. The pulse input to the rate sensing circuit is denoted by $r^*(t)$ (fig. 28(a)) for an input to the system of five pulses. Thus ten $r^*(t)$ pulses are fed in at a frequency of $2/T_r$ pulses/sec. The rate circuit produces a square wave from these pulses as shown in figure 28(b). The time $T_r/2$ is measured by a counter and a fixed frequency pulse generator. The square wave is differentiated to produce the negative pulses shown in figure 28(c) which are then fed to the pulse-data system as the input pulses $r(t)$.

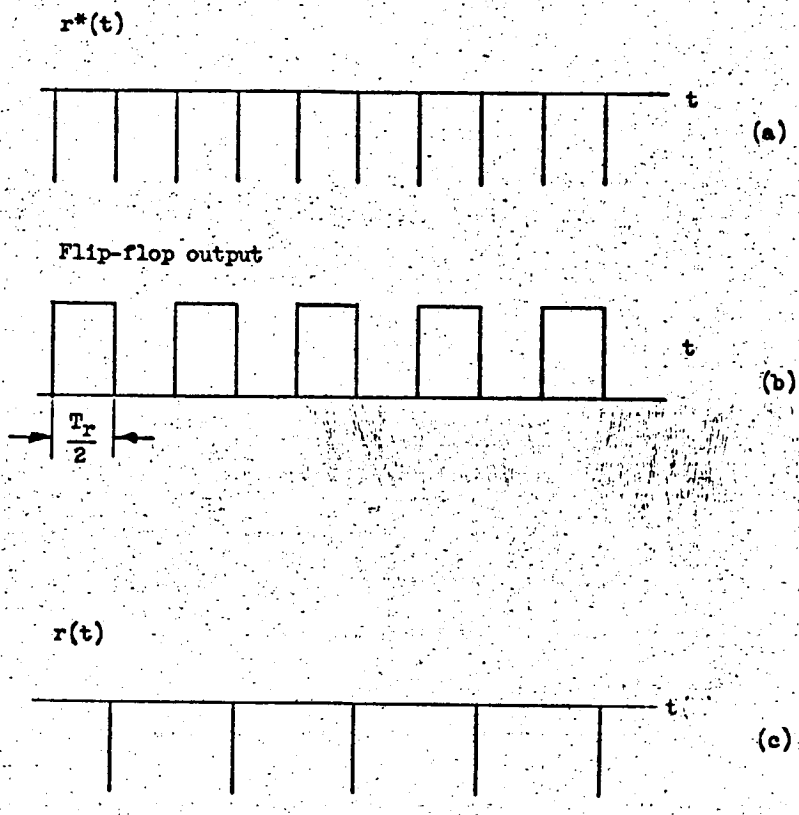

Figure 28. - Input rate sensor waveforms.

There are two counters used to measure $T_r/2$ each with a ten count capacity. A given counter measures $T_r/2$ every other cycle of the square wave. The counter state is converted to a d-c voltage. The counter is a cold cathode tube which is used as a voltage source in a divider network to accomplish the digital to analog conversion directly. The d-c voltage conversion is nonlinear so that the voltage is proportional to input pulse frequency. The d-c signal indicating pulse frequency at a given time is obtained from the counter which is not counting. Thus the input pulse rate signal is obtained from one counter, then the other to provide a continuous rate signal. In this way input pulse rate is determined continuously.

The ten count capacity of the counters limits the range over which gain can be changed. Gain could be controlled as a linear function of input rate over a ten to one range in ten steps. It was actually controlled over a ten to one range in nine steps because of factors in the digital to analog conversion process in the counters.

Multiplier

The d-c output voltage produced by the Rate Sensor Circuit was then used to control the gain of a multigrid vacuum tube. The multigrid tube then serves as the multiplier (X in fig. 25). In this tube the modulated signal e(t) is amplified by an amount depending on the d-c signal from the Rate Sensor.

The resulting gain versus pulse rate relation is shown in figure 29. Since the counter has only nine usable states there are only nine different gains over the range of adaption. If for example the input

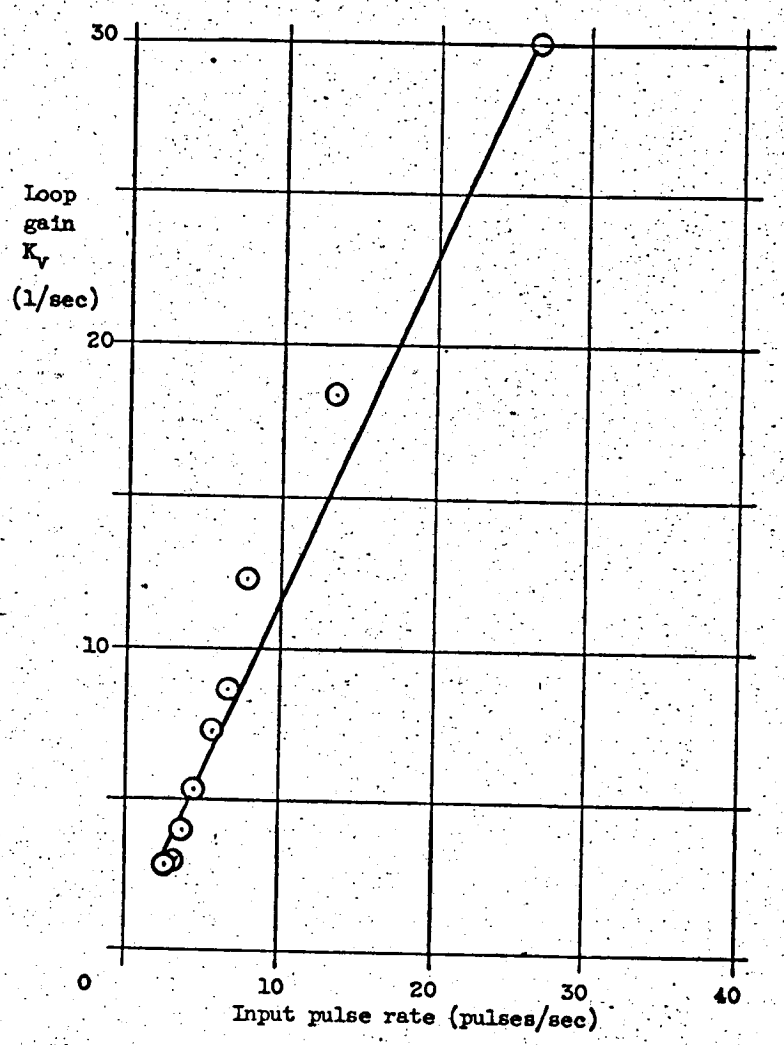

Figure 29. - Gain-rate relation.

pulse rate were 20 pulses/second the count in the rate counters would vary from one to two producing an average gain of about K_v = 23/sec. This causes a ripple in the steady state velocity due to the gain change. It could be reduced by increasing the number of counter states and making the gain-rate relation nonlinear. The largest amount of ripple in the gain occurs at the high rates where the frequency of this ripple would also be high. This ripple does cause an increase in the value of I the smoothness criterion at high rates.

The pulse-data system described here was tested with and without the adaptive circuit. The next chapter describes the results.

CHAPTER VI

EXPERIMENTAL RESULTS

The self-adaptive system described in chapter V was tested as was the same system without the adaptive section.

The two systems tested are shown in the form of mathematical models of the type described in chapter I (fig. 30). The notation used is the same as that developed in chapter I. In addition:

R denotes the transfer function of the input rate sensor. This element accepts an input $r^*(t)$.

$$r^*(t) = \sum_{n=0}^{\infty} A_n \left[\delta\left(t - T_{rn} + \frac{T_{r(n+1)} - T_{rn}}{2}\right) + \delta(t - T_{rn}) \right]$$

This is illustrated in figure 28. It produces two outputs $r(t)$ and K'/T_r.

$$r(t) = \sum_{n=0}^{\infty} A_n \delta(t - T_{rn})$$

K'/T_r = rate signal to multiplier (X in fig. 30).

The delay term in the integrator block is due to the synchronizer as was described in chapter V.

The self-adaptive system of figure 30 was converted to the non-adaptive system by removing the K'/T_r signal. This signal was replaced by a fixed voltage.

Ramp Inputs

An input $r(t)$ of fixed period was fed to the system. With this type of input the desired output $\theta(t)$ is a ramp. The two methods of

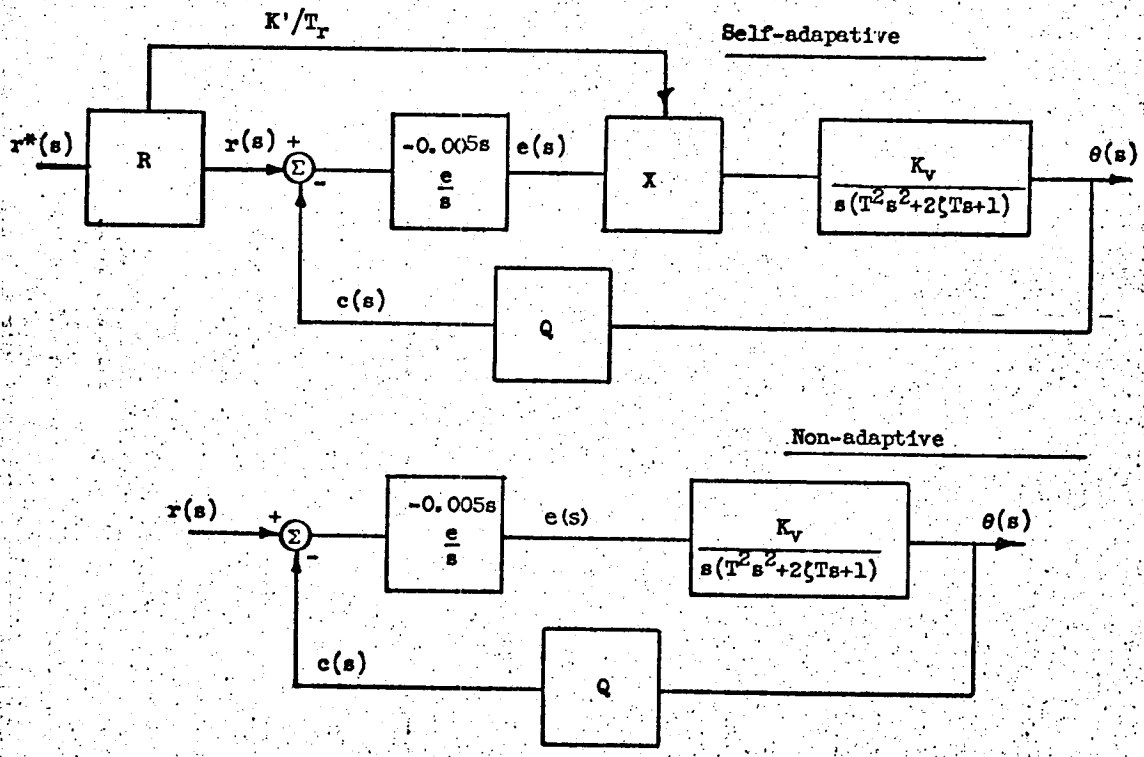

Figure 30. - Systems tested.

chapter III were used to specify the desired output

$$r(t) = \sum_{n=0}^{K} A\, \delta(t - nT_r)$$

$$A = +1$$

$$= -1 \text{ depending on the desired direction}$$

$$T_r = \text{pulse period}$$

The following system variables were recorded:

$\theta(t)$ = controlled variable position

$\dot{\theta}(t)$ = controlled variable rate

$r(t)$ = reference input

$c(t)$ = feedback pulses

K'/T_r = rate signal

Figures 31 and 32 show the response of both systems to an input rate of 3.2 quanta per second. The values of the system parameters are:

$$K_v = 30 \text{ sec}^{-1}$$

$$K'K_v/T_r = 3 \text{ sec}^{-1}$$

$$T = 0.0125 \text{ sec}$$

$$\zeta = 0.25$$

The desired path of $\theta(t)$ is also shown. This path is based on the assumptions of chapter III. The adaptive system not only has a smoother response but it follows the desired path with better accuracy. The smoothness criterion yields

$$I = | 1 - \dot{\theta}_{ss}(t)\, T_r | \text{ max}$$

$$I_{\text{adaptive}} = 0.85$$

$$I_{\text{nonadaptive}} = 10.5$$

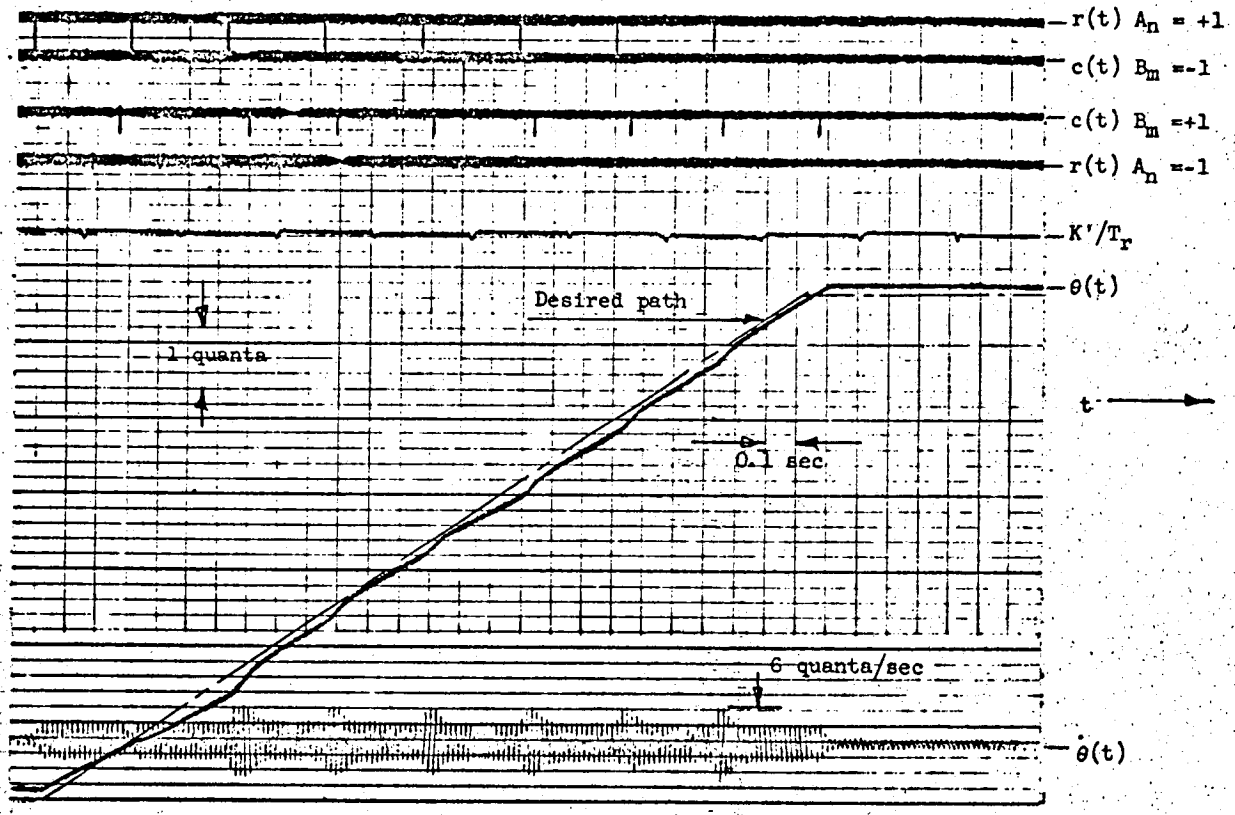

Figure 31. - Adaptive ramp response 3.2 quanta/sec.

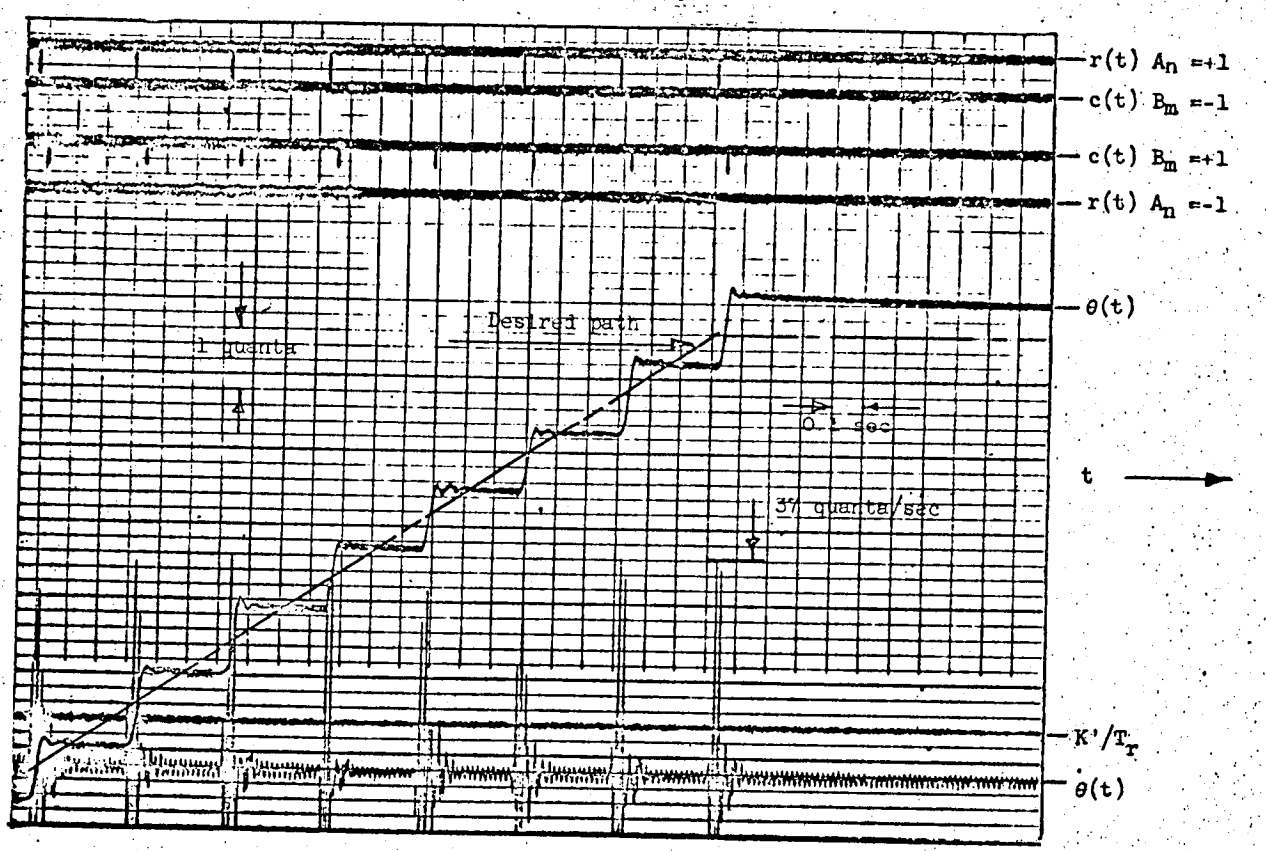

Figure 32. - Nonadaptive ramp response 3.2 quanta/sec.

Triangular Wave

A triangular wave is representative of the type of input which would be applied to a pulse-data path control with linear interpolation. The response to this type of signal provides some insight into the transient behavior. This form of input also illustrates the smoothness.

In these records $r(t)$ has the following form:

$$r(t) = \sum_{n=0}^{7} A\,\delta(t - nT_r) - \sum_{n=0}^{7} A\,\delta\,[t - (n+8)\,T_r] + \ldots$$

Where A and T_r are defined as before.

This form of $r(t)$ instructs the system to follow a triangular wave path as shown.

Figures 33 and 34 show the adaptive and nonadaptive response to a triangular wave at an input rate of 3.2 quanta per second. The values of the system parameters are:

$$K_v = 30\ \text{sec}^{-1}$$

$$K'K_v/T_r = 3.5\ \text{sec}^{-1}$$

$$T = 0.0125\ \text{sec}$$

$$\zeta = 0.3$$

Both responses are within one quanta of the desired response. The adaptive response is much smoother with $I = 1$ compared with $I = 10.6$ for the nonadaptive response. The flatting of the triangular wave is due to the quantized nature of the feedback.

A triangular wave at an input rate of 5.5 quanta per second is shown in figures 35 and 36. Where:

$$K_v = 30\ \text{sec}^{-1}$$

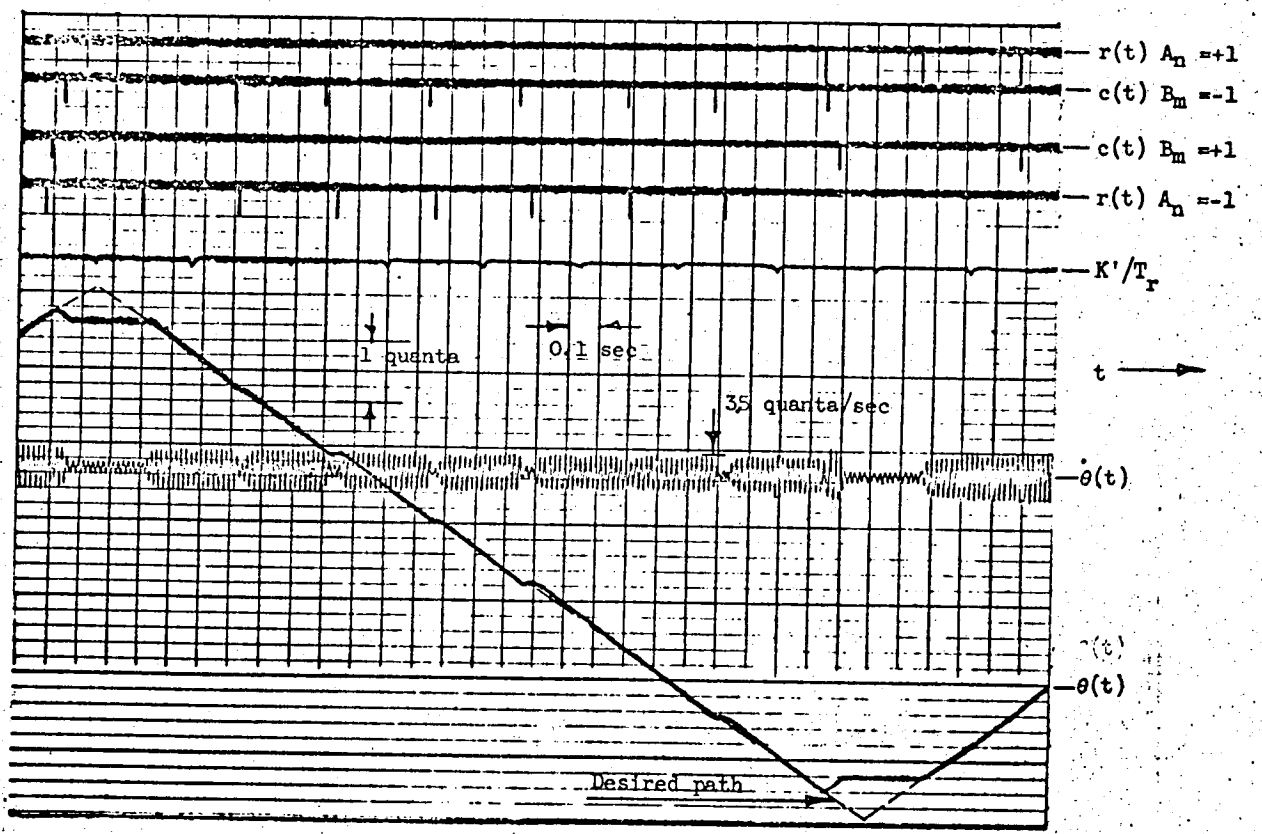

Figure 33. - Adaptive triangular wave 3.2 quanta/sec.

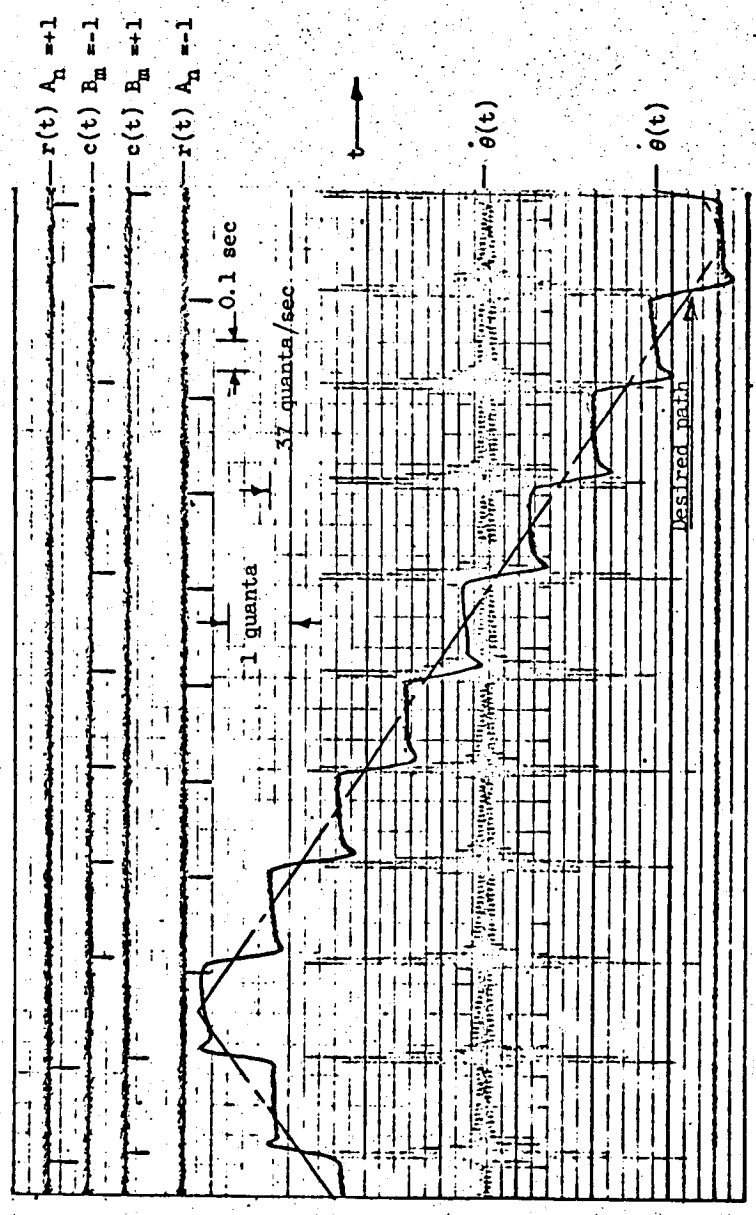

Figure 34. - Nonadaptive triangular wave 3.2 quanta/sec.

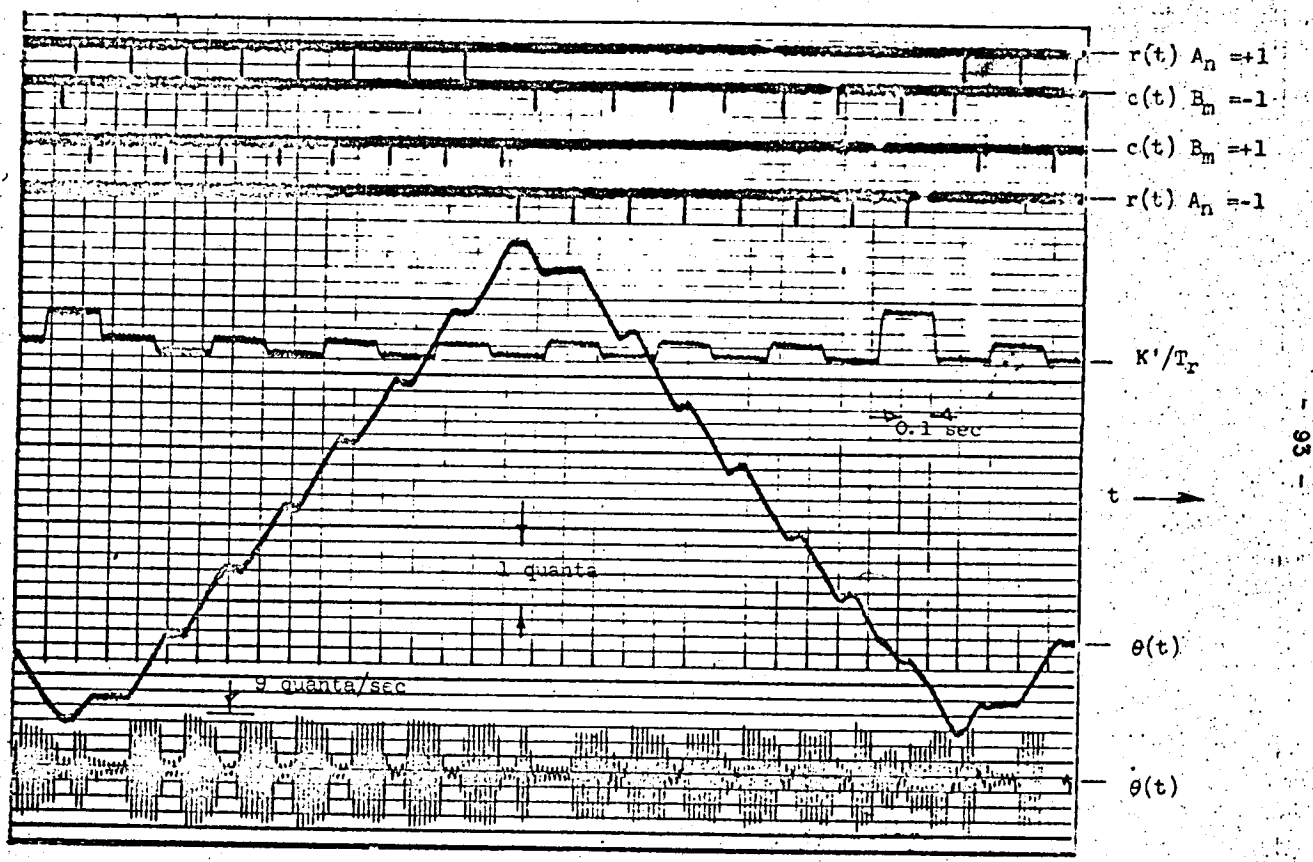

Figure 35. - Adaptive triangular wave 5.5 quanta/sec.

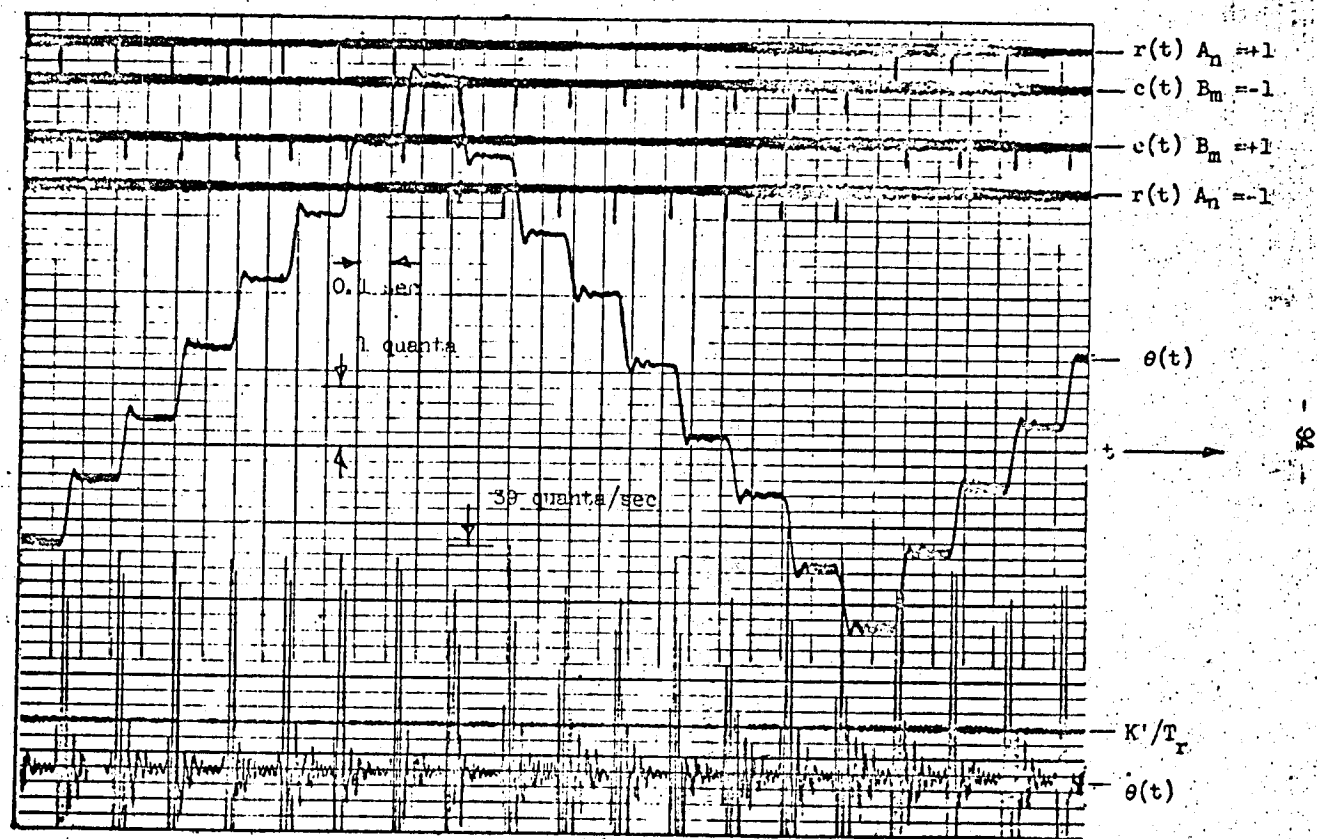

Figure 36. - Nonadaptive triangular wave 5.5 quanta/sec.

$$K'K_v/T_r = 8 \text{ sec}^{-1}$$

$$T = 0.0125 \text{ sec}$$

$$\zeta = 0.3$$

The adaptive response is much smoother than the nonadaptive response. The adaptive gain is not quite low enough since the controlled variable stops occasionally. The rate counter counts one more clock pulse from time to time which causes the rate signal K'/T_r to decrease as shown. The value of $I = 5.2$ for the nonadaptive response compares to $I = 1$ for the adaptive response.

The response to a triangular wave at an input rate of 13.5 quanta per second is shown in figures 37 and 38.

The system parameter values are:

$$K_v = 28 \text{ sec}^{-1}$$

$$K'K_v/T_r = 16.5 \text{ sec}^{-1}$$

$$T = 0.0125 \text{ sec}$$

$$\zeta = 1$$

Again the adaptive system has smoother reponse.

$$I_{adaptive} = 0.56$$

$$I_{nonadaptive} = 1$$

The improvement is not as great as that shown in figures 31 to 36 for two reasons.

(1) The damping ratio of the prime mover transfer function is greater. This reduces the overshoot in velocity $\dot{\theta}(t)$ and increases the rise time. However this also necessitates reducing K_v to maintain stability.

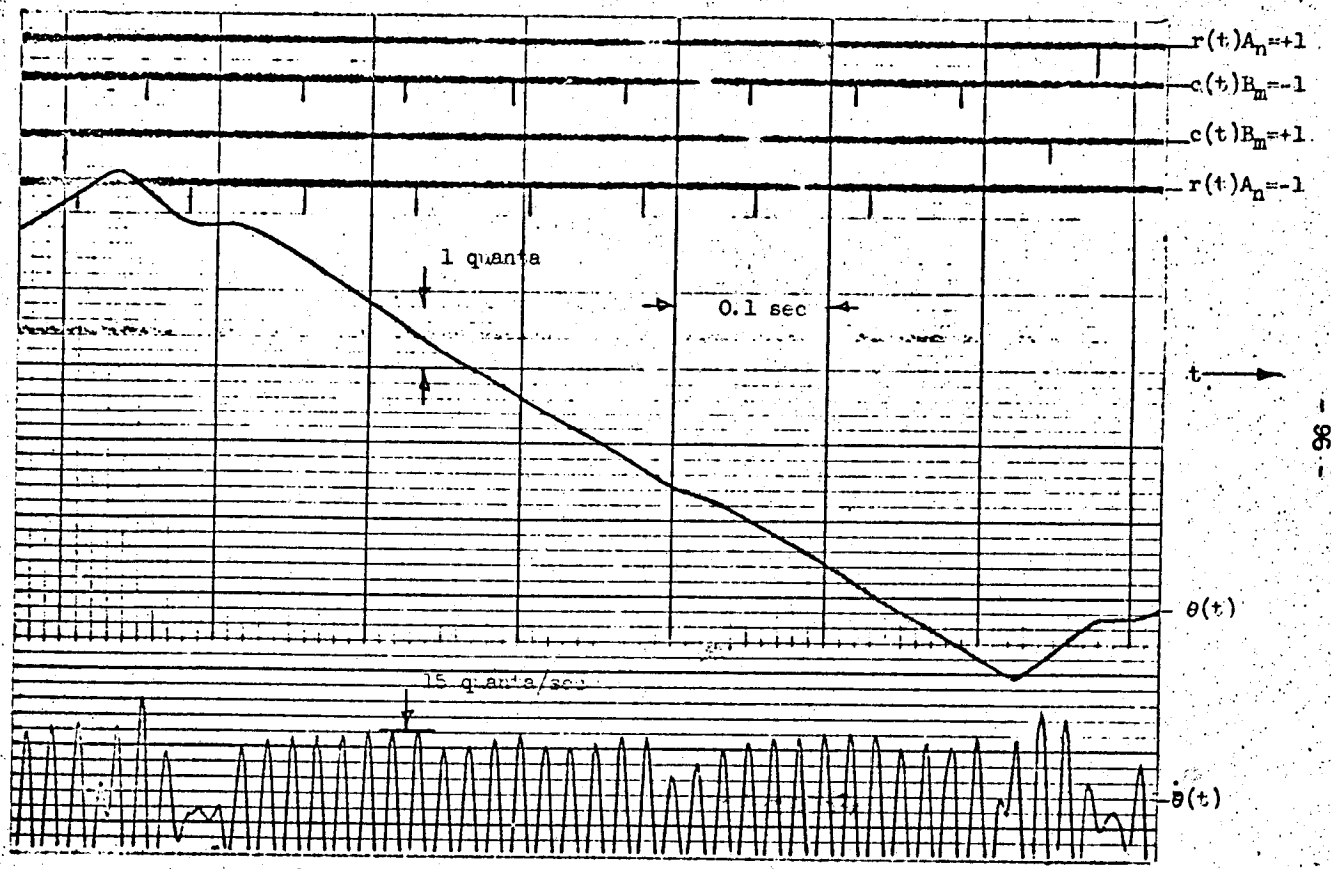

Figure 37. - Adaptive triangular wave 13.5 quanta/sec.

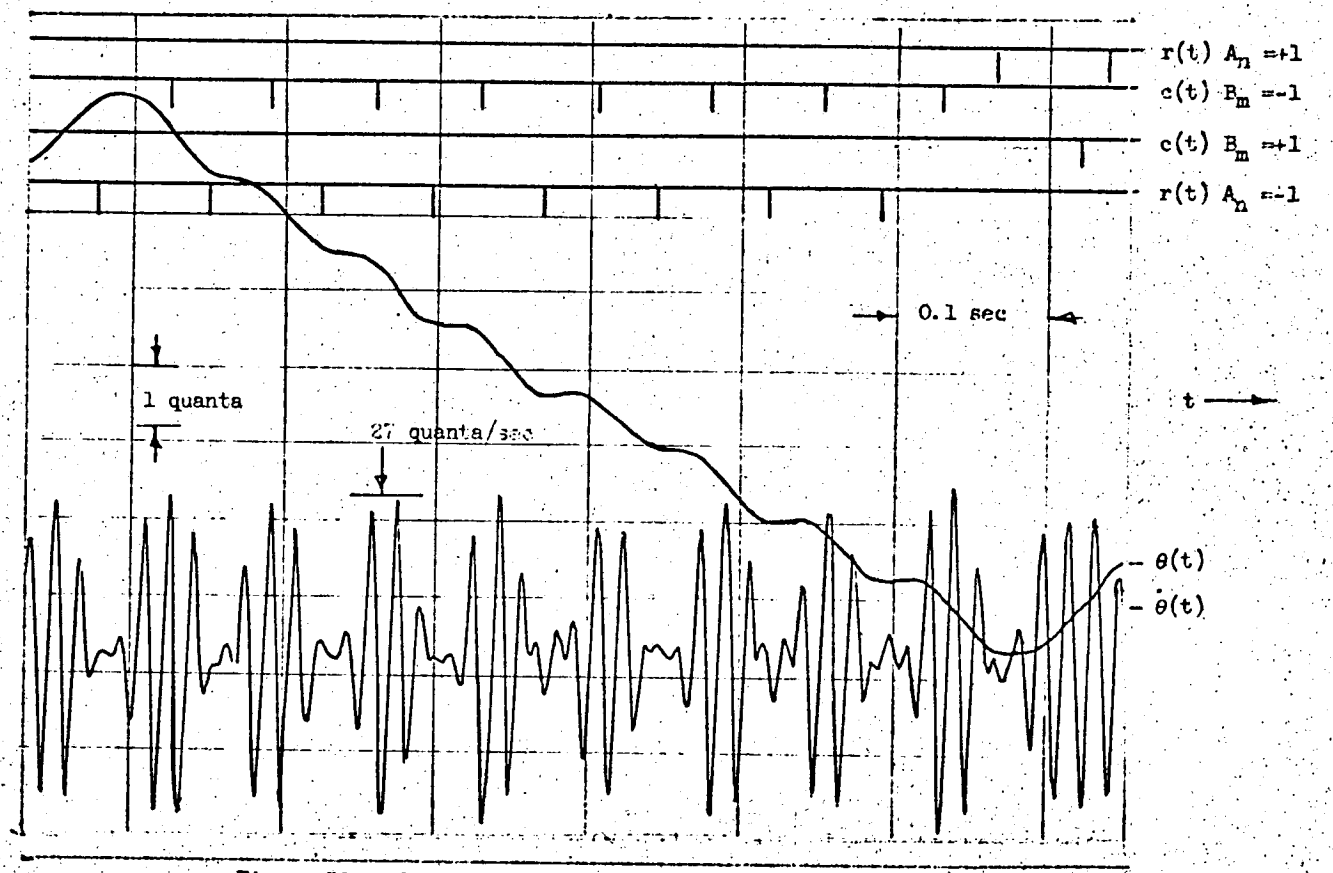

Figure 38. - Nonadaptive triangular wave 13.5 quanta/sec.

(2) The rate of the input pulses is greater than in the other records. As $1/T_r$ approaches K_v the errors in rate diminish. Hence the improvement obtained by making $K_v = 1/T_r$ diminishes.

Change in Rate

The most difficult input for the adaptive system to reproduce is a change in rate. The system must measure the rate and change the gain to obtain smooth operation. The transient during the period of rate measurement and gain change is of interest.

A change of input rate from 27.5 quanta per second to 3.2 quanta per second is the maximum which can occur in the adaptive range.

Figure 39 shows this transition. The values of the system parameters are:

$$K_v = 28 \text{ sec}^{-1}$$

$$K'K_v/T_r = 3.5 \text{ sec}^{-1}$$

$$T = 0.0125 \text{ sec}$$

$$\zeta = 1$$

The rate sensing circuit requires one pulse period to measure the rate. The output from the counters is not switched until one-half pulse period later. This is done to prevent timing problems in the counting process. As a result the gain is not changed until one-half pulse period after the first pulse at the new rate has been received. This is evident in figure 39. There is some advantage to this in the transition from fast to slow rates. If the gain were changed as soon as the rate changed the system would have to be brought to the lower rate at a

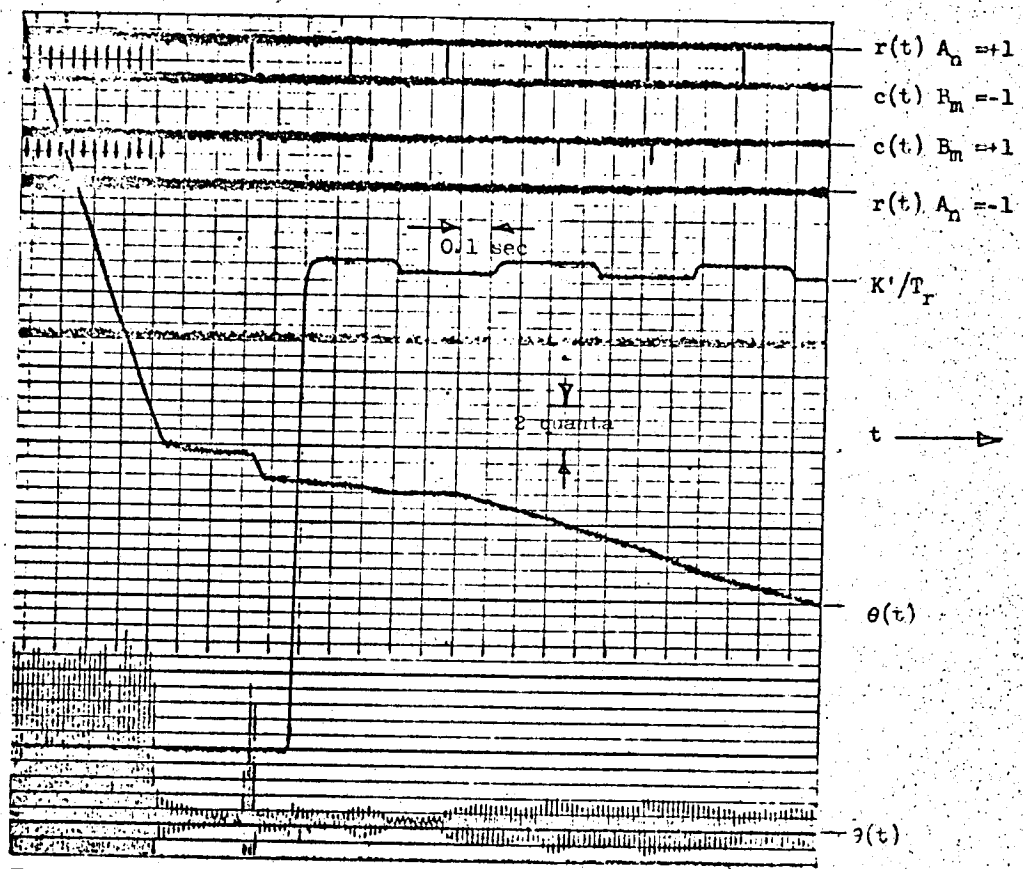

Figure 39. - Adaptive change in rate 27.5 quanta/sec to 3.2 quanta/sec.

lower position loop gain. This delay in the gain change does cause a flat spot in the response since the first slow rate input pulse is executed at high gain.

At the transition from a slow input rate to a fast rate the delay in the gain change causes a slightly larger initial error. At worst this error is equivalent to a delay in G(s) of $3T_r/2$. The amount of the error would depend on the difference in rates and the system dynamics.

Summary

The self-adaptive system definitely has smoother response at low input pulse rates than the nonadaptive system. Figure 40 shows the value of:

$$I = |1 - \dot{\theta}_{sg}(t)\ T_r|\ \max$$

This is shown for the self-adaptive and the nonadaptive pulse-data systems at several input pulse rates. As was illustrated in figures 31 to 38 the improvement at lower pulse rates is much greater than that at higher rates. The amount of improvement depends on the value of K_v and the form of G(s). If K_v is large and G(s) does not contain large time constants the improvement is great. If K_v is small and, or G(s) has large time constants, the improvement will not be as great. This is due to the larger velocity errors and the smoothing action of G(s).

The theoretical values for I are also shown in figure 40. These are calculated in appendix I. The values of I for the adaptive system would be zero if $K_v = 1/T_r$. However because of variations in

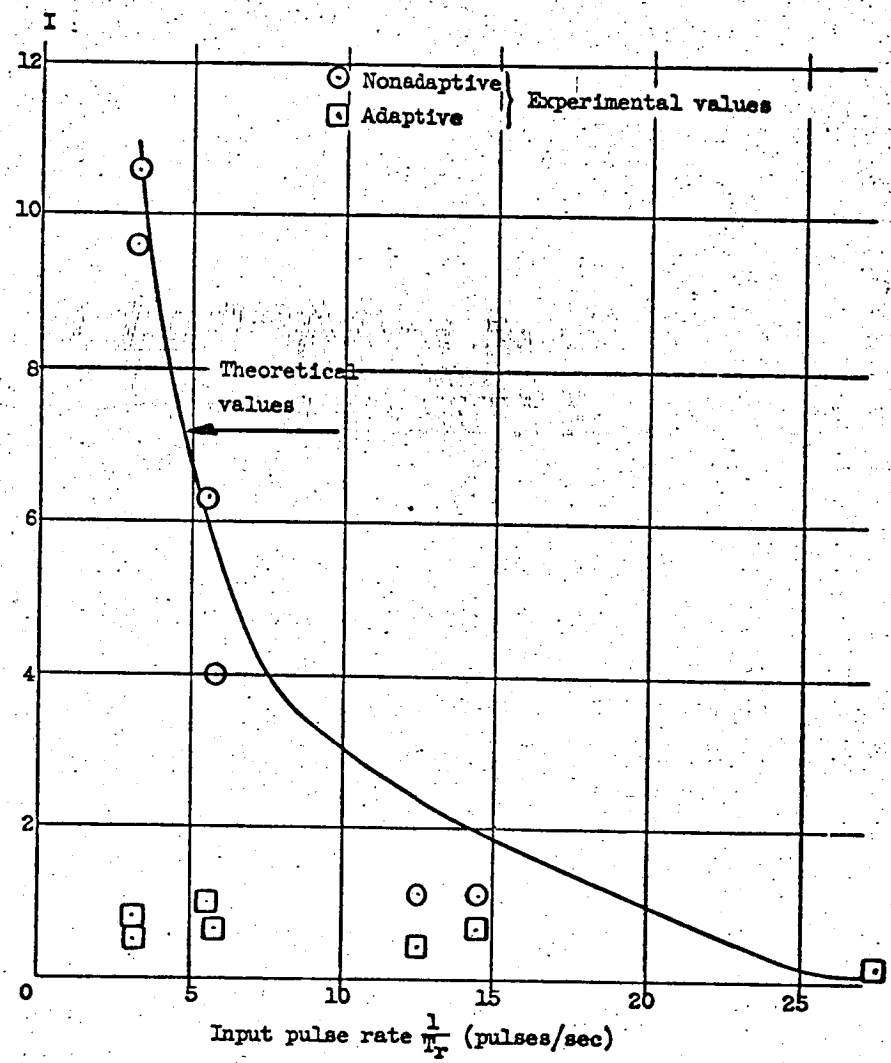

Figure 40. - Adaptive and nonadaptive smoothness.

friction and prime mover parameter variations the actual values are higher.

In any practical pulse-data system G(s) will have time constants as small as possible. This will insure that K_v can be made large so that the velocity error will be small at high rates. In this case the self-adaptive control exhibits very substantial improvements in the response to inputs at low rates.

CHAPTER VII

CONCLUSIONS AND AREAS OF FUTURE WORK

The self-adaptive system described in this thesis has the advantage of digital accuracy with analog smoothness of operation. The low speed smoothness has been improved without impairing the accuracy.

Methods for the analysis and synthesis of pulse-data systems are developed here. The methods are applied to the design of an actual system.

(1) The time response of a pulse-data system may be obtained using the convolution integral. This can be done graphically or could be performed on a digital computer.

(2) An exact method to determine the critical value of one system parameter is developed. This is based on the system response to a single input pulse. The method determines the critical parameter value for which the "error" $e(t)$ does not change sign.

Existing methods are also used in the analysis to present a "synthesis program" for use in the design of pulse-data systems.

There are several areas of future work which could prove fruitful.

(1) Statistical control theory might be applied to this type of system. The process of quantization has been handled by statistical methods, perhaps some of these methods could be applied here.

(2) The self-adaptive method used here might be applied to a relay servomechanism. This would improve its response to ramp inputs and still preserve the simplicity and quick response obtained on this type of system.

(3) The optimum time to exercise the change in gain used in the adaptive control might be investigated. For example the input pulses $r(t)$ might be delayed in time while the rate was being measured. The gain change could then be made as soon as the rate changed. The change might be made instantly when the rate change was slow to fast. A delay could be included when the change was fast to slow to permit reducing the system velocity at high gain. The time constant of the gain change could also be controlled. Some combination of these methods might improve the response still more.

(4) Stabilization methods to increase loop gain are of interest. The nonlinear methods applied in relay servomechanisms might be used to improve the open loop gain at high speeds. If linear compensation were used the graphical method of determining the critical parameter value for no reversal of $e(t)$ could be used.

(5) Other system parameters might be controlled in addition to the loop gain to provide adaptive control. For example the damping ratio of $G(s)$ might also be controlled as a function of input rate.

APPENDIX I

DESIGN OF AN ADAPTIVE PULSE-DATA SYSTEM

This section will illustrate the application of the methods described in chapter II. The analysis consists of the following parts:

1. Prime mover and gear box selection.
2. Prime mover transfer function.
3. Synthesis of pulse-data position loop gain.
4. Steady state response.
5. High speed errors.
6. Step input response.
7. Adaptive range.
8. Errors when input pulse rate changes in the adaptive control.
9. Ripple due to adaptive gain quantization.

Prime Mover and Gear Box Selection

It is desired to design and construct a pulse-data system to illustrate the advantages of the adaptive control. This leads to the following requirements for the prime mover and gear box:

(a) The prime mover power level can be small but the methods of data handling must be applicable to high power systems.

(b) The major time constants of the prime mover transfer function must be small.

(c) Backlash between the prime mover and the quantizer must be as small as possible. The effects of backlash are quite serious in this type of system. If it is not carefully controlled it may obscure the test results.

(d) A position transducer is to be coupled to the quantizer. Any system transients should be confined to the linear range of this transducer which is plus or minus 60°.

A 60 cycle per second a-c voltage carrier was selected as the signal medium in the prime mover section of the system. An a-c voltage is easier to amplify without drift than are d-c voltages. Alternating current is readily available. A signal of this form can control a prime mover of nearly any power level and type. This method does have the disadvantage that it is difficult to compensate a carrier system. However, by choosing the prime mover carefully and employing tachometer feedback it is hoped that compensation will not be required.

A prime mover power level of 15 watts appears to be optimum in this application. This provides a stall torque of one lb-in which can be easily handled by instrument-type gear trains. Higher power levels would require special gear trains. Lower power levels would be more sensitive to gearing friction.

An a-c two phase servomotor possesses the most desirable characteristics for this application. There is no brush friction. There are no pulsations due to armature voltage ripple which can occur with d-c servomotors powered by rectifiers. A motor with a coupled a-c tachometer was selected so that the prime mover time constants could be reduced by velocity feedback.

A breadboard-type gear box was used to couple the quantizer and position transducer to the prime mover. The overall ratio of the gear box was selected in the following manner:

(a) Backlash had to be less than 0.1 quanta. The quantizer had 100 quanta points per revolution. Thus backlash had to be less than 0.36° reflected to the quantizer end. This is less than most precision instrument gear trains. The number of meshes should therefore be a minimum.

(b) The position transducer linear range of 120° determined the minimum gear ratio. At top speed the velocity constant of a continuous system would be 12 sec^{-1} or better. At 3600 revolutions per minute the motor would lag 5 revolutions behind. Thus the 120° of transducer rotation should equal at least 5 motor revolutions.

$$\frac{5}{1/3} = 15 = \text{minimum gear ratio}$$

A gear box of three meshes 2:1, 2.5:1, and 3.5:1 was constructed. This provided an overall ratio of 17.5:1. The measured backlash at the quantizer end of the train was 0.16°.

Prime Mover Transfer Function

The two phase servomotor and amplifier can be represented by a transfer function of the following form:

$$\frac{\theta(s)}{e'(s)} = \frac{K}{s(T_m s + 1)(T_L s + 1)}$$

where $e'(s)$ is the Laplace transform of the voltage input to the prime mover amplifier. T_m is due to the motor and load inertia and the slope of the motor torque-speed curves. T_L is due to the motor reactances.

In order to reduce T_m and T_L a velocity loop was closed around the motor. This produces an overall transfer function:

$$\frac{\theta(s)}{e(s)} = \frac{K_v}{s(T^2s^2 + 2\zeta Ts + 1)}$$

where $e(s)$ is the digital to analog converter output whose units are quanta.

The synchronizer circuit introduced a delay of 0.005 sec. This delay will be included in the overall transfer function.

$$\frac{\theta(s)}{e(s)} = \frac{K_v e^{-0.005s}}{(T^2s^2 + 2\zeta Ts + 1)s} = G(s)$$

Figure 41 shows the prime mover velocity response to a change of $e(t)$ of one quanta. The values of T and ζ from figure 41 are:

$T = 0.0125$ seconds

$\zeta = 0.3$

This is the minimum value of T which can be obtained with this system. Further increases in velocity feedback gain did not materially improve the value of T but did reduce ζ. Since T is close to the carrier period further reductions of T could only be accomplished by increasing carrier frequency.

Some testing was performed with slightly different velocity loop gains. This resulted in values of ζ from 0.25 to 1.0.

Synthesis of Pulse-Data Position Loop Gain

In both the adaptive and nonadaptive systems it is desirable to have the response as smooth as possible at all rates. Thus it is desirable to have the output of the digital to analog converter $e(t)$ as smooth as possible. This will be accomplished if K_v is selected such that $e(t)$ does not reverse sign for a single input pulse.

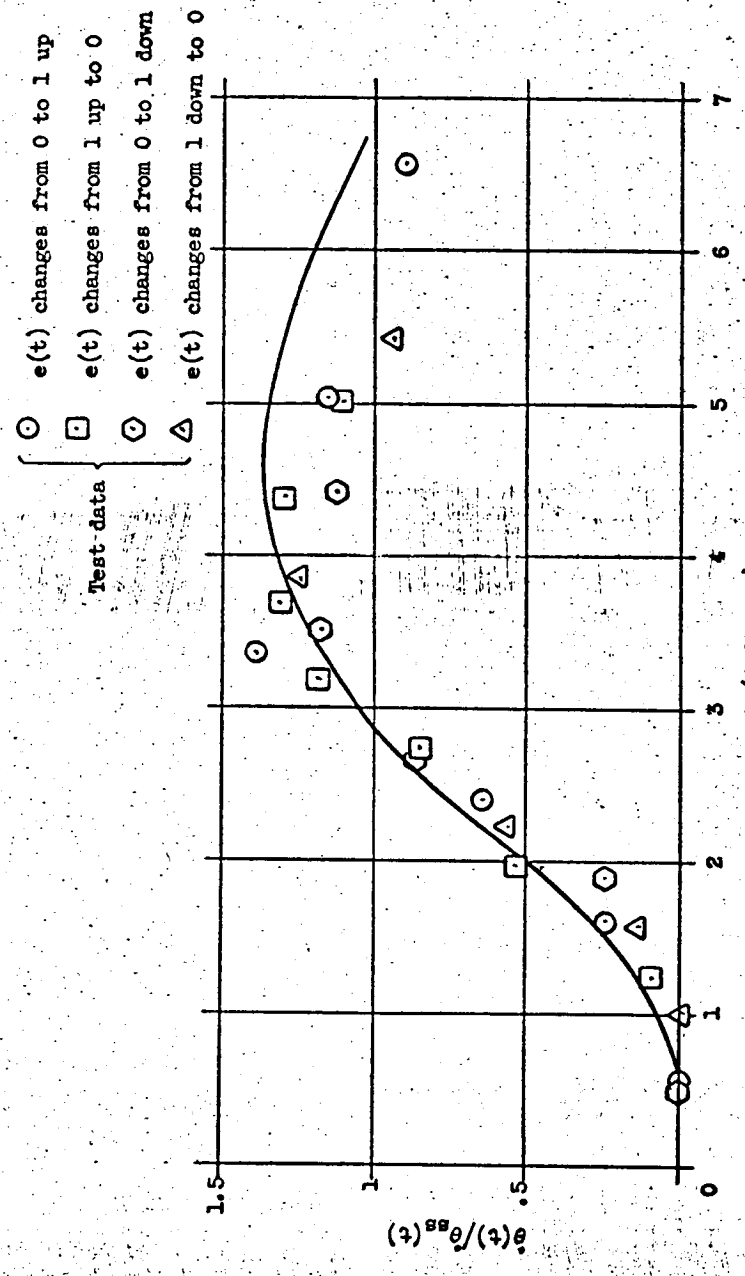

Figure 41. - Prime mover transient response.

Chapter II presented a graphical method for determining the critical value of a parameter for a controlled variable overtravel of one quanta.

Since the prime mover has complex poles in its transfer function the method for case II must be used.

$$G(s) = \frac{K_v T e^{-0.4s}}{s(s^2 + 0.6s + 1)}$$

Where $t = T\tau = 0.0125\tau$. This makes the prime mover equations dimensionless in time.

(a) The response to a unit step $q_u(\tau)/K_vT$ is plotted versus time in figure 42.

(b) The value of τ_1, the time at which the first quanta point is passed, is plotted versus b the distance from the initial position to the first quanta point (fig. 43). This is plotted for various values of K_vT.

(c) Figure 44 shows τ_m the time at which $q_u(\tau)-q_u(\tau-\tau_1)u(\tau-\tau_1)$ is a maximum versus τ_1. This is determined by plotting $q(\tau)$ the impulse response of G(s). A second plot of $q(\tau)$ is shifted by $\tau = \tau_1$ and the time where $q(\tau) = q(\tau-\tau_1)u(\tau-\tau_1)$ is τ_m.

(d) Also plotted in figure 44 is $\theta(\tau_m)/K_vT$ where $q_u(\tau_m) - q_u(\tau-\tau_1)u(\tau_m-\tau_1) = \theta(\tau_m)$. This curve is formed by selecting a value of τ_1, this yields τ_m from figure 44. Then figure 42 produces a value of $\theta(\tau_m)/K_vT$ by subtracting the ordinates of $q_u(\tau)/K_vT$ at $\tau = \tau_1$ and at $\tau = \tau_m$.

(e) Then using the relations plotted in figures 43 and 44, figure 45 may be developed. This is a plot of $\theta(\tau_m)$ versus b. A

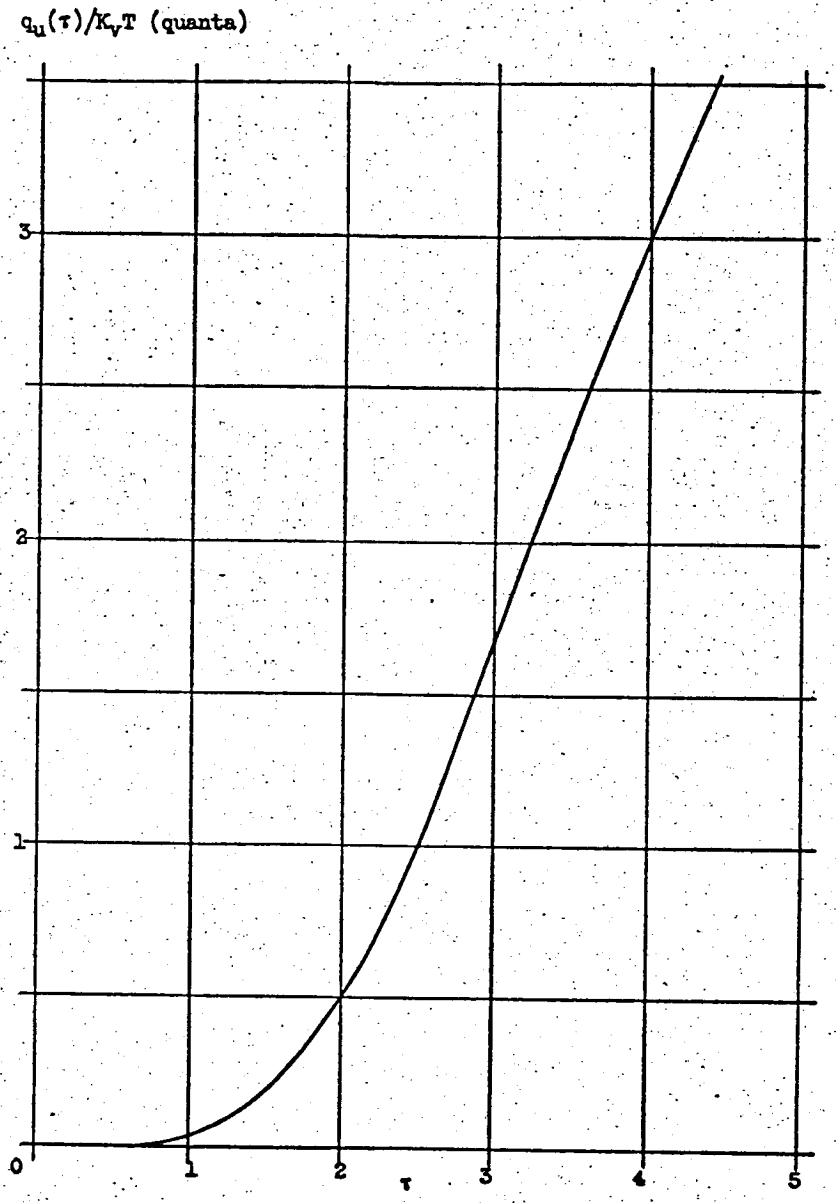

Figure 42. - Unit step response.

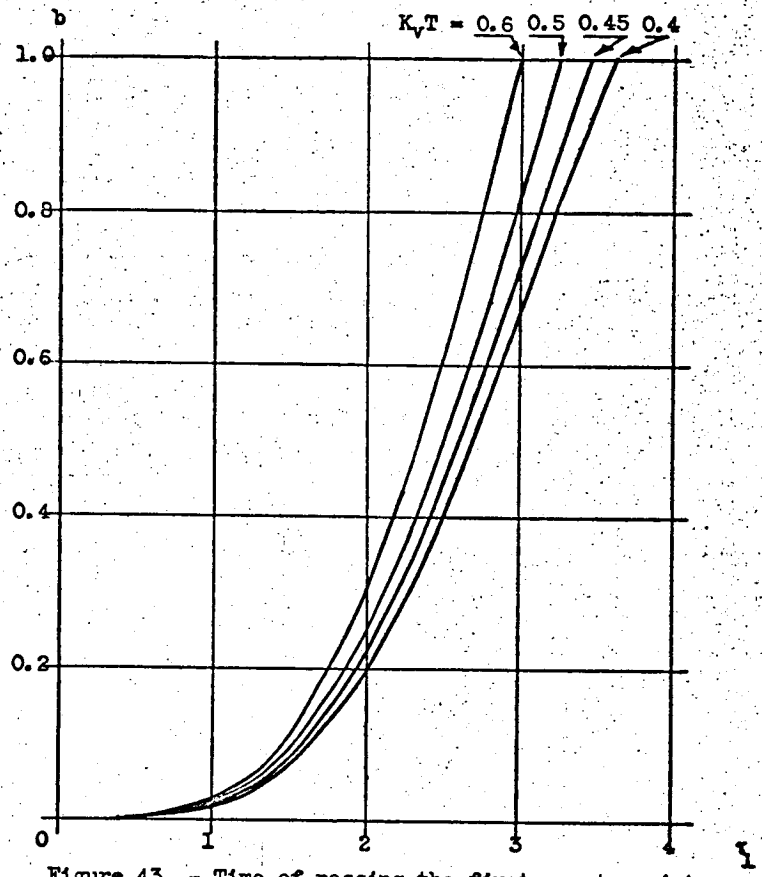

Figure 43. - Time of passing the first quanta point τ_1 versus distance to first quanta point b.

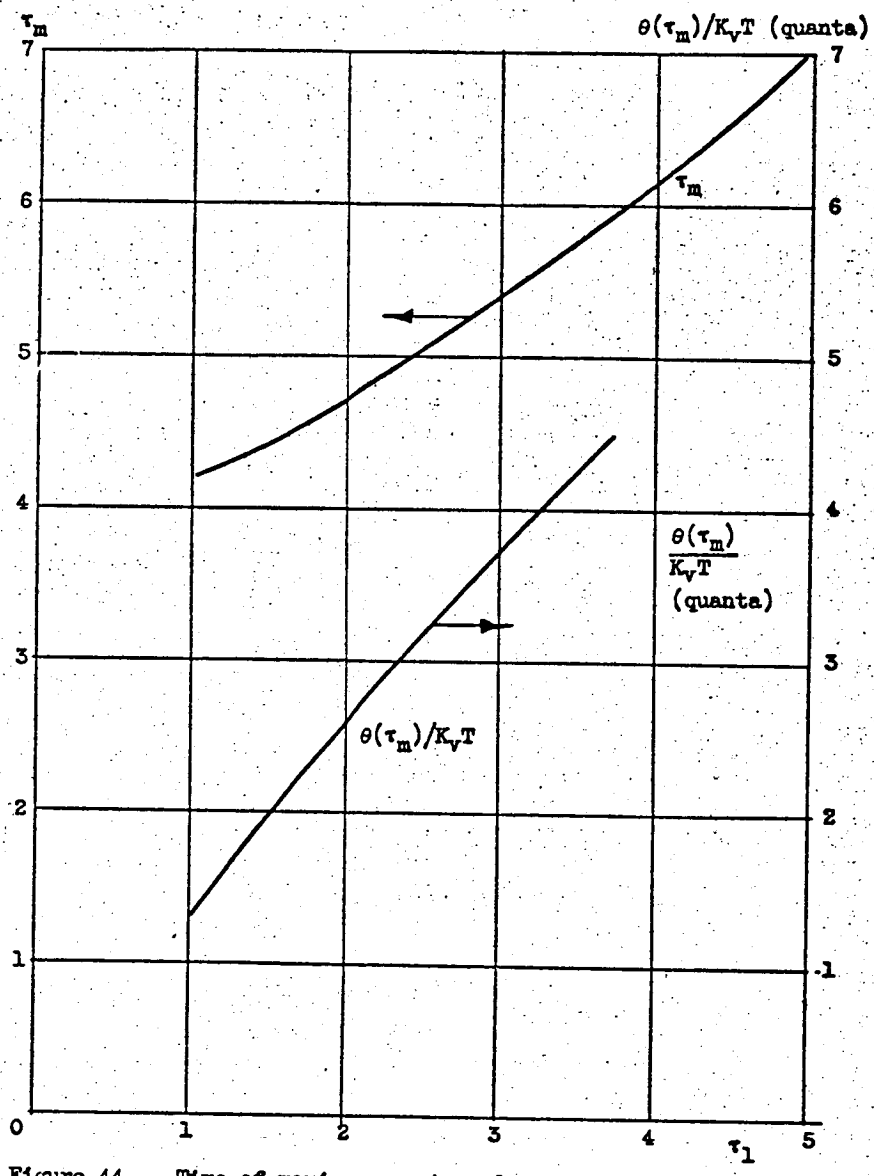

Figure 44. - Time of maximum overtravel τ_m and maximum travel $\theta(\tau_m)/K_vT$ versus time of passing first quanta point τ_1.

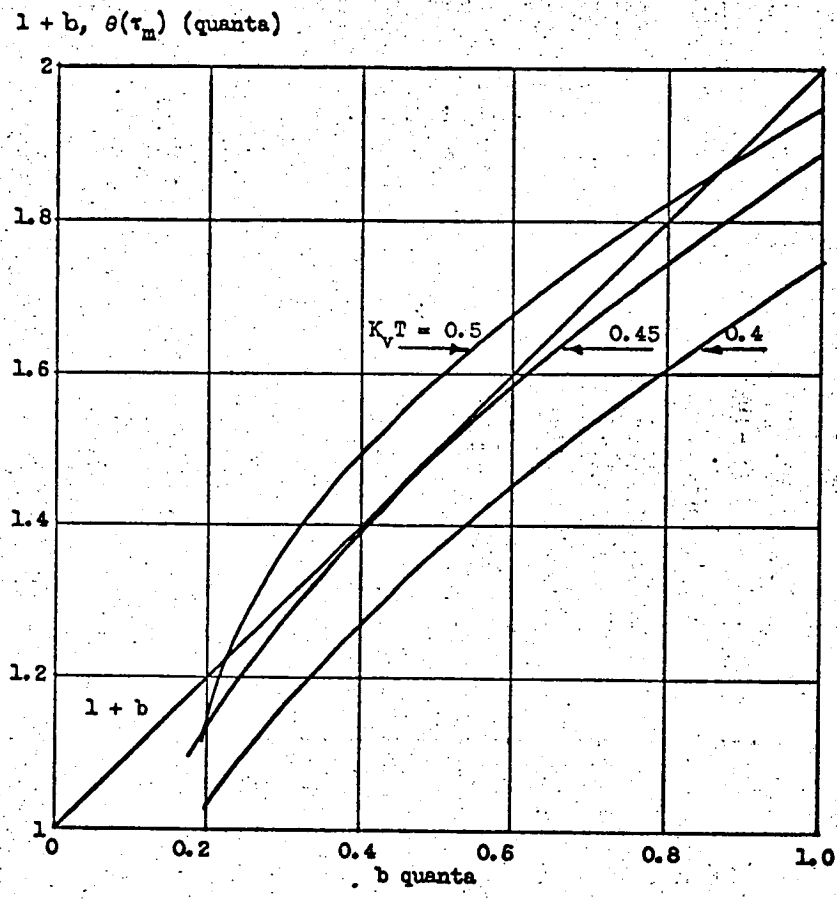

Figure 45. - Maximum travel $\theta(\tau_m)$ versus distance to first quanta point b.

value of K_vT is selected. Then for each value of b a value of τ_1 is found from figure 43. For this value of τ_1 figure 44 supplies $\theta(\tau_m)/K_vT$ which when multiplied by K_vT yields $\theta(\tau_m)$ for the specified K_vT and b. 1 + b is also plotted in figure 45. Then the requirement for an overtravel of one quanta or less is:

$$\theta(\tau_m) \leq 1 + b$$

The $K_vT = 0.45$ curve is tangent to the 1 + b line and lies below it for all values of b. Thus this is the critical value.

Therefore for no reversal of $e(\tau)$ when a single input pulse is applied

$$K_vT < 0.45$$

The curves shown in figure 45 also indicate that the maximum overtravel for $K_vT = 0.45$ occurs at $b = 0.45$. This is illustrated in figure 46 where the system response with $K_vT = 0.45$ is plotted for three values of b. The response for $b = 0.5$ overtravels more than the others. For $b = 0.2$ the overtravel is 0.98 quanta. When $b = 0.9$ the overtravel of $\theta(\tau)$ is 0.9 quanta. At $b = 0.5$ it overtravels one quanta. Since $T = 0.0125$ sec the critical value of K_v is:

$$K_v = 37.5 \text{ sec}^{-1}$$

A value lower than this is selected to make sure that there will be no overtravel with variations in the system parameters. The value selected is:

$$K_v = 30 \text{ sec}^{-1}$$

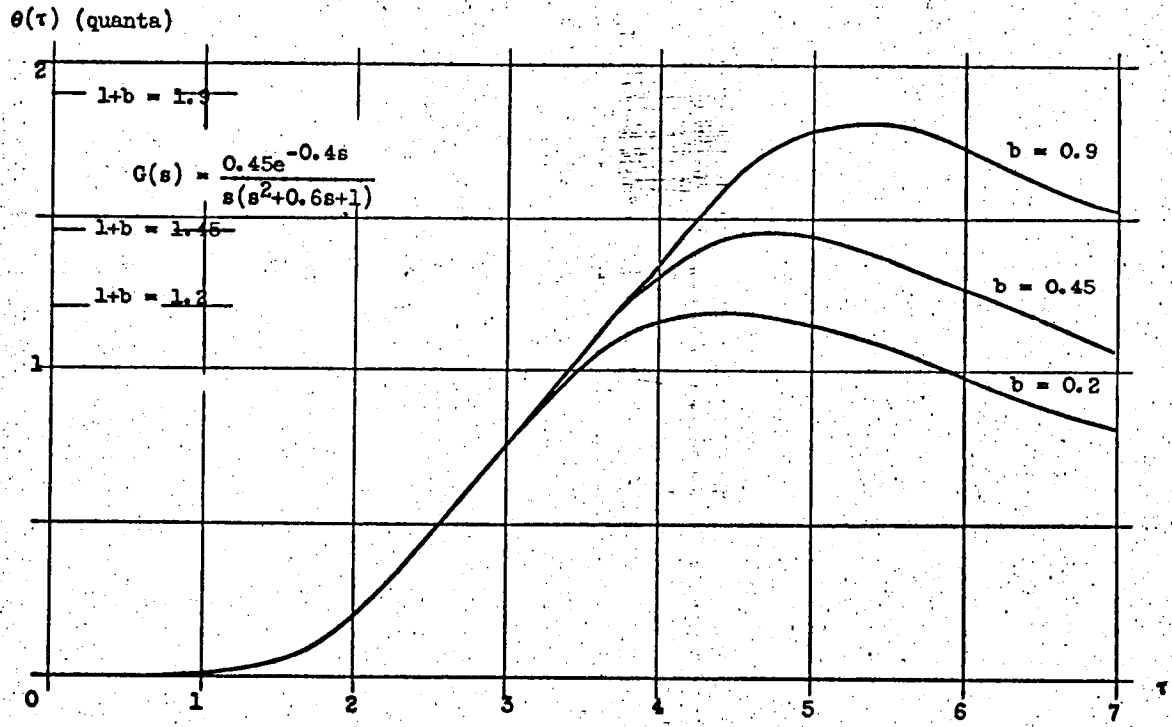

Figure 46. - Response for various values of b, distance to first quanta point.

Steady State Response

In order to predict the low speed smoothness of the pulse-data system an analysis of the steady state response was performed. The input $r(t)$ is assumed to consist of a train of pulses of fixed period T_r. The deviations of the controlled variable velocity from the desired value will then provide a measure of smoothness. The smoothness for a given value of system gain $K_v T$ will be worst at low rates.

The steady state Laplace transform method outlined in chapter II will not work for the system to be constructed. This is due to the transport lag. The steady state solution for controlled variable velocity $\dot{\theta}_{ss}(t)$ is the difference between the total solution over the first period and the transient solution for the first period. Both of these solutions are zero at $t = 0$ since both Laplace transforms involve $e^{-0.45}$ in the numerator. Thus the total solution must be zero at time zero according to this method. However at high input pulse rates the output rate cannot be zero at the time of an input pulse. This does not correspond to the actual velocity as determined by graphical methods.

The graphical method outlined in chapter II employing the convolution integral is used to obtain the steady state response.

(a) The system is started from rest with an input pulse train of period T_r starting at $t = 0$. The solution for $\theta(t)$ is plotted as was outlined in chapter II. However, only the straight line approximation is plotted. The points where $\theta(t) = b + \sum_0^\infty B_m$ are noted by using the paper strip to convolve $\dot{e}(t-\tau)$ with $q_u(\tau)$ in the regions around the quanta points.

(b) This process is continued until $e(t)$ reaches the steady state as noted by a constant time between feedback pulses. Then $\Delta\tau$ the time from an input pulse to a feedback pulse is noted. This specifies $e(t)$ in the steady state.

(c) Then a paper strip is marked with $r(-\tau)$ and $c(-\tau)$ for steady state conditions. The sign of $r(-\tau)$ and $c(-\tau)$ pulses are noted. The impulse response $q(t)$ is also plotted. The steady state velocity can then be plotted versus t. The paper strip is located under the abscissa of $q(t)$ so that the $\tau = 0$ point on the strip is located opposite a value of t at which the transients of $q(t)$ have died out. The steady state velocity can then be plotted point by point by adding algebraically the ordinates of $q(t)$ which occur above $c(-\tau)$ and $r(-\tau)$ pulses.

The method is applied to the system with an input pulse period $T_r = 0.074$ sec. In order to use dimensionless plots T_r and $\Delta\tau$ are normalized by dividing them by T the prime mover time constant. This defines two dimensionless numbers.

$$\frac{T_r}{T} = \beta = 5.92 \qquad \frac{\Delta\tau}{T} = \alpha$$

Then:

$$G(s) = \frac{K_v T e^{-0.4s}}{s(s^2 + 0.6s + 1)}$$

Where:

$$K_v T = 0.375$$

Figure 47 shows how α is determined. The straight line approximation to unit step response $q_{uss}(\tau)$ and the correction $q_{ut}(\tau)$ are plotted first. Using the correction ordinates the exact response near

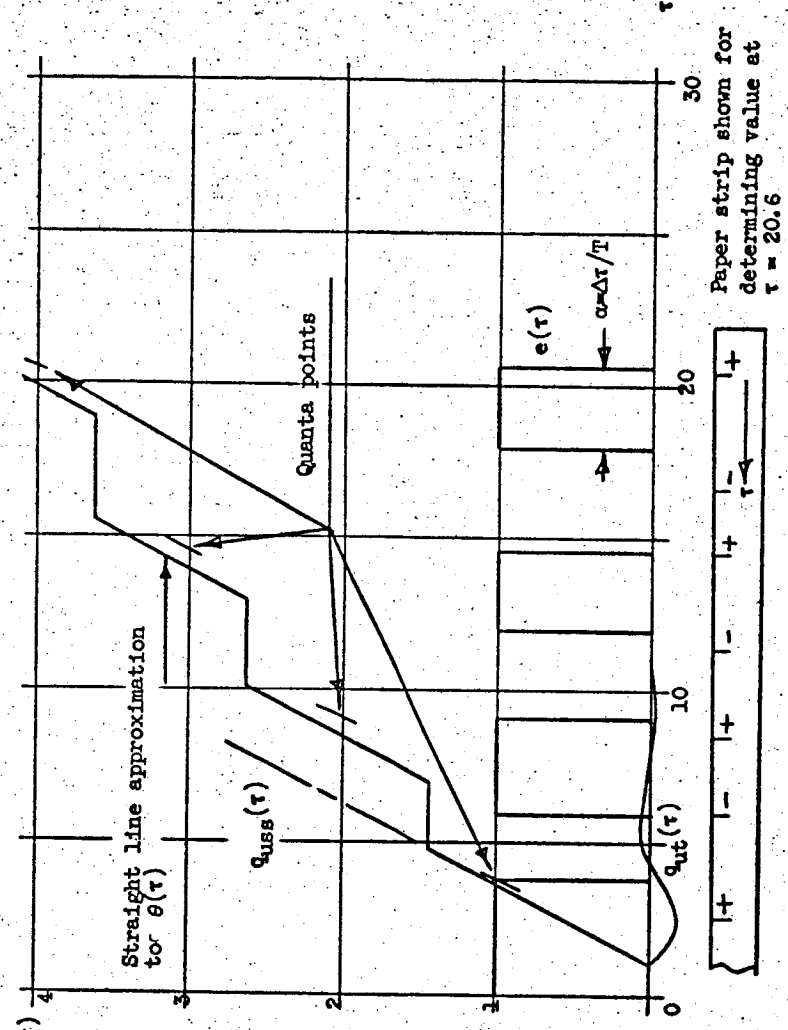

Figure 47. - Graphical construction for $\alpha = \Delta\tau/T$, the steady state time between an input pulse and a feedback pulse.

$\theta(\tau) = 1$ is determined. This yields T_{f0} the time of the first feedback pulse. At this time the straight line approximation starts to change due to the feedback pulse. At $\tau = 4.7$ the approximation slope becomes zero. At $\tau = 5.92$ a second input pulse is recieved. $e(\tau)$ is also plotted to indicate when equilibrium is reached. When $e(\tau)$ becomes periodic the response has reached the steady state and the width of $e(\tau)$ is equal to α. The paper strip is shown in the proper orientation for determining $\theta(\tau)$ at $\tau = 20.6$. The plus marks indicate input pulses. The minus marks denote feedback pulses. The ordinates of $q_{ut}(\tau)$ above these marks are added according to the signs to produce the correction to the approximate path. In this case the correction is minus 0.25 quanta. Thus this distance is subtracted from the straight line approximation to yield a value $\theta(\tau) = 4$. The quanta point is assumed to be located at $\theta(\tau) = 4$ so a feedback pulse is received at $\tau = 20.2$. This construction yields a value of $\alpha = 2.66$.

Now the response $\theta(\tau)$ over one cycle can be plotted and differentiated to produce $\dot{\theta}(\tau)$. The method used will be the one described in part (c) above. Figure 48 illustrates the method for $\beta = 5.92$. A paper strip is made with a zero point arbitrarily located. $q(\tau)$ is plotted. The zero point on the strip determines the location of $\dot{\theta}_{ss}(\tau)$, the steady state velocity, on the paper. Starting from somewhere to the left of the zero point plus marks are made $\beta = 5.92 = \tau$ units apart moving to the left. Since $\alpha = 2.66$ a minus mark is made $2.66 = \tau$ units to the left of every plus mark. The strip is then placed parallel to the τ axis with one of the plus marks opposite the

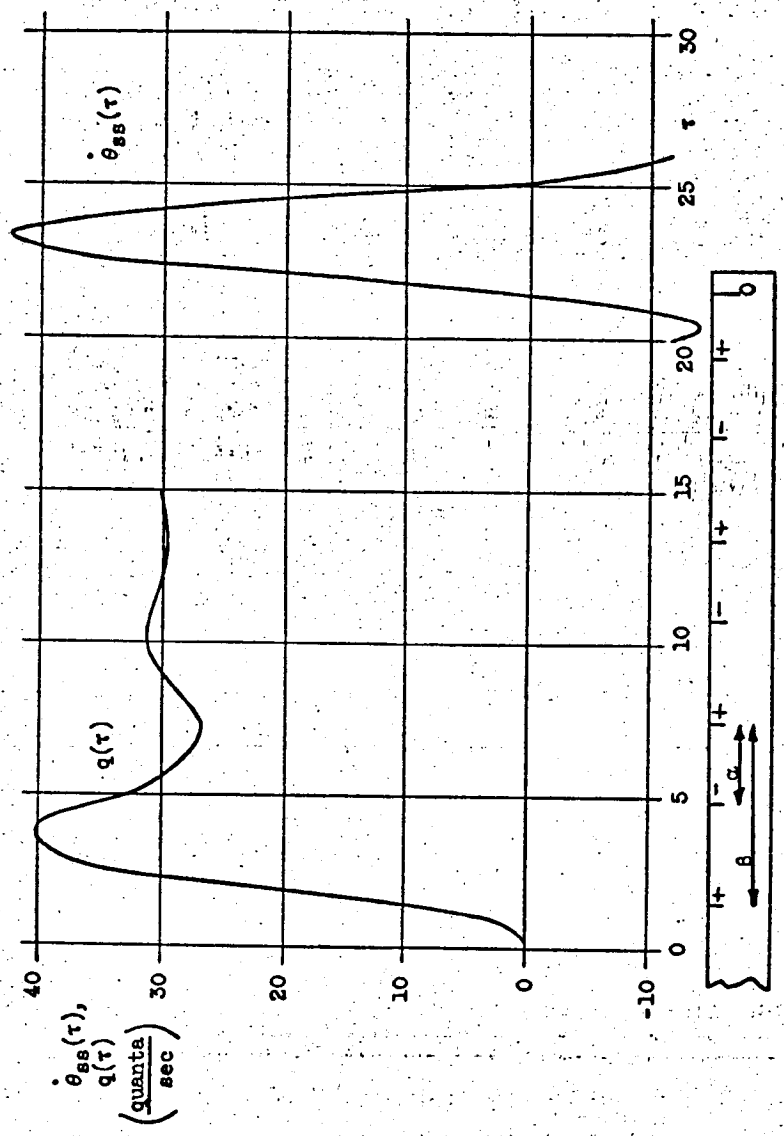

Figure 48. - Steady state response T_r = 0.074 sec.

$\tau = 0$ abscissa. The first plus mark to the left of the zero mark should be opposite an ordinate of $q(\tau)$ which has reached the steady state. Now the ordinates of $q(\tau)$ above the strip are added according to the sign adjacent to the mark on the strip. The sum yields the value of $\dot{\theta}_{ss}(\tau)$ at the time of an input pulse. The strip is moved to the right and the process is continued until $\dot{\theta}_{ss}(\tau)$ is determined over one input pulse period. The strip is shown in figure 48 located to determine $\dot{\theta}_{ss}(\tau)$ at $\tau = 21.5$ [illegible] (note the time scale for $\dot{\theta}_{ss}(\tau)$ is arbitrary in its location). The ordinates above the plus marks are added with a pair of dividers those above the minus marks are subtracted to produce $\dot{\theta}_{ss}(\tau)$. It is sometimes useful to note the ordinates in pairs, one plus and the other minus. The difference in ordinates is then the net contribution of the two. In this way the plus mark at $\tau = 19.4$ and the minus mark at $\tau = 16.74$ for the strip location shown produce no net contribution.

In order to evaluate the smoothness of the steady state response the criterion developed in chapter III will now be used.

$$I = \left|1 - \dot{\theta}_{ss}(\tau)\, T_r\right|_{max}$$

The maximum and minimum values of $\dot{\theta}_{ss}(\tau)$ are determined and applied to this relation. For $K_v T = 0.375$ $\beta = 5.92$ figure 48 shows:

$$\dot{\theta}_{ss}(\tau)_{max} = 42.2 \text{ quanta/sec}$$

$$\dot{\theta}_{ss}(\tau)_{min} = -14.0 \text{ quanta/sec}$$

Thus:

$$I = \left|1 - 42.2 \times 0.074\right|_{max} = 2.12$$

Note that it is only necessary to determine the maximum and minimum values of $\dot{\theta}_{ss}(\tau)$ to evaluate I.

The process outlined above was carried out for several values of T_r at a fixed loop gain $K_v = 30\ sec^{-1}$. The resulting values of I were determined.

Figure 49 shows the values of I versus the input pulse rate $1/T_r$. As would be expected I is large for low input pulse rates and becomes smaller as the pulse rate approaches $K_v = 1/T_r$. Thus at a fixed position loop gain the errors in the steady state velocity become large at low rates. The output smoothness deteriorates very rapidly for low input pulse rates. The adaptive pulse-data system will improve the smoothness at these low input pulse rates.

High Speed Errors

In order to check the errors which occur at high input pulse rates the graphical techniques of chapter II are applied.

An input of a finite number of pulses at a fixed frequency was applied. Where:

$$r(\tau) = \sum_{0}^{35} \delta\left(\tau - \frac{nT_r}{T}\right)$$

$$\frac{T_r}{T} = \frac{0.0032}{0.0125} = 0.256 \cong \beta$$

This corresponds to a servomotor speed of 3280 rpm. According to the relation developed in chapter II:

$$\Delta\tau = \frac{1}{K_v} - a\,T_r$$

In this case $K_v = 30\ sec^{-1}$, $T_r = 0.0032$sec. Thus:

$$a = 10 \text{ quanta}$$

The expected steady state error should be ten quanta. However,

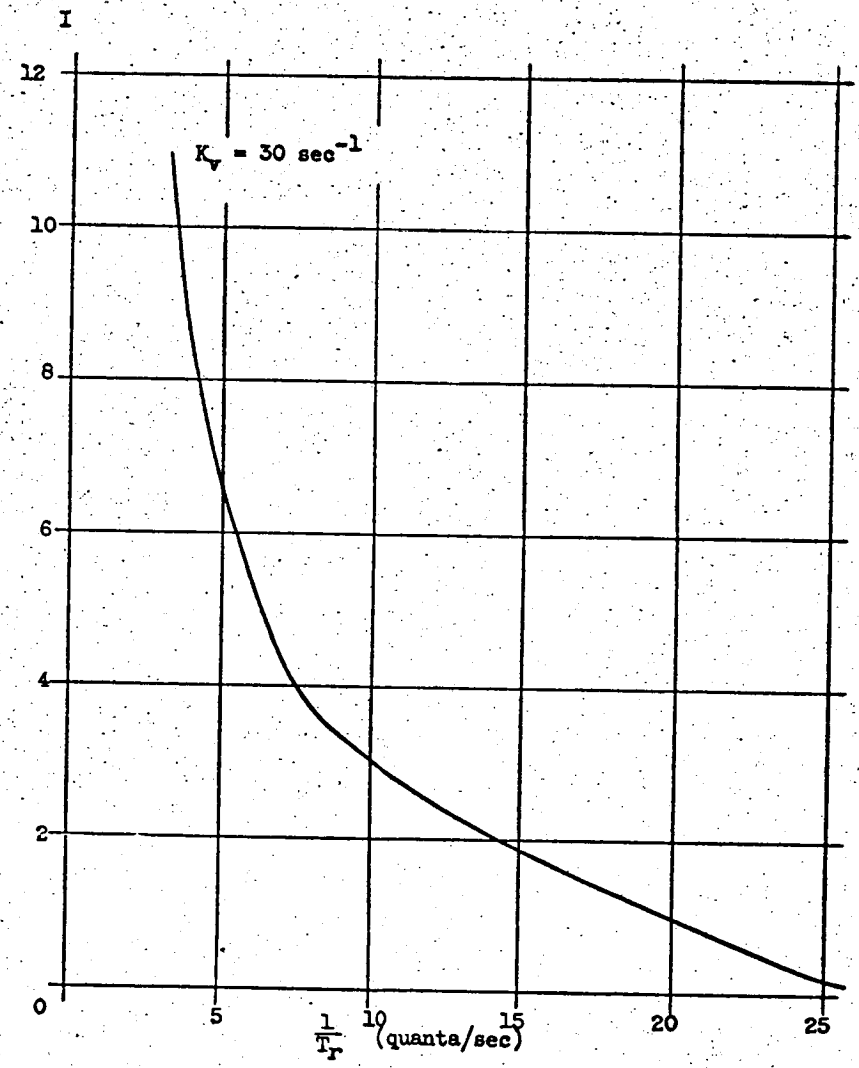

Figure 49. - Smoothness versus input pulse rate.

if the input pulses are programed as outlined in chapter III for the case where $1/K_v > T_r$, the steady state variation from the desired path should only be nine quanta.

Figure 50 shows the starting and stopping transient. The maximum deviation from the desired path is ten quanta. This occurs at $\tau = 4$. In the steady state the error does approach nine quanta. The overshoot at stopping is 0.9 quanta.

Since this is very close to the maximum prime mover rate, ten quanta is about the maximum error which can occur during a ramp input.

In this way the maximum required capacity of the bidirectional counter can be specified. In view of the above analysis a counter capacity of plus or minus 15 quanta should be satisfactory.

The transients in the ramp have substantially ceased after the total displacement is 33 quanta or 1/3 of a revolution of the quantizer. Since the displacement transducer linear range is 120° this verifies that the gear ratio should be satisfactory from that standpoint.

Step Input Response

The pulse-data path control does not normally receive pulses at a rate faster than it can execute. Thus T_r the input pulse period is never less than the period of the quantizer output $c(t)$ when the motor is operating at top speed. This minimum period is 0.003 sec. Thus a step input cannot occur during normal operation.

However the bidirectional counter might malfunction due to a short power failure or some other disturbance. Then a sudden change in the digital to analog converter output $e(t)$ could occur. This would produce a step input.

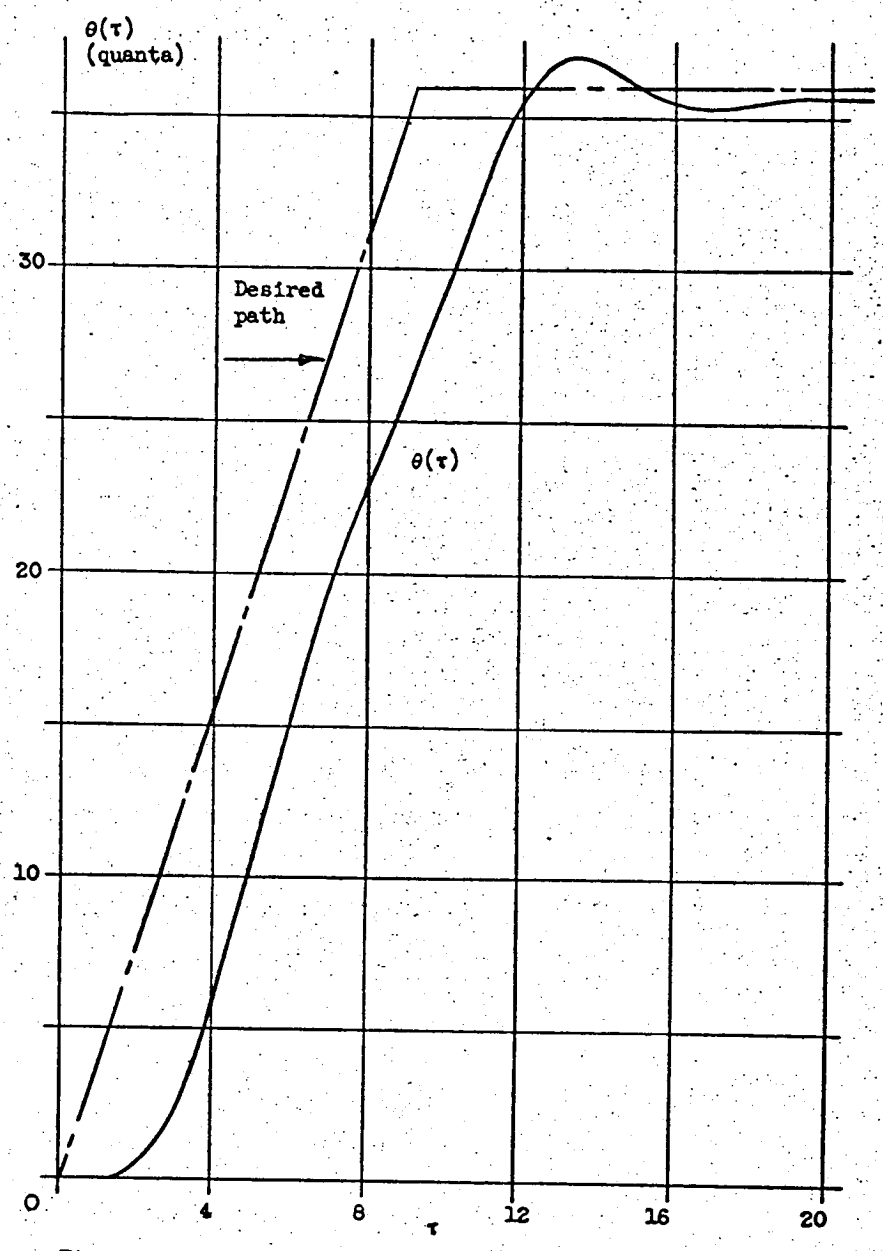

Figure 50. - Ramp response at 313 quanta/sec.

In order to insure that the system will not be unstable in this situation its response to a step input is determined. The graphical construction employing the convolution integral is used. As outlined in chapter II the system must start at rest so that the step is applied as an instantaneous change in $e(t)$ equal to the amount of the step. In the graphical construction this amounts to weighting the initial mark on the paper strip an amount proportional to the step. The initial slope of the straight line approximation is also weighted.

Figure 51 shows the resulting response for four and eight quanta steps. In the case of the eight quanta steps the initial mark on the paper strip has a weight of eight. The ordinate of the correction curve $q_{ut}(\tau)$ above this mark is multiplied by eight. The initial slope of the straight line approximation has eight times the value it would have if only one input pulse was received.

The resulting response is quite oscillatory but stable. Thus if possible any short duration disturbances which might cause $e(t)$ to change suddenly by more than one quanta should be avoided. If they do occur they will not cause instability, however.

Adaptive Range

The counters to be used in the rate circuit had a ten count capacity. For reasons mentioned in chapter V the useful range was nine counts. This means that adaptive control can be exercised over a 9:1 range of input rates.

Theoretically smoothness would be perfect when $K_v = 1/T_r$. The value of I in this case would be zero. In an actual system small

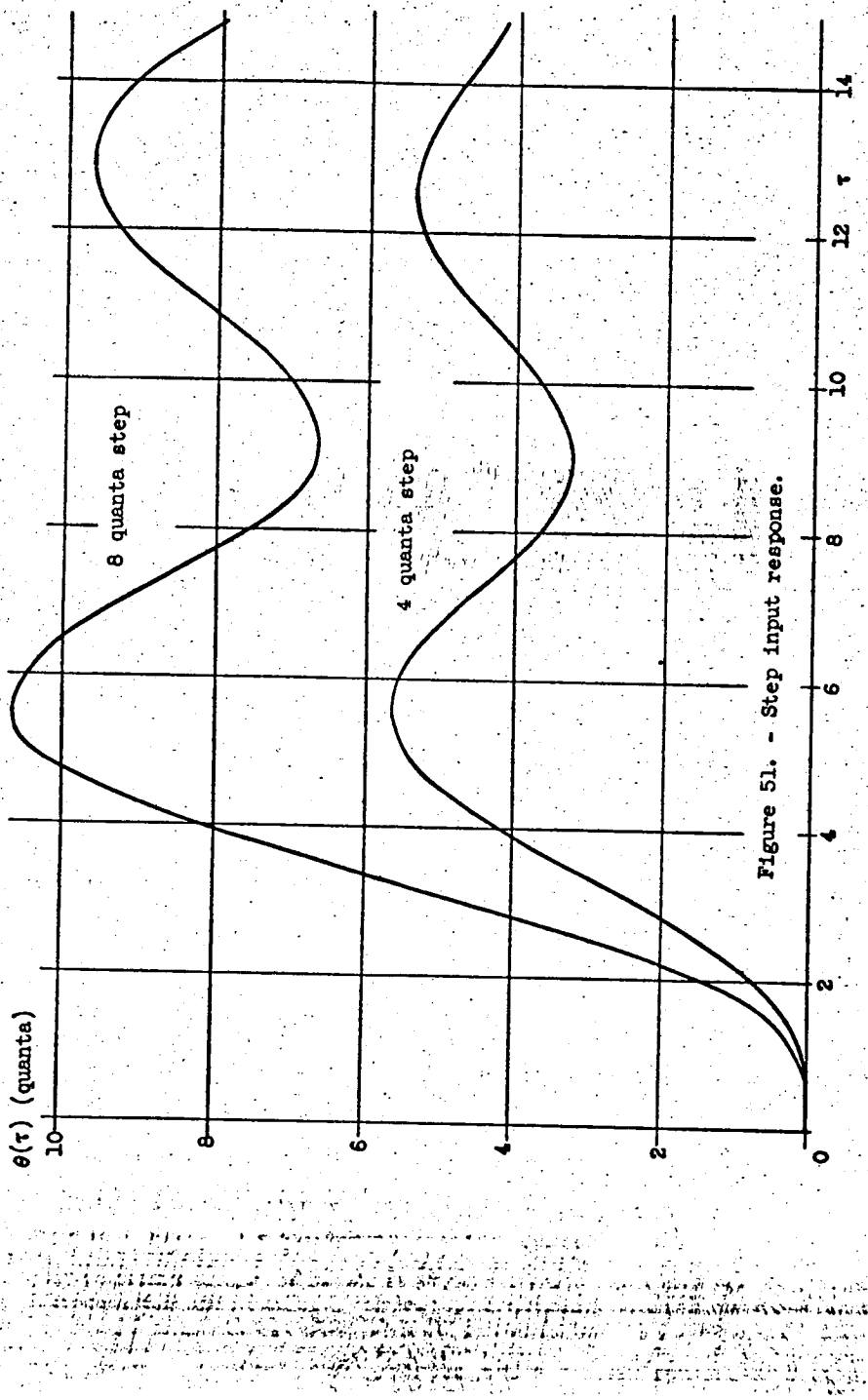

Figure 51. - Step input response.

disturbances due to friction changes and variations in gain make this ideal value of I difficult to achieve.

It was decided to start the adaptive region near $1/T_r = K_v = 30$ quanta/sec. At this point the ideal value of I would be zero. Above this input pulse rate the gain K_v would be fixed at 30 sec^{-1}. Below this pulse rate the gain K_v would be decreased linearly with input rate. The minimum value would occur at approximately 3.3 quanta/sec.

In order to evaluate the improvement in smoothness for a given reduction in loop gain K_v, I was plotted versus K_v for an input pulse rate of 3.2 quanta per second. The method described in section 4 of this part of the appendix was used to obtain the theoretical values of I. Figure 52 shows the resulting relation. The value of I decreases as the loop gain decreases until the loop gain is $K_v = 6$ sec^{-1}. There is not much further improvement until $K_v = 3.2$ sec^{-1}. This is due to the velocity transient of the prime mover. When $K_v > 3.2$ sec^{-1} the controlled variable velocity becomes negative during part of the steady state period between input pulses. When $K_v < 3.2$ sec^{-1} this does not occur. In fact the controlled variable velocity never becomes zero in the steady state. When $K_v = 3.2$ sec^{-1} the steady state value of I is zero since there is no ripple.

Figure 52 indicates that making K_v the loop gain decrease with decreasing input pulse rate definitely improves smoothness. The indicated gain at an input pulse rate of 3.2 quanta per second is about 3-3.2 sec^{-1}.

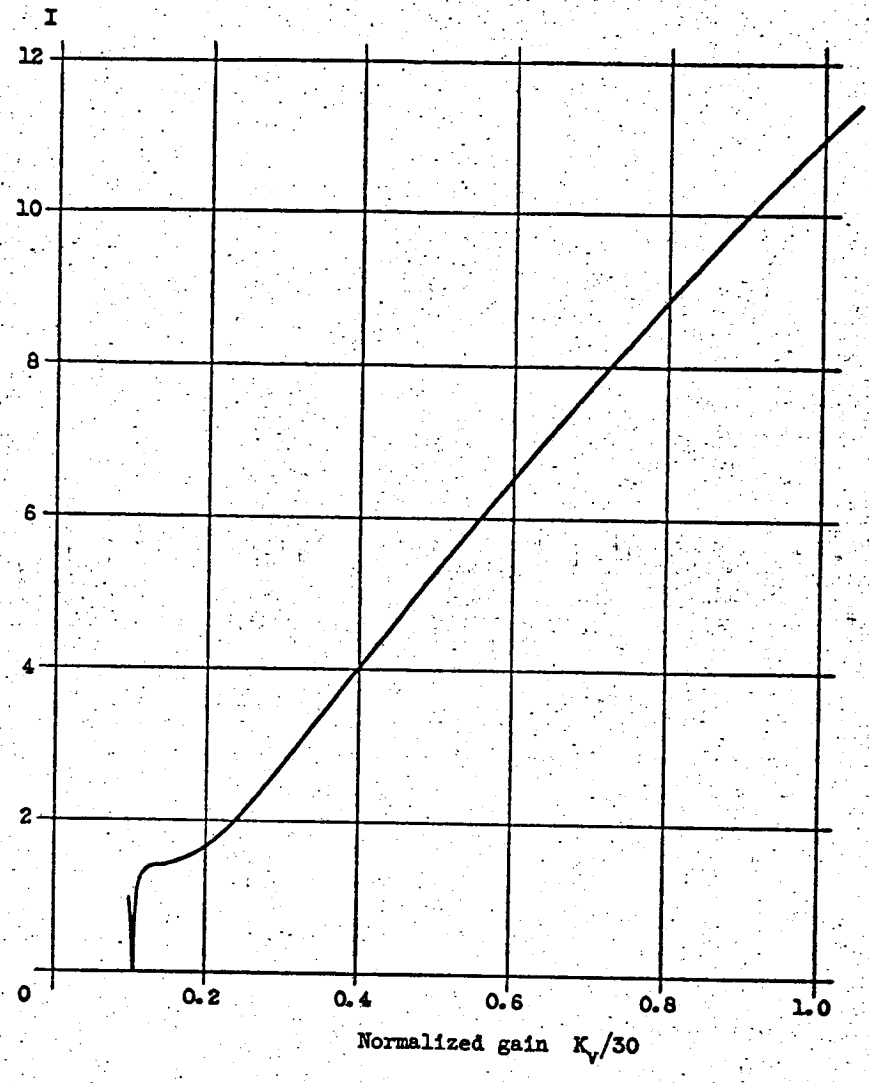

Figure 52. - Smoothness-gain relation for T_r = 0.31 sec.

Errors When Rate Changes In The Adaptive Control

The adaptive control measures the input pulse period. It then controls the loop gain K_v to make it proportional to the input pulse rate over a nine to one range of rates. When the system is operating at a high rate then suddenly changes to a low rate errors can occur. The adaptive process can be made instantaneous relative to the prime mover dynamics. However it takes a finite time to measure the rate change, which could allow errors to occur.

Figure 53 shows the system response for a change in rate from 27.5 quanta per second to 3.2 quanta per second. This covers the entire adaptive range of the system. The response was obtained by assuming that the velocity at 27.5 quanta per second was constant and $\theta(t)$ followed the ideal path. This is not exact but very nearly correct.

$$G(s) = \frac{K_v T e^{-0.4s}}{s(s^2 + 0.6s + 1)}$$

Where:

$K_v T = 0.375$ at 27.5 quanta per second.

$= 0.0375$ at 3.2 quanta per second.

Errors of up to 1.6 quanta occur because the first "slow" input pulses are executed at high gain. The input rate change is not detected by the rate circuit until $\tau = 28$. The gain change is accomplished at $\tau = 40$. These errors are not excessive although some improvement might be obtained if the gain were changed as soon as the rate change was detected. This would eliminate the second high gain response and bring the system to the correct rate sooner. This was not done here because there would be timing problems.

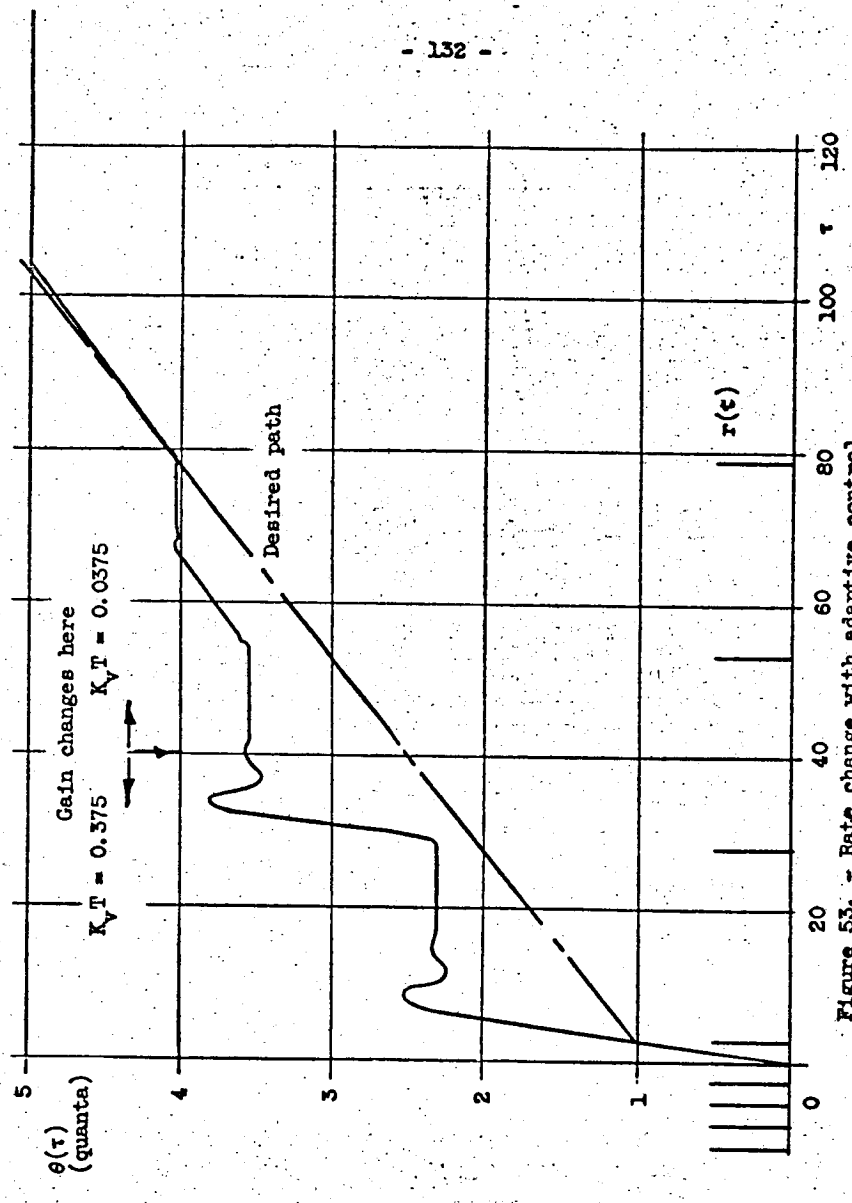

Figure 53. - Rate change with adaptive control.

When the input pulse rate changes from a low rate to a high one errors can also occur. However in this case only the first pulse at the high rate is executed at the wrong gain. At worst this introduces a delay of one and a half times the faster pulse period in the execution of the first high rate pulse.

Ripple Due to Adaptive Gain Quantization

The adaptive control changes the loop gain K_v over a 10:1 range in nine steps. The rate circuit measures the input pulse period by counting the number of clock pulses which occur during one half this period. The count in the counters and hence the gain will be constant for a constant input pulse period only when this period is an integral number of clock periods. At low input pulse rates the gain does not change much between two counter states. However a change of from one clock period to two clock periods is a input pulse rate change of 2:1. The gain also changes by about a factor of two. Thus there is a large range of input pulse rates which will not have constant gain. For example the maximum loop gain is $K_v = 30\ sec^{-1}$ at 27.5 quanta/sec and above. At 13.75 quanta/sec the gain is $K_v = 15\ sec^{-1}$. If the input pulse rate is 20.6 quanta/sec the counters will alternately count one and two clock pulses. Thus the gain will change from 30 sec^{-1} to 15 sec^{-1} in a periodic manner. The counters are switched in time halfway between two input pulses. Whenever the gain changes it has the effect of doubling or halving $e(t)$ the digital to analog converter output.

The response can be plotted using the graphical method by plotting $e(\tau)$ at the same time as $\theta(\tau)$. Whenever the gain changes it has the

same effect as a feedback or input pulse, without the 0.005 sec delay. Since the gain change is exercised on the modulator output, see figure 30, there is no delay. In order to plot the response under these conditions $q_u(\tau)$ and $q_u(\tau + 0.4)\ u(\tau + 0.4)$ are plotted with $K_v = 15\ \text{sec}^{-1}$. A paper strip is used with the input pulse times T_{rn} marked and the time when the gain changes also marked. When $e(\tau)$ changes due to an input or a feedback pulse the magnitude of the mark is weighted with a value of one or two depending on the gain at that instant. These marks are used with $q_u(\tau)$ to obtain $\theta(\tau)$, the controlled variable response. In addition, when $e(\tau)$ changes due to a gain change the mark has a value one or two depending on $e(\tau)$. The gain change marks are used with the $q_u(\tau + 0.4)u(\tau + 0.4)$ curve since no delay is involved. Figure 54 shows the steady state response $\theta_{ss}(\tau)$ and $e(\tau)$ the digital to analog converter output. The response has a period $2/T_r$ instead of $1/T_r$ because of the periodic gain change. This gain ripple makes the velocity deviations at this rate worse than they were without adaptive control. The value of I, the smoothness factor, is 1.53 compared with $I = 0.9$ without adaptive control. However, the gain ripple is largest at the rate shown in the example. Lower rates are not effected seriously. There is a substantial improvement in smoothness over the entire speed range in spite of the gain ripple.

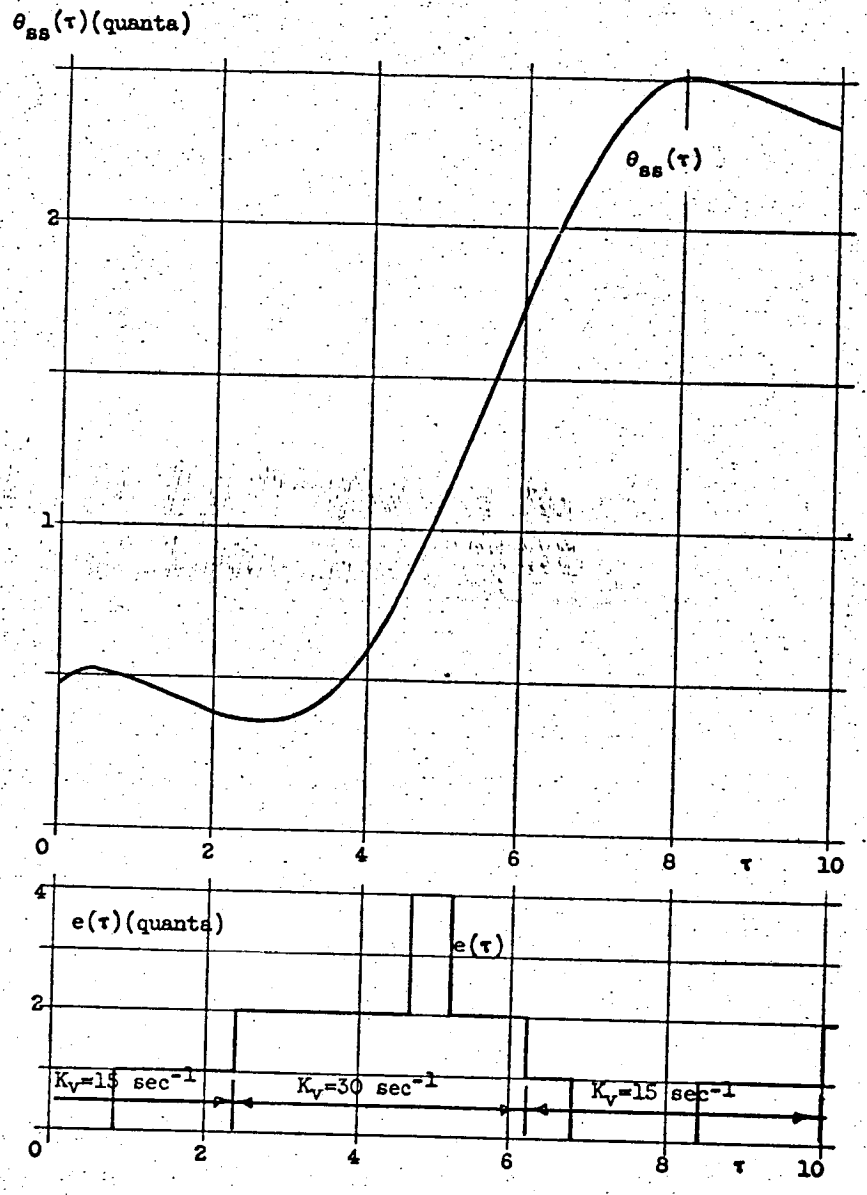

Figure 54. - Steady state response with gain ripple.

APPENDIX II

DETAILED SELF-ADAPTIVE SYSTEM DESCRIPTION

The purpose of this section is to describe the self-adaptive pulse-data system which was constructed. This description is to be in enough detail to permit future researchers to reproduce all or part of the system.

Most of the electronic circuits are composed of combinations of plug-in units. Several types of units were used. In the case of these circuits the following method of description is used.

(1) A logical diagram of each of the circuits is shown. The plug-in units are represented symbolically. The type of unit is noted by a number of the form Z90000, which is an Engineered Electronics Company part number, or a letter designation. The signal connections are numbered referring to the pin connections on the plug-in unit. All elements external to the plug-in units are shown.

(2) Each plug-in is shown in detail in a separate schematic. The bias voltages and plate voltages are noted in the plug-in descriptions.

This method of representation tends to highlight the function of each circuit element. The circuit can be easily constructed from the logic diagram and the plug-in description.

Figure 55 shows the symbols used to represent the plug-in units.

(a) Flip-Flop. This element has two stable states. When a pulse is received at the "R" input it goes into the reset state. A pulse at the "S" input sends it into the set state. If a pulse is received at the "T" input the flip-flop changes state.

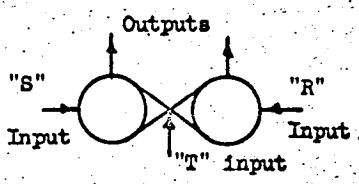

Bistable multivibrator (flip-flop)

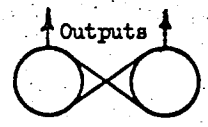

Astable multivibrator
(free-running multivibrator)

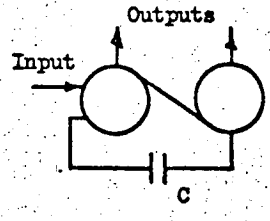

Monostable multivibrator
(One shot)

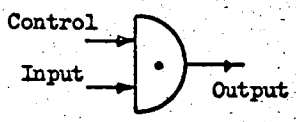

"And" gate

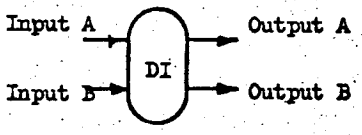

Dual inverter

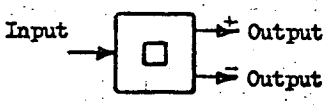

Squaring circuit

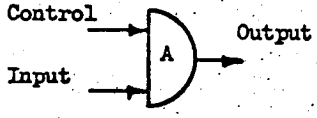

Analog gate

Figure 55. - Logical element symbols.

(b) Free-Running Multivibrator. This is an oscillator which produces a square wave of fixed frequency.

(c) One Shot. A one shot goes into the set state when an input pulse is received. It stays in the set state for a period of time determined by capacitor c. After this period of time it returns to the reset state.

(d) "And" Gate. In the "and" gate there is no connection from input to output unless a specified signal appears at the control. If the control signal is present then the input pulses pass through inverted, to the output.

(e) Dual Inverter. This element has two separate sections. Each section inverts the polarity of its respective input pulse.

(f) Squaring Circuit. The squaring circuit reduces the rise and fall time of an input signal. Thus it "squares" the input waveform.

(g) Analog Gate. The analog gate operates in the same manner as the "and" gate. However the input and output are d-c voltages.

A photograph of the complete self-adaptive pulse-data system circuitry is shown in figure 56. The system consists of several sections:

(1) Input rate sensing and adaptive section.

(2) Synchronizer.

(3) Bidirectional counter.

(4) Digital to analog converter.

(5) Modulator.

(6) Prime mover amplifier.

(7) Quantizer circuit.

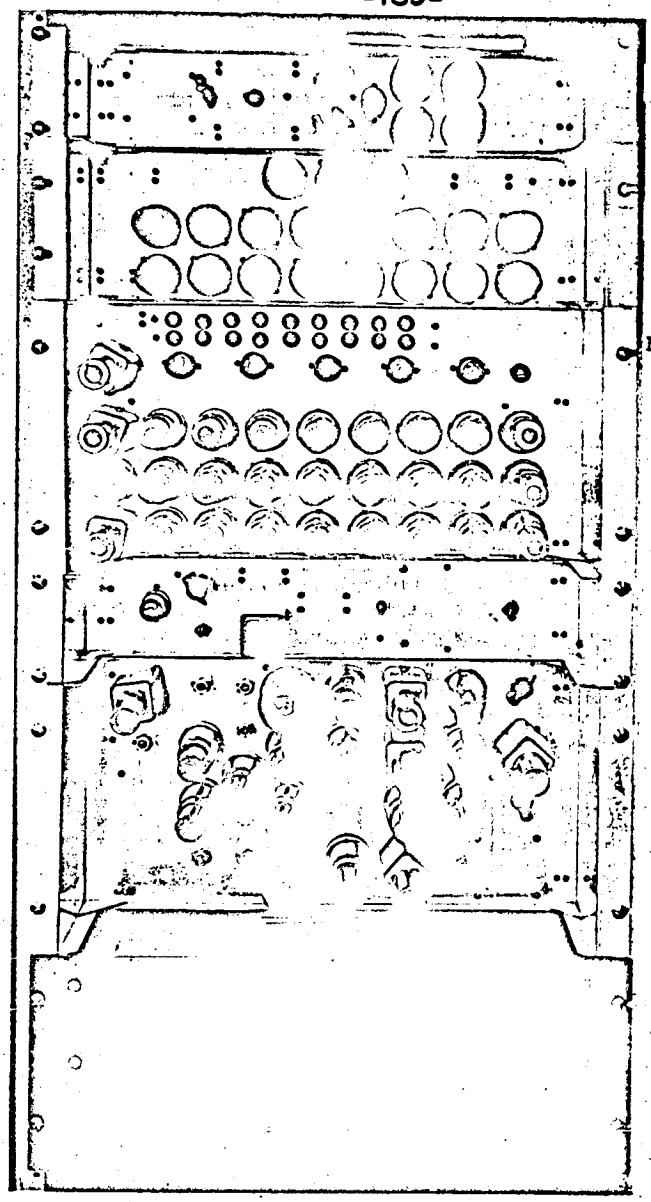

Figure 56.- Self-adaptive pulse-data system circuit photograph.

These sections are described in detail in the remainder of this appendix. The relationship of these sections is shown schematically in figure 25.

Input Rate Sensing and Adaptive Section

This section has three subsections:

(a) Control

(b) Counter

(c) Blender and multiplier

The control subsection is shown in figure 57. The input $r^*(t)$ which has twice the desired frequency is connected to the "T" input of a flip-flop. The output of the flip-flop is a square wave whose period is the desired period of the input to the pulse-data system $r(t)$. The square wave is differential and fed to the synchronizer by either the up or down gate. The positive-going portion of the square wave opens an "and" gate. The input of the gate is the output of a 53 cycle per second free-running multivibrator. The gate output is then a burst of pulses equal in number to 26.5 T_r. The bursts of pulses are alternately gated to one of two counters. These gates are controlled by a second flip-flop which is triggered at its "T" input by the first flip-flop. This flip-flop resets the counter which is to receive the burst of pulses. It also supplies a trigger signal to the blender circuit.

There are two identical counters in the counting subsection. Figure 58 shows one of these counters. The counter uses a cold cathode bidirectional decade counter tube similar to a Sylvania 6476. The reset pulse from the flip-flop in the control subsection makes cathode

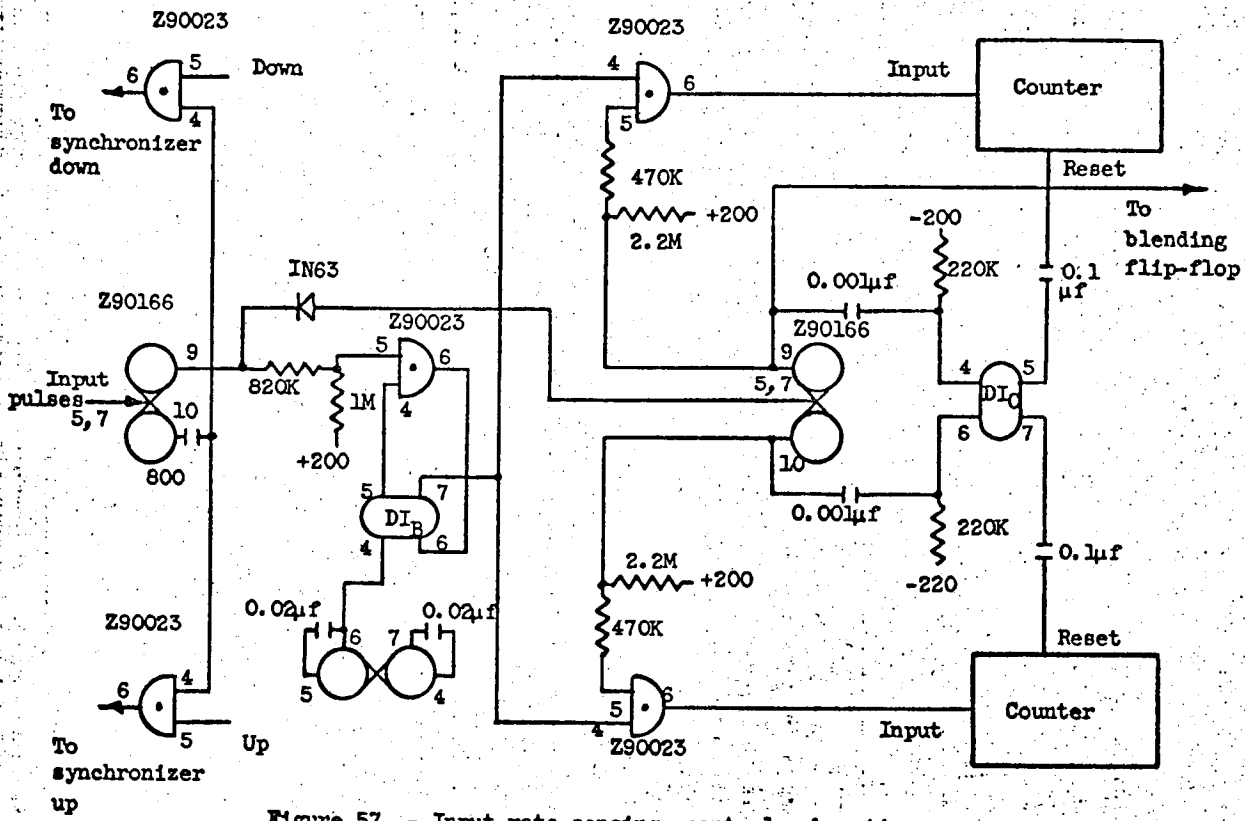

Figure 57. - Input rate sensing, control subsection.

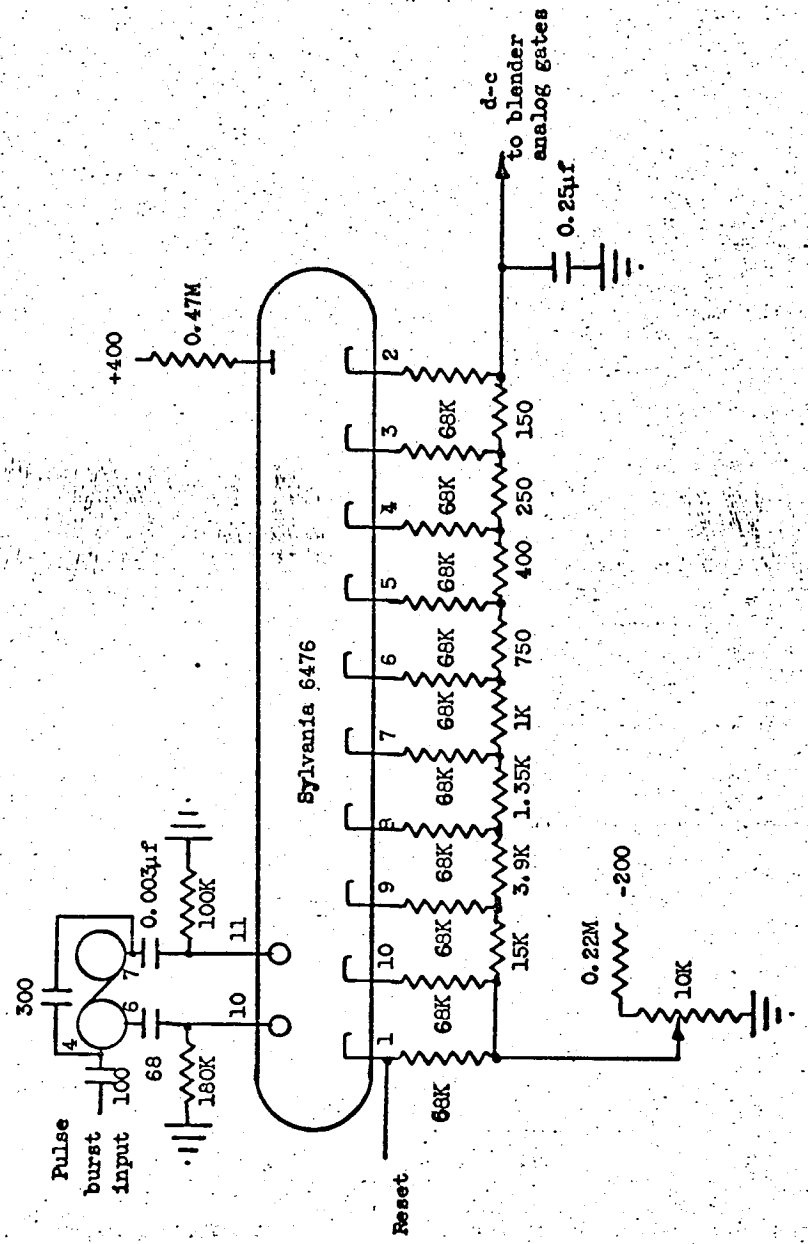

Figure 58. - Counter subsection of rate sensing circuit.

number 1 become more negative than the rest. This causes the glow to jump to this cathode. Each of the pulses in the burst from the gate in the control subsection sets the one shot. The one shot activates two sets of guide cathodes, number 11 and 12, in succession. This moves the glow one cathode to the right for each pulse in the burst. When the burst is over the counter remains at the last cathode until it is reset. The tube drop is constant so that the 0.47 meg plate resistor, the 68K cathode resistor, and several resistors in series, depending on which cathode is conducting, serve as a divider. The d-c voltage across the 0.25 mfd capacitor then depends on which cathode is conducting. The resistors between the bottom end of the 68K cathode resistors are weighted. The values are chosen so that the output voltage change is proportional to input pulse frequency. The 10K bias potentiometer is set so that the voltage across the 0.25 mfd capacitor always operates the analog gates in their linear range. The bases of the number 1 and 10 cathode resistors are tied together so that there is no change in output for one or zero pulses in the burst. This is done because the presence of no pulses in the burst could indicate an input pulse period of 1/26.5 sec or less. Instead of defining a definite input frequency, a zero count defines a whole range of frequencies. Then the input frequency indicated by a count of one bears no fixed relation to that defined by a count of zero. This ambiguity was removed by eliminating the difference between a one and a zero count.

Figure 59 shows the blender and multiplier subsection. The output of each of the counters is fed to an analog gate. The gates are opened

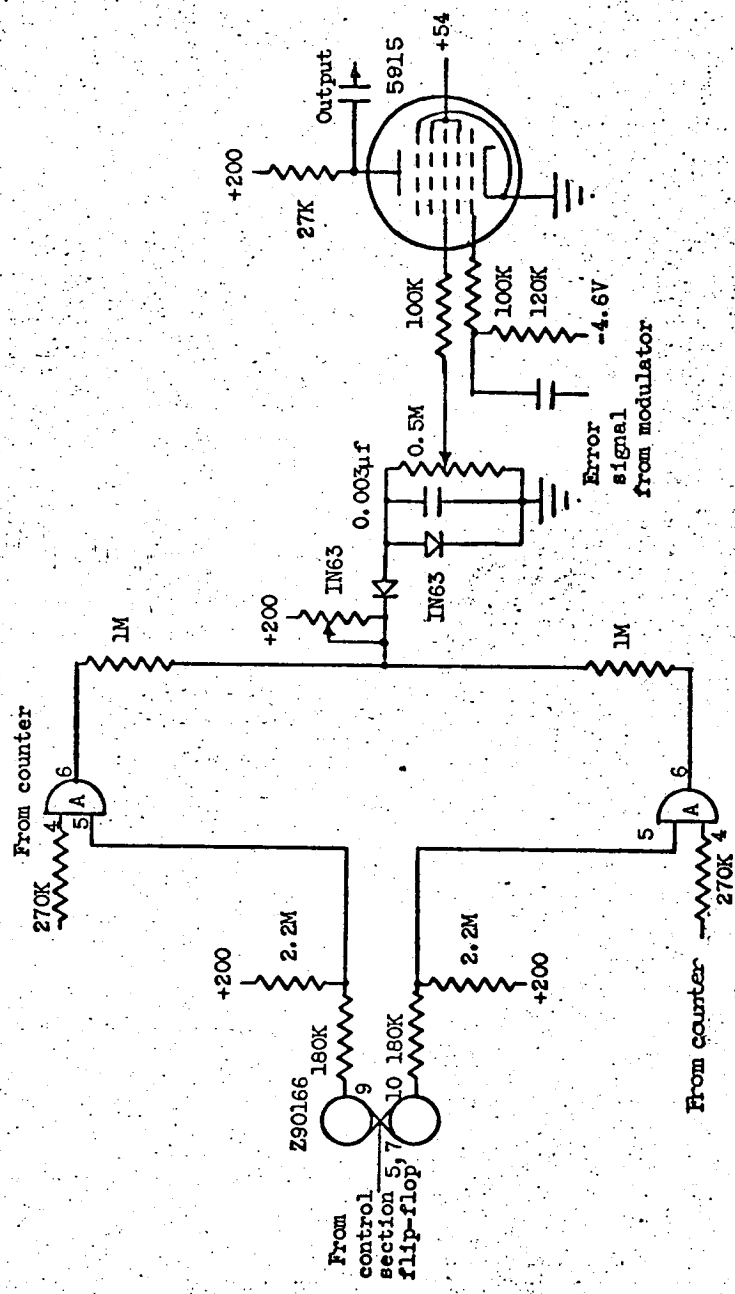

Figure 59. - Blender and multiplier subsection of rate sensing circuit.

alternately by the flip-flop which is driven by the flip-flop in the control subsection. The analog gate connected to the counter which is not counting a pulse burst is the gate which is open at any instant. The voltage across the 0.5 meg potentiometer is zero for zero or one count in the counter. It decreases to -8 volts at nine counts. The 0.5 meg potentiometer is set for the desired amount of gain reduction at nine counts. This voltage, fed to grid number 3, controls the gain of the 5915 tube. The modulator output is fed to grid number 1. The a-c voltage on the plate is then proportional to input pulse rate for a given modulator output.

No provision has been made in this circuit for input pulse rates lower than 3.2 pulses/sec. At rates lower than this the counters will not measure T_r correctly. This could be remedied by increasing counter capacity or limiting the number of clock pulses in a burst to nine.

Synchronizer

The synchronizer developed by D. R. McRitchie[10] is composed of a clock pulse generator and four identical memory and gating channels.

The clock pulse generator and one channel are shown in figure 60. A free-running multivibrator drives two flip-flops at their "T" inputs. This produces one positive pulse every two periods of the free-running multivibrator from each output of the two flip-flops. The four resulting pulses are spaced equally in time and none are coincident with any others. Each of the four memory and gating channels is activated by one of these four pulses.

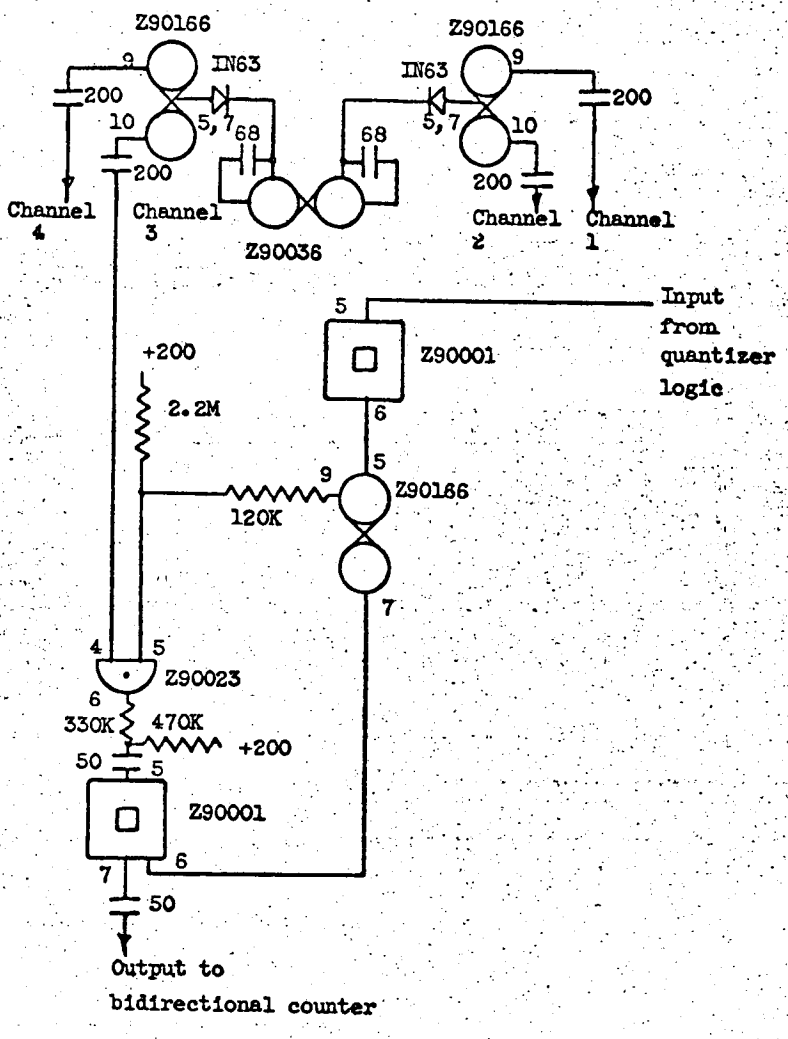

Figure 60. - Synchronizer; clock pulse generator and one channel.

The memory channel number three is shown. The input pulses will come from the plus output of the quantizer. The other channels are connected to the minus output of the quantizer and the plus and minus gate outputs on the rate sensing control subsection. The input pulse is shaped by the squaring circuit and sets the flip-flop. The flip-flop opens the "and" gate. When a pulse is produced by the clock pulse generator at the gate input it passes through the gate. The gate output is shaped and fed to the bidirectional counter. It is also used to reset the flip-flop. In this way one pulse is delivered to the bidirectional counter for each input pulse. The pulse is delivered at the time when that channel receives a pulse from the clock pulse generator. Only one channel at a time gets a pulse from the generator. This prevents pulses from entering the bidirectional counter simultaneously.

If a pulse enters a memory channel just after a clock pulse has been fed to that channel it will be delayed. The maximum delay is equal to twice the free-running multivibrator period. In this case that is 0.005 sec.

Bidirectional Counter

A seven stage binary counter designed by D. R. McRitchie[10] is used. The stages are identical so only the first two stages and the up and down controls will be shown in figure 61.

The reference or feedback pulses from the synchronizer are inverted and set one of two one shots. Each one shot controls a string of "and" gates, one gate at the input to each stage. If the input pulse comes in on the up line the left one shot opens the left string of gates

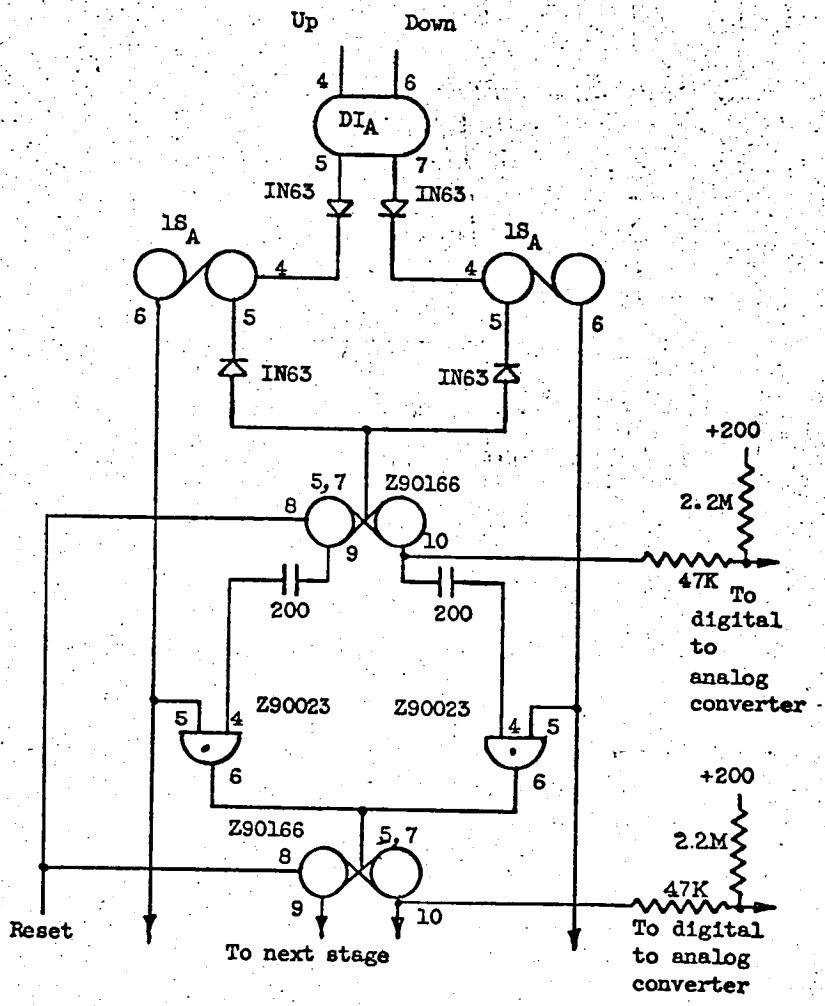

Figure 61. - First two stages of bidirectional counter.

for 50 microseconds. Now if one of the flip-flops changes from the set state to the reset state, as a consequence of the input pulse, a carry pulse will be fed to the next stage. If the input pulse enters the down line the right one shot opens the right gates. Now whenever one of the flip-flops changes from the reset to the set state a borrow pulse is fed to the next stage. The input pulse is always fed to the first stage flip-flop. This stage changes state regardless of the counting direction. The one shots remain set long enough for the counter to change stage as a consequence of the input pulse. Both one shots are never set simultaneously. The synchronizer insures that the time spacing of the input pulses is long enough to prevent this and allow for one shot recovery.

All flip-flops are reset when the line connecting pin 8 to -200 volts is opened.

Pin 10 of each flip-flop, except the one in the last stage, is d-c coupled to the grid of a digital to analog converter stage. Pin 9 of the last stage is connected to its corresponding converter stage. In this way the bidirectional counter appears to be half full to the digital to analog converter when it is reset. This permits the digital to analog converter to convert the state of the counter to a linearly varying d-c voltage over a ±63 count range on either side of the reset state.

Digital to Analog Converter

This circuit is shown in figure 62. The grid of each of the triodes is d-c coupled to a flip-flop output in one of the counter stages.

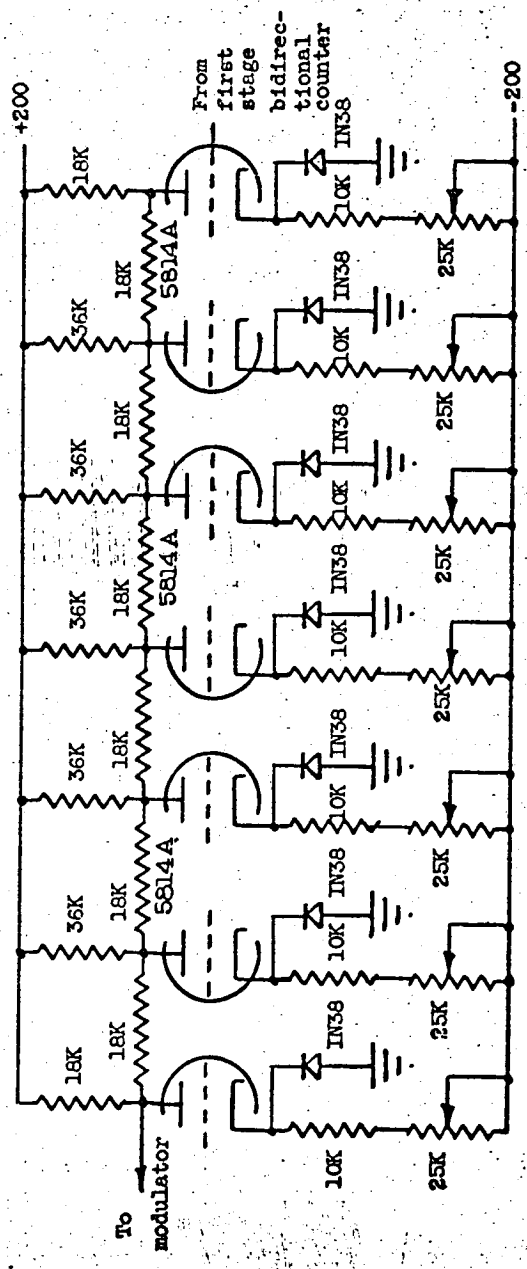

Figure 62. - Digital to analog converter.

When the flip-flop is in the set state the triode is conducting, otherwise it is cut off. The triode connected to the 2^6 stage is conducting when that stage is in the reset state as discussed in the bidirectional counter description.

Each triode acts as a current source feeding the ladder network composed of 18K and 36K resistors. The d-c voltage deviation from +178 volts appearing at the plate of the last stage of the converter is proportional to the count in the counter.

The IN38 diodes prevent the cathodes from becoming negative. This permits the triodes to be cut off with small signals which provides positive action. The 25K potentiometers permit adjustment of the current supplied by each stage to the ladder. This allows the use of resistors of ±5 percent tolerance. Two watt resistors should be used to minimize temperature effects. 5814A tubes are used for reliability and their consistent characteristics.

Modulator

The d-c output of the digital to analog converter is modulated on a 60 cycle per second carrier (fig. 63). A C. P. Clare and Company type HGS 1004 Mercury-Wetted Contact Chopper is used. The signal from the digital to analog converter is connected to the wiper of the chopper. The two chopper contacts are connected to the ends of the primary of a center-tapped transformer. The center-tap is connected to a potentiometer which is adjusted for +178 volts.

The chopper coil is excited by a 60 cps voltage. This causes the wiper to apply the digital to analog converter output alternately

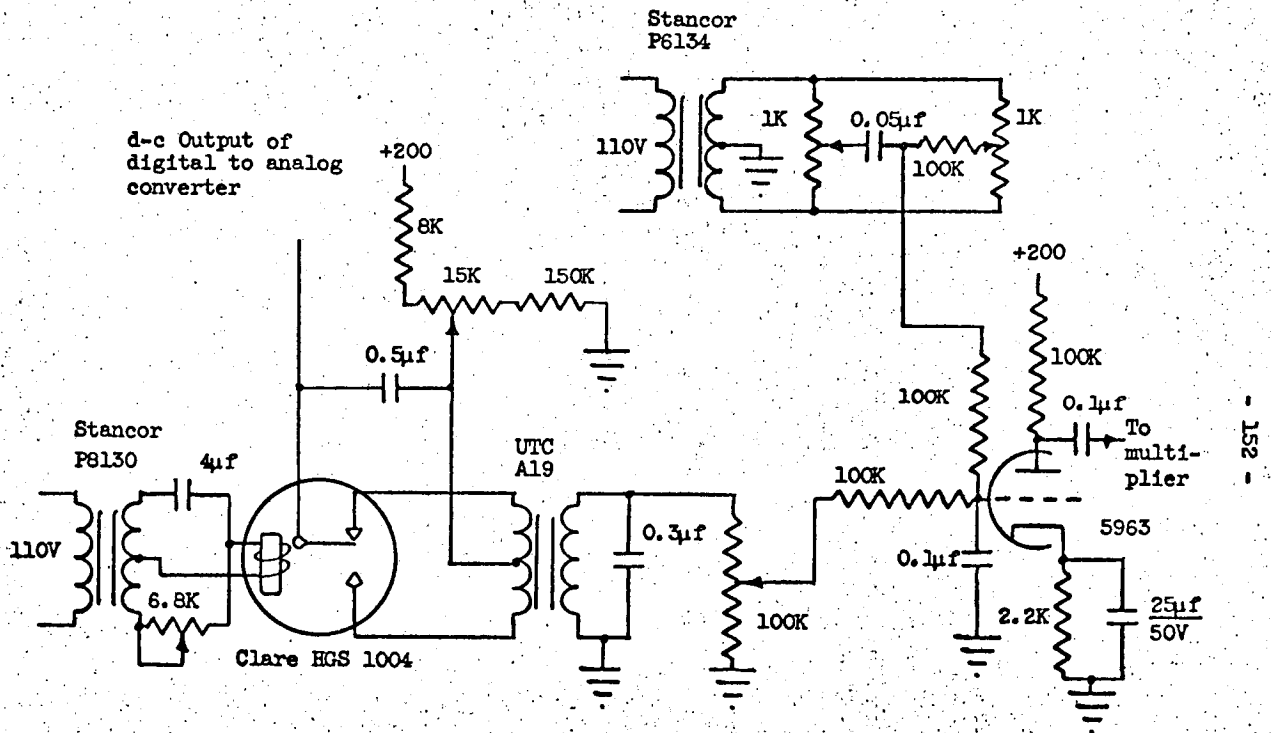

Figure 63. - Modulator.

to opposite ends of the transformer primary. The voltage across the primary is proportional to the count in the bidirectional counter and is a-c with a 60 cps frequency. This voltage is filtered and amplified. The output is then an a-c voltage whose amplitude and phase are dependent on the state of the bidirectional counter. This voltage is fed to the multiplier in the adaptive circuit.

The phase of the a-c voltage output is adjusted by varying the 6.8K resistor in the chopper coil circuit. The servo loop gain K_v is adjusted by the 100K potentiometer.

A small a-c signal is fed to the grid of the triode to correct for errors in the null of the servomotor tachometer. The 1K potentiometers are adjusted to supply the correct amount of correction.

Prime Mover Amplifier

The a-c servomotor has a fixed 110 volts a-c winding and a variable voltage control winding. The voltage on the control winding determines the motor speed. Its phase determines the motor direction of rotation. The control winding is supplied by a pair of 6L6 tubes in push-pull. This winding is a high impedance center-tapped winding for operation directly from the tubes. This eliminates the need for an output transformer.

Figure 64 shows the amplifier developed by C. C. Crabs. The phase of the a-c signal from the tachometer is adjusted by the network shown. The feedback gain is controlled by the 100K potentiometer. The signal from the wiper of this potentiometer is combined with the signal from the multiplier. The output of the first stage

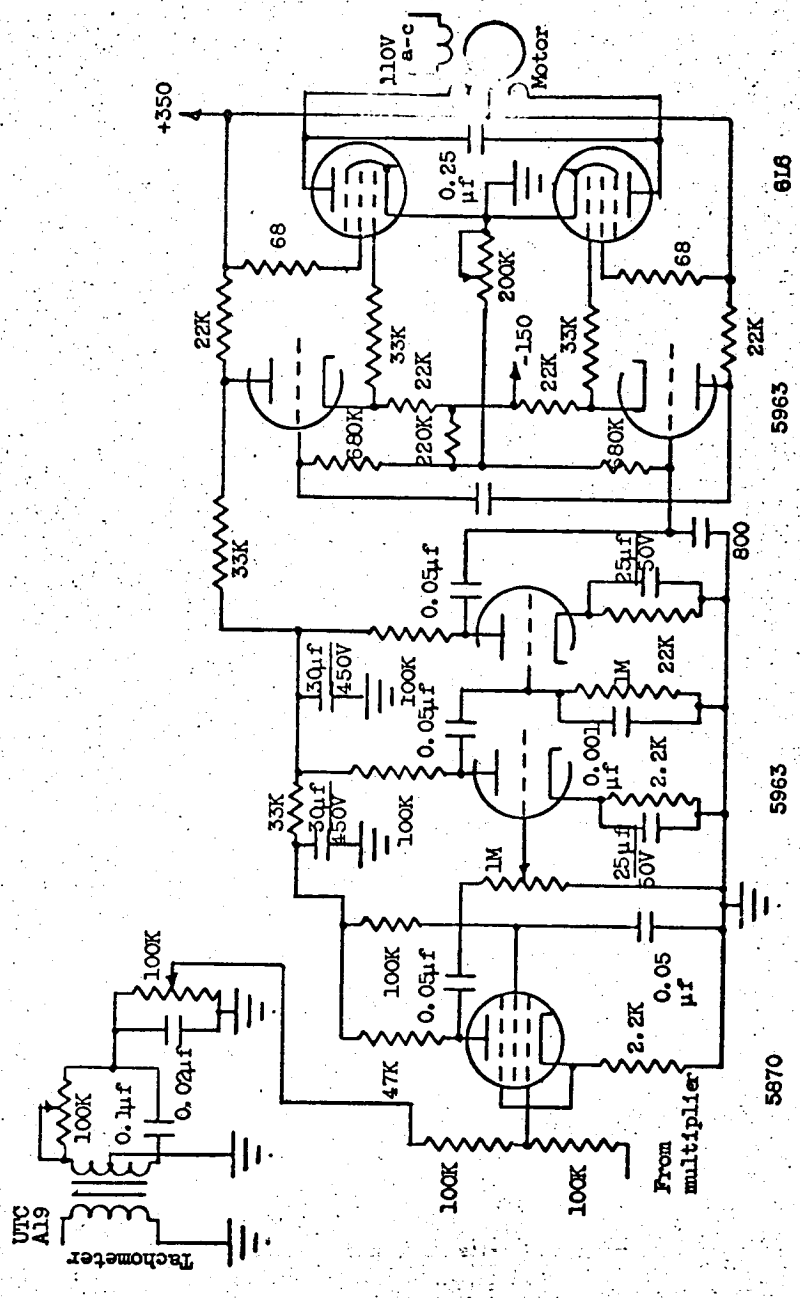

Figure 64. - Prime mover amplifier.

is the difference since the signal from the tachometer is 180° out of phase with the signal from the multiplier.

This signal is amplified and inverted to drive the 6L6 tubes in push-pull.

Quantizer

The quantizer operation is described in detail in chapter V. The circuitry used consists of two subsections.

(1) Oscillator

(2) Demodulator and logic

The oscillator circuit shown in figure 65 was developed by the Applied Science Corporation of Princeton, New Jersey for use with their quantizer. The circuit produces a 45 kilocycle sine wave of 1.5 volts peak to peak amplitude. The transformer is wound with number 26 enamel wire on a toroidal core. A Magentics Incorporated number E29-55206-A2 or equivalent is suggested.

The demodulator shown in figure 66 was also developed by the quantizer manufacturer. The two quantizer outputs as described in chapter V are modulated on a 45 kilocycle carrier. The 2N94 is biased off to provide demodulation and amplification. The resulting d-c signal is amplified by the 2N321 and the 5963. The output of the 5963 drives a squaring circuit which decreases the signal rise and fall time. The resulting signal from input A is used to control the two "and" gates. The signal resulting from input B is differentiated and serves as the input to the gates. In this way direction sensing is accomplished as outlined in chapter V. The gate outputs are directed to the synchronizer.

Note: Transformer is wound on a Magnetics Inc. E29-55206-A2 toroidal core or equivalent. No. 26 enamel wire is used.

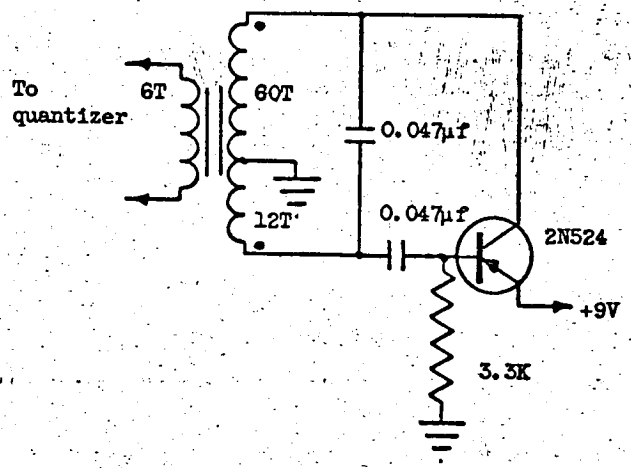

Figure 65. - Quantizer oscillator.

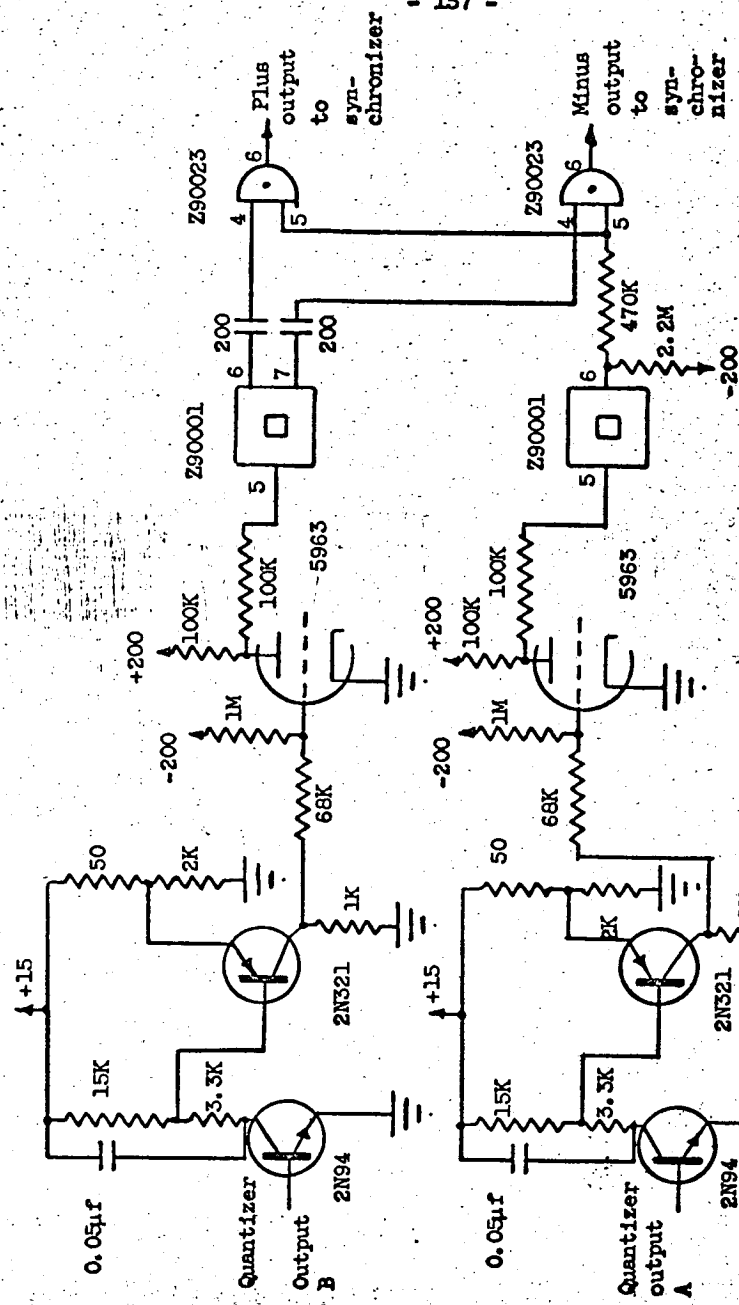

Figure 66. - Quantizer demodulator and logic.

Plug-In Schematics

The plug-in units used in the circuits are shown in figures 67 to 76. All of the units use a plate voltage of +200 volts except where noted.

Flip-flop Z90166 figure 67. This unit is connected as a "T" flip-flop by feeding the input pulses to pins 5 and 7. In the circuits shown pin 2 is always grounded and pin 1 is connected to -200 volts. The flip-flop is reset by opening the contact between pins 1 and 8 which is normally closed.

Free-running multivibrator Z90036 figure 68. External capacitors between pins 5 and 6 and pins 4 and 7 determine the frequency.

One shot Z8889 figure 69. This one shot requires +30 volts bias on pin 5 relative to pin 1.

One shot A figure 70. This one shot, developed by Dr. H. W. Mergler, is used in the bidirectional counter. The 500 mmfd capacitor determines the time that the one shot remains set. Pin 1 is connected to -200 volts and pin 2 is grounded.

"And" gate Z90023 figure 71. Two bias voltages are required. Pin 8 must be -50 volts with respect to pin 1. Pin 7 must be +70 volts with respect to pin 1.

Dual inverter figures 72, 73, and 74. The basic inverter in figure 72 was developed by D. R. McRitchie[10]. The other forms are modifications for different grid bias arrangements.

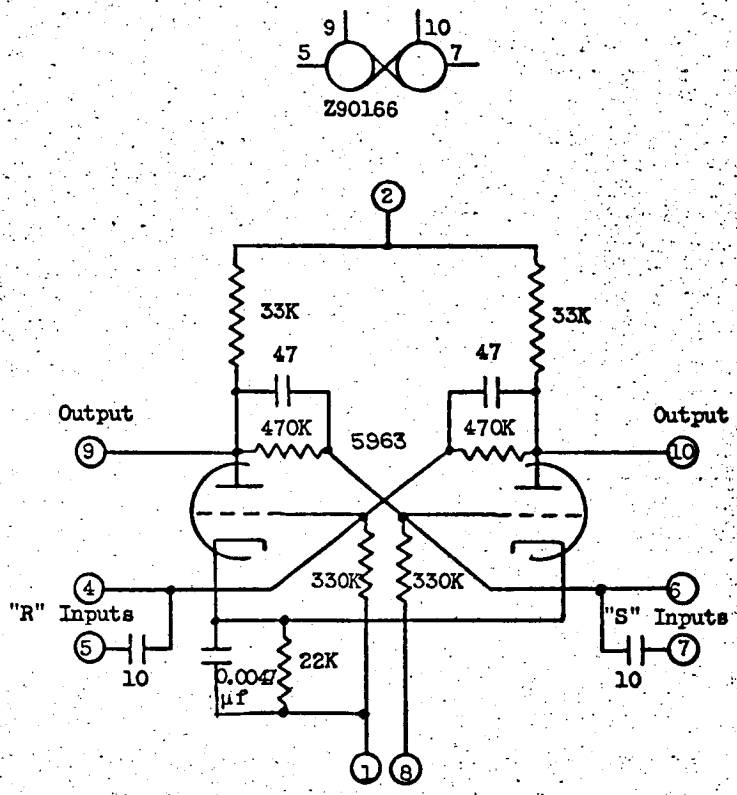

Figure 67. - Z90166 Engineered Electronics Company flip-flop.

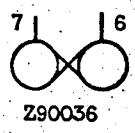

Z90036

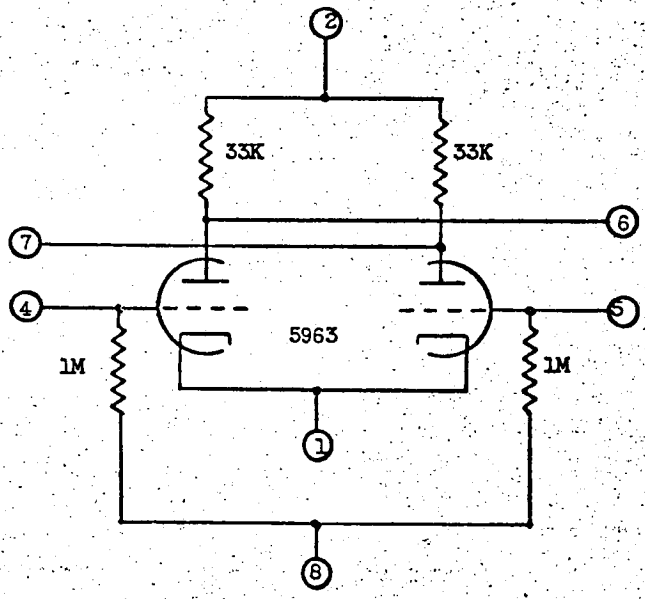

Figure 68. - Z90036 Engineered Electronics Company free-running multivibrator.

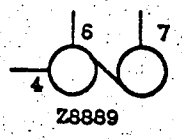

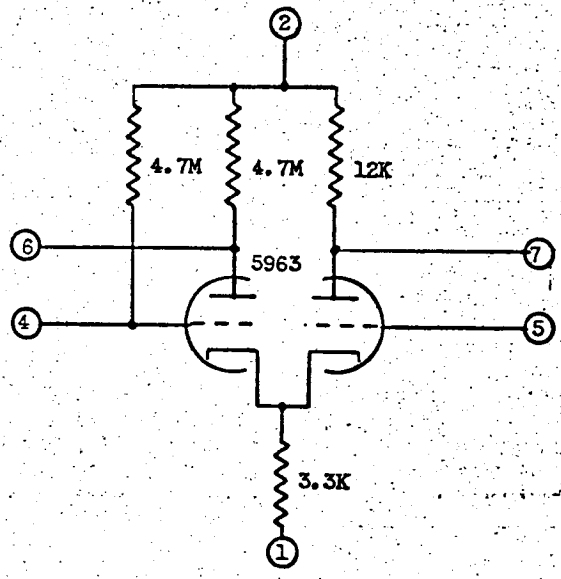

Figure 69. - Z8889 Engineered Electronics Company one shot.

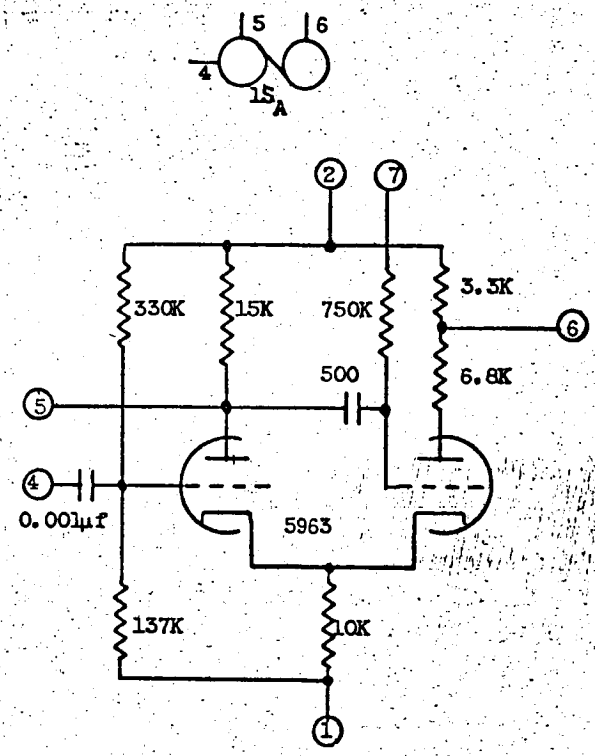

Figure 70. - One shot A.

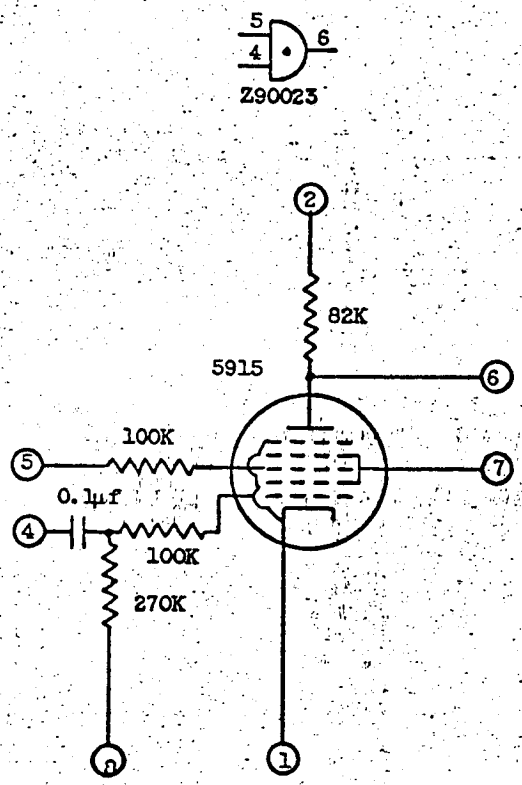

Figure 71. - Z90023 Engineered Electronics Company "and" gate.

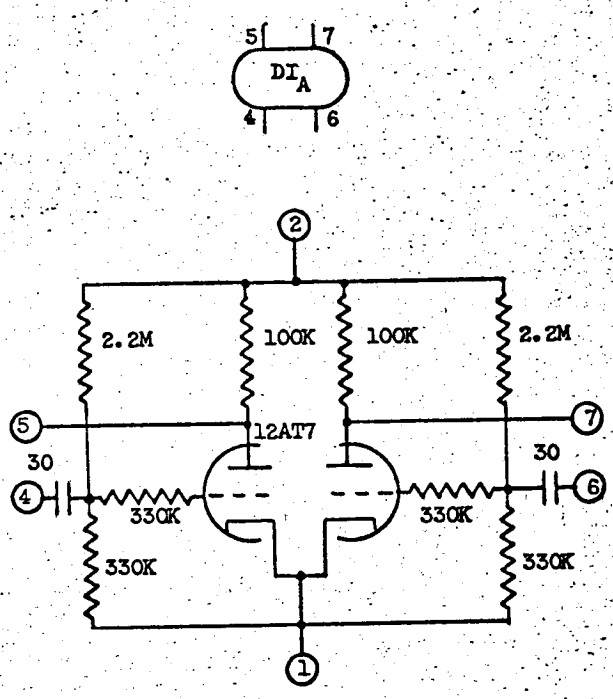

Figure 72. - Dual inverter A.

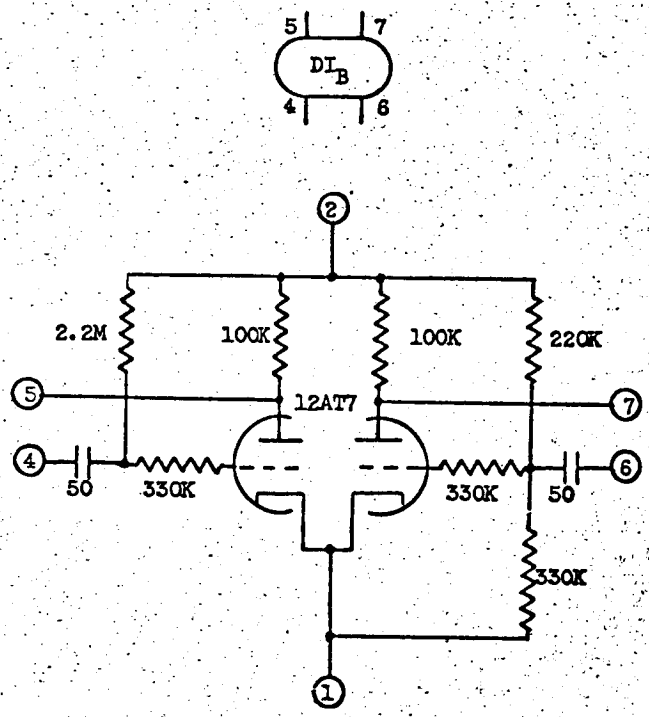

Figure 73. - Dual inverter B.

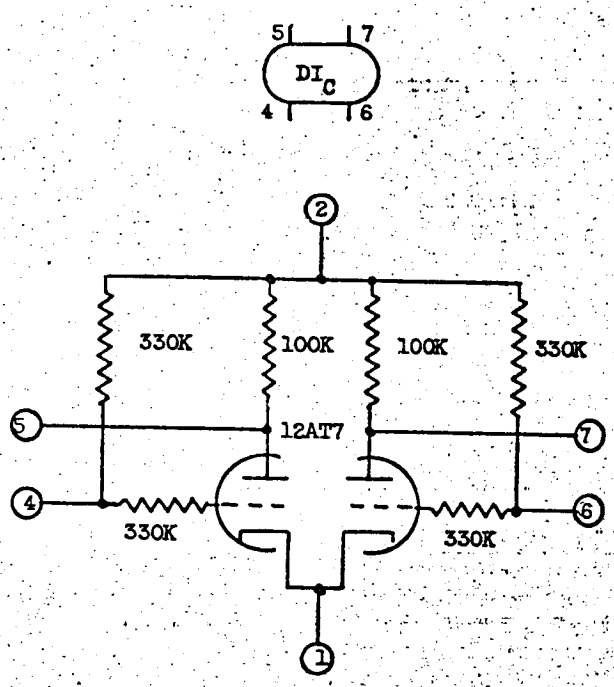

Figure 74. - Dual inverter C.

Squaring circuit Z90001 figure 75. In the synchronizer pin 1 is grounded and pin 2 is connected to -200 volts.

Analog gate figure 76. This gate requires two bias voltages. Pin 7 must be +54 volts with respect to pin 1. This voltage must be supplied by a low impedance source since changes in this voltage due to grid current changes effect the gate characteristics. This grid draws a current of up to 14 ma. A bias of minus one or two volts applied to pin 8 is used to match the gate outputs.

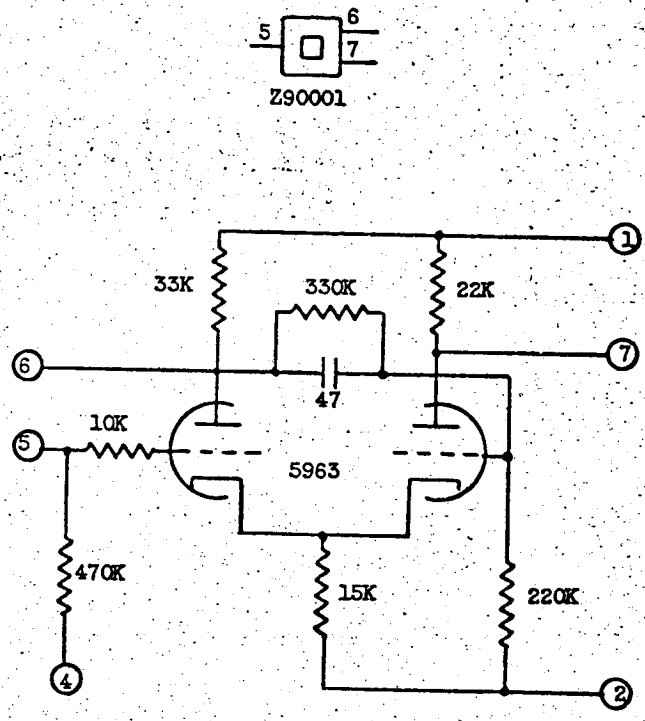

Figure 75. - Z90001 Engineered Electronics Company squaring circuit.

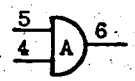

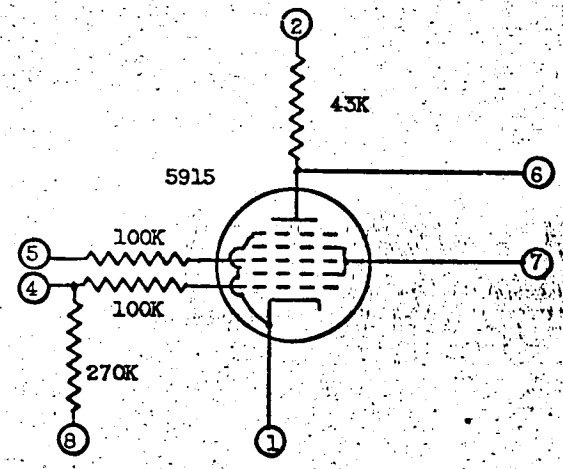

Figure 76. - Analog gate.

REFERENCES

1. Cunningham, W. J. Introduction to Nonlinear Analysis. New York: McGraw-Hill Book Company, Inc., 1958, pp. 28-48.

2. Truxal, John G. Automatic Feedback Control System Synthesis. New York: McGraw-Hill Book Company, Inc., 1955, pp. 48-51, pp. 613-656.

3. Savant, C. J. Jr. Basic Feedback Control System Design. New York: McGraw-Hill Book Company, Inc., 1958, pp. 333-347.

4. Gille, J-C., Pélegrin, M. J., Decaulne, P. Feedback Control Systems: Analysis, Synthesis, and Design. New York: McGraw-Hill Book Company, Inc., 1959, pp. 394-398.

5. Ragazzini, John R., Franklin, Gene F. Sampled-Data Control Systems. New York: McGraw-Hill Book Company, Inc., 1958.

6. Farmanfarma, G. "Analysis of Linear Sampled-Data Systems With Finite Pulse Width: Open Loop," American Institute of Electrical Engineers Transactions, Vol. 75, part I, 1956, pp. 808-819.

7. Waidelich, D. L. "The Steady State Operational Calculus," Proceedings of the Institute of Radio Engineers (February, 1946), pp. 78-83.

8. Hinde, William L. "Analysis of Feedback Control Systems Using Pulse Width Error Detection", Master of Science Thesis. Cleveland: Case Institute of Technology, 1959, pp. 79-90.

9. Seshu, Sundaram; Balabanian, Norman. Linear Network Analysis. New York: John Wiley and Sons, Inc., 1959, pp. 168-186.

10. McRitchie, David R. "The Program and Comparison Unit for a Numerically Controlled Machine Tool Operating From Magnetic Tape," Master of Science Thesis. Cleveland: Case Institute of Technology, 1959.

11. Susskind, Alfred K. (ed.) Notes on Analog-Digital Conversion Techniques. New York: John Wiley and Sons, Inc., 1957, pp. 5-29 to 5-32.